MATHEMATICAL MODELING OF AUTOIMMUNE DISEASE

by

James R. Moore

A dissertation submitted to the faculty of
The University of Utah
in partial fulfillment of the requirements for the degree of

Doctor of Philosophy

Department of Mathematics

The University of Utah

May 2015

The University of Utah Graduate School

STATEMENT OF DISSERTATION APPROVAL

The dissertation of **James R. Moore**

has been approved by the following supervisory committee members:

Frederick Adler	, Chair	October 29th, 2014 (Date Approved)
Aaron Fogelson	, Member	October 22nd, 2014 (Date Approved)
Robert Fujinami	, Member	October 23rd, 2014 (Date Approved)
James Keener	, Member	October 22nd, 2014 (Date Approved)
Matthew Williams	, Member	October 23rd, 2014 (Date Approved)

and by Peter Trapa , Chair/Dean of

the Department of Mathematics

and by David B. Kieda, Dean of The Graduate School.

ABSTRACT

A fundamental challenge for the immune system is the distinction between self and nonself, or infected and uninfected. Autoimmune disease arises when the immune response mounts an immune response against the hosts tissues. Via a mathematical model, we show that the immune system can distinguish self from nonself via the interaction of T-cells and and dendritic cells (DCs) and explain how autoimmunity is avoided in most people most of the time. The NOD mouse develops Type 1 diabetes, an autoimmune disease, spontaneously with an incidence of about 80% in females. The progression of Type 1 diabetes may be either accelerated or delayed by viral infection. We first create a mathematical model to understand the factors that affect progression in uninfected mice and how it may be interrupted via certain treatments. We categorize which types of viral infection should accelerate Type 1 diabetes or delay. We find that the timing of infection is important, as well as the cell type infected.

CONTENTS

LIST OF TABLES

ACKNOWLEDGMENTS

I wish to acknowledge my advisor, Professor Fred Adler, for helping me find this project and keeping me on track. I also would like to acknowledge the rest of my committee for helping me narrow my focus and for teaching me humility.

The math biology group in this department is a very cooperative environment, and I'd like to acknowledge everyone who made suggestions or asked me a question in a group meeting that I couldn't answer satisfactorily: Parker, Cheryl, and Megan in particular. I'd like to thank Ross for critiquing my early terrible attempts at color maps. Laura Strube helped me while I was off-campus and attended roughly 18 of my group meetings. I'm also grateful to Allie for proofreading a bewilderingly complex 150 page thesis in a subject completely foreign to her.

CHAPTER 1

INTRODUCTION

One of the primary challenges of the mammalian immune system is to distinguish self from foreign. Fundamentally, the immune system does this at the molecular level, as immune responses form against specific molecules called antigens. These immune responses consist of adaptive immune cells called lymphocytes, which each respond specifically to a limited range of molecules. We focus here on a subset of lymphocytes, T-cells, which can respond to protein fragments about 8-10 amino acids long. An amino acid sequence that is expressed by the cells of the host's body is a self antigen, and the T-cells that recognize it are self reactive T-cells. The generation and activation of a large number of self reactive T-cells is an autoimmune response. Autoimmunity is the cause of a large number of diseases, in particular Type 1 Diabetes, one of the subjects of this thesis.

The generation of self reactive T-cells is difficult to avoid entirely, but the immune system has several regulatory mechanisms that limit their numbers. In the first chapter, we describe these mechanisms and develop a mathematical model to examine how they work together to control autoimmunity. Although there is no fundamental difference at the molecular level between self antigens and foreign antigens, as each are composed of the same amino acids, the context in which these antigens appear can be quite different. If an antigen is associated with a dangerous pathogen, then wherever it appears there should be signs of tissue damage. These environmental cues are sensed by dendritic cells, another immune cell that is required to activate T-cells. Dendritic cells continuously gather antigen, present it to T-cells and then, based on the environmental cues they have received, either activate or suppress the T-cells that bind to them. In this manner, the body effectively measures the correlation between the presence of an individual antigen and the presence of tissue damage. This results in the generation of immune responses against antigens associated with infectious disease and the repression of autoimmune responses.

It is thought that viral infection plays an important role in the initiation of many autoimmune diseases [27]. One proposed mechanism, epitope spreading, suggests that if the

expression of antigen A and antigen B is strongly correlated and antigen A is associated with a pathogen that causes tissue damage, then the immune system might detect a correlation between antigen B and damage. The immune system might mount a response to antigen B instead of, as well as or subsequent to, a response to antigen A. This general mechanism can apply to the spread of an immune response from a viral antigen to a self antigen or even between responses to different self antigens.

The 'hygiene hypothesis' seemingly runs counter to the notion of viral initiation of autoimmunity via epitope spreading [59]. Broadly speaking, this hypothesis states that lack of exposure to pathogenic foreign antigens makes our immune systems more likely to generate autoimmune responses or allergic responses, which are overly strong responses to otherwise harmless molecules.

Type 1 diabetes, an autoimmune disease of the pancreas, is thought to either be triggered or delayed by viral infection depending on the context. In the NOD mouse, an animal model of Type 1 diabetes, infection by the same virus, at different ages, can have opposite outcomes. Infection at a young age can prevent or at least delay diabetes, whereas infection later in life can precipitate it rapidly [16]. This system provides an excellent opportunity to better understand the role of infection in Type 1 Diabetes.

NOD mice develop diabetes spontaneously in the absence of infection. It is due to multiple breakdowns in immune regulation, which have analogs in the human disease [38]. Before investigating the role of viral infection, we first study the progression of this spontaneous diabetes. In Chapter 3, we develop a mathematical model of Type 1 Diabetes to study the factors that affect the incidence of diabetes among NOD mice and the distribution of the age of onset. Then in Chapter 4, we create a mathematical model of viral infection of NOD mice and test the prevailing hypotheses about their mechanisms of action.

In this thesis, we attempt to address why and how regulatory mechanisms fail and, more specifically, why some individuals develop autoimmune disease while others do not. The differences between two individuals may be genetic, environmental or a combination of both. These are factors that we consider in the first three chapters. However, it may be that the underlying process within an organism can be intrinsically stochastic so that two individuals with identical parameters and initial conditions may experience different outcomes. In Chapter 5, we develop a simple stochastic model of the development of autoimmune disease and compare the results to the corresponding deterministic model.

CHAPTER 2

HETEROGENOUS DC POPULATIONS ALLOW FOR IMMUNITY AND TOLERANCE

2.1 Introduction

The immune system must destroy harmful pathogens within the body without destroying the body itself. It must recognize what is self and what is foreign, even though individual immune cells remain ignorant of this. We use mathematical models to test whether immune cells following simple rules can self-organize to generate a protective immune response while avoiding autoimmunity. Our mathematical model tracks a relatively small number of variables amidst the greater complexity of the immune system.

2.1.1 Biological background

Immune cells called **T-cells** recognize a specific peptide (see Figure 2.1), an **antigen**. The T-cell population is composed of many subpopulations each with a different antigen-specificity. Some of these populations recognize molecules associated with dangerous pathogens or other molecules not produced by the body (**foreign reactive**), while others recognize endogenous molecules such as collagen or insulin (**self reactive**). The activation and proliferation of self reactive T-cells is responsible for many autoimmune diseases including type 1 diabetes, multiple sclerosis, and rheumatoid arthritis. The lack of a response is called immune self tolerance or, more simply, **tolerance**. As both foreign and self antigens are present during an infection, there is the potential for some self reactive T-cells to become activated [66]. Animal models and epidemiological studies suggest that infection can act as a trigger in autoimmune diseases [2, 16, 54]. In this paper, we examine how regulatory mechanisms prevent infection-triggered autoimmunity under normal conditions.

Reprinted with permission from J. R Moore, *The benefits of diversity: heterogenous dc populations allow for both immunity and tolerance*, J. Theor. Biol. **357** (2014), 86–102

There are several known mechanisms of tolerance. Here, we focus on thymic selection, regulatory T-cells, and tolerogenic dendritic cells. Thymic selection is the deletion of cells in the thymus, through which all newly created T-cells must pass before entering circulation. As this process takes place only in the thymus, we also call it **central tolerance**. By contrast, **peripheral tolerance** is a collective term for any mechanism that prevents the survival, proliferation, or activation of self reactive T-cells that escape deletion in the thymus. The thymus expresses many self antigens and can thus bind most self reactive T-cells. A T-cell that binds strongly within the thymus is either deleted or induced to become a regulatory T-cell (see [57] and Figure 2.2). These regulatory T-cells or **Tregs** take part in peripheral tolerance once they have left the thymus and constitute a second level of protection against autoimmunity. Finally, context is very important in the immune system. A self reactive T-cell that encounters its antigen in the periphery will not become activated without an accompanying **danger signal** of an infection. This danger signal could be either evidence of excessive cell damage [10] or of molecules that are made only by bacteria or viruses [52].

During an immune response, T-cells must be activated by dendritic cells (**DCs**). DCs collect antigens from the environment, often by phagocytosing dead cells, and then present those antigens on their surfaces. T-cells bind to the presented antigens to initiate a response, but this often happens away from the infected tissue in secondary lymphoid organs such as **lymph nodes**. The DCs also collect environmental danger signals, such as bacterial polysaccharides or molecules associated with necrosis, the presence of which they then communicate to the bound T-cells. There are many subpopulations of DCs, but we divide them into two broad categories: **immunogenic DC** that have seen a danger signal and **tolerogenic DC** that have not. Immunogenic DC cause T-cells to differentiate into **effector cells**, which fight infection, whereas tolerogenic DC cause T-cells to enter an unresponsive state called anergy [66].

Multiple T-cells can bind to a DC simultaneously and can interact with each other while bound. In particular, Tregs can suppress the activation of other T-cells that are bound to the same DC [57]. A Treg can prevent the activation, proliferation, and even survial of other T-cells, but all of these processes require the presence of the DC to mediate signals. This means that Treg activity is not necessarily antigen specific, as DCs may present more than one antigen simultaneously [43]. Prior models, such as [43], assumed that Tregs must therefore act uniformly on all T-cells in the lymph node. However, this is only true if we assume that all DCs present the same antigens in the same quantities.

2.1.2 Prior modeling

The question of how the immune system can simultaneously avoid autoimmunity while mounting a defensive immune response has rarely been approached by math modeling. However, there have been numerous models of autoimmune disease, immune tolerance, and, more generally, the activation of T-cells by DCs.

Some of the earliest models of autoimmune disease concerned the positive feedback inherent to **immunopathology**, disease caused by the immune system. When the immune system mounts a self reactive response, a danger signal is created by the resulting tissue damage, which then further stimulates the autoimmune response. The onset of diabetes is thought to be due to an initial trauma either during development [71] or due to viral infection [16] that can precipitate a self-sustaining autoimmune disease. Several groups [18, 47] have studied this system and demonstrated that the importance of this positive feedback in the early stages of the disease. Iwami et al. [37] made a more general, minimalistic model including only T-cells, tissue damage, and the level of target cells. They showed that this model could produce behavior characteristic of several different autoimmune diseases by simply changing the parameters. In particular, they found that they could reproduce the 'relapsing-remitting' behavior of multiple sclerosis. In this case, the levels of self reactive T-cells and target cells oscillate stably, with the self reactive T-cell population declining when there is no longer enough target antigen available to promote a response.

Several authors have extended the self immune response/target cell model to incorporate regulation by Tregs. Borghans and de Boer investigated the use of treatment of multiple-sclerosis (a T-cell mediated autoimmune disease of nerve tissue) with self reactive T-cells [11]. In their model, Tregs proliferate in response to the presence of effector T-cells. They showed that treatment with a small dose of effector T-cells could move the system from a naive state with a small number of Tregs to a 'vaccinated' state. This vaccinated state has an ongoing, subclinical immune response held in check by Tregs. Importantly, perturbation of the vaccinated equilibrium, such as by a large influx of T-cells or by antigen release, results in a much smaller immune response than the peturbation of the naive state. Alexander and Wahl [5] investigated different proposed mechanisms of Treg action. They found that the presence of Tregs has no impact on the initiation of an autoimmune response, but can limit its size. Magombedze et al. [45] had a similar finding when they modeled the role of Tregs in Type 1 Diabetes (T1D). In the progression of T1D, Tregs initially control an autoimmune response preventing the destruction of pancreatic β-cells, despite the presence of an ongoing immune response.

It is widely accepted that infectious disease can act as a trigger for autoimmune disease [16, 27]. Burroughs et al. [13] modeled the non-antigen-specific activation of autoreactive T-cells via growth factors secreted by foreign reactive T-cells during infection, a mechanism known as Bystander Activation. They found that at certain parameter values, the self reactive T-cell population has two stable equilibria. Bystander activation can move the system from the 'controlled' equilibrium to the uncontrolled, self-sustaining response, despite the activation of Tregs.

Our hypothesis is that the antigen specificity of Tregs is relevant as they can colocalize to the same DCs as effector T-cells with the same specificity. Therefore, it is necessary to explicitly model the multicell conjugates of T-cells and DCs. The formation of these conjugates is vital for both the activation of T-cells and their repression by Tregs. De Boer et al. [19] proposed a basic model for the interaction of DC and T-cells, with the primary goal of deriving a realistic T-cell growth rate. They assumed, as we do, that T-cells divide only when bound to DCs (or, equivalently, that proliferation is proportional to the amount of time spent bound), and so the growth rate of T-cells saturates with respect to both T-cells and DC. They generalized their model to include multiple different T-cell lineages binding to a single population of DCs. As there is finite binding space on the surface of a DC, the proliferation of a given T-cell lineage is indirectly limited by the presence of others. The T-cells that bind to DCs with the highest affinity dominate the population, generating an antigen-specific response. This framework was also used by [44] to investigate competition between Tregs and effectors. They found that competition for space is not strong enough for effective regulation and that Tregs must actively inhibit the growth of effectors. They assume that Tregs and effectors only interact on DCs in an antigen nonspecific manner. Leon and colleagues extend their model to include multiple lineages controlled by central tolerance [43]. They hypothesized that thymic selection ensured that self antigen would never be presented strongly, and so there could only be an immune response when a foreign antigen is present. They found that this behavior was only possible under strict assumptions on model parameters. Further analysis of this model [14] revealed that Tregs could suppress a T-cell population whose antigen is sufficiently common, but the result depended on initial conditions as the system is bistable.

2.1.3 Outline of our approach

In this paper, we have two objectives. First, we hypothesize that heterogenous antigen presentation by DC is necessary for the robust promotion of simultaneous immunity to foreign antigens and tolerance to self. This heterogeneity, which leads to some DC presenting

more self than others, may lead to tolerance either via tolerogenic DC, Tregs or both. To show this, we construct a minimal mathematical model of immune tolerance. We focus on the short-term initiation of an immune response during an infection, prior to either the clearance of disease by foreign reactive T-cells or the initiation of immunopathology. Therefore we assume that antigen availability in the tissues and presentation in lymph node remain constant.

The immune system has several, seemingly redundant, mechanisms of regulation, some or all of which we may select when creating a minimal model. Thus, the second objective in this paper is to investigate how each mechanism contributes to tolerance and how they work together. The steps we take are as follows:

- Introduce the modeling framework of T-cell and DC interaction used by [43] and discuss its basic behavior.
- Extend the model to tolerogenic DC, regulatory T-cells, and heterogenous self antigen presentation by DC. We represent thymic selection via the initial self reactive T-cell population size. These changes and extensions are modular and can be added in any combination.
- Evaluate each combination by its ability to produce a strong foreign response (immunity) while limiting the self response (tolerance) across a wide variety of possible antigenic environments.
- Adjust control parameters governing the relative importance of different Treg mechanisms, to test whether they are synergistic or redundant.

We then discuss the limitations of the model, as well as possible extensions and applications.

2.2 Model description

2.2.1 T-cell proliferation

The interaction of T-cells and DCs is crucial for the induction of both immune responses and tolerance. In this section, we will describe the binding of T-cells and their resulting proliferation. This model has been used before to study T-cell and Treg interaction [44] as well as in a more general setting of competition between different T-cell lineages [19].

Let T be the total number of T-cells of one lineage in a lymph node. Some of these T-cells are bound to DCs and others are free moving. We assume that there are N DCs with enough surface area to bind N_S T-cells each. Let $\bar{S} = NN_S$ be the total number of potential 'spots' for T-cells. The total number of bound and unbound T-cells are B and U, respectively, with

$$T = U + B \tag{2.1}$$

Bound T-cells divide at a rate γ. We assume that the death rate of T-cells within the lymph node is small compared to the rate of egress. Chemotaxis controls the trafficking of T-cells through the lymph node. Upon an initial contact with a DC, T-cells change the surface expression of certain chemotactic receptors, trapping themselves in the lymph node for several days until the expression level reverts [48]. We assume this expression reverts at a constant rate δ, regardless of whether or not they are bound, and that the T-cell immediately leaves.

$$\begin{aligned} \frac{dT}{dt} &= \gamma B - \delta T \\ &= (\gamma - \delta)B - \delta U \end{aligned} \tag{2.2}$$

When a T-cell comes in contact with a spot on a DC, S, it binds at a rate c. It unbinds at a rate $\mu = \lambda^{-1}$ where λ is the average duration of the T-cell:DC contact. Assuming mass action for the cellular interaction, the number of bound cells obeys

$$\begin{aligned} \frac{dB}{dt} &= cSU - \mu B \\ &= c(\bar{S} - B)U - \mu B \end{aligned} \tag{2.3}$$

We shall assume that the process of binding and unbinding is near equilibrium as this process is much faster than the rate of at which the T-cell populations change. The steady state of (2.3) gives an expression for B as a function of U.

$$B = \bar{S}\frac{c\lambda U}{1 + c\lambda U}$$

We substitute the above into (2.1) and (2.2) to get a differential-algebriac system for T and U.

$$\begin{aligned} \frac{dT}{dt} = f(U) &= (\gamma - \delta)\bar{S}\frac{c\lambda U}{1 + c\lambda U} - \delta U \\ T = g(U) &= U + \bar{S}\frac{c\lambda U}{1 + c\lambda U} \end{aligned} \tag{2.4}$$

The value $c\lambda$ is the affinity of a T-cell for a DC. Due to the assumption that (2.3) is near equilibrium, changing c has the same effect as changing λ. Throughout this paper, we shall assume (as in [43]) that c is fixed for all interactions but that λ may change for different T-cells. To avoid solving the DAE, we temporarily eliminate the variable T and write our equations with respect to the number of unbound T-cells, U. Differentiating (2.4) with respect to time yields $g'(U)\frac{dU}{dt} = f(U)$. Prior modeling papers [19, 44] have derived a

differential equation in terms of the more 'natural' variable T. Their methods, unlike ours, do not readily generalize to more T-cell and DC populations.

2.2.2 Multiple T-cell lineages

To exhibit tolerance and immunity, the model must include at least two lineages—one self reactive and one foreign reactive. To allow for this and the later introduction of Tregs, we will describe how to extend our model to an arbitrary number of lineages, indexed by j. Let T_j, U_j and B_j be the total, unbound and bound number, respectively, of T-cell lineage j and $\lambda_j = \mu_j^{-1}$ be its residence time on DCs (see Table 2.1).

For each j,

$$\frac{dB_j}{dt} = c(\bar{S} - \sum_k B_k)U_j - \mu_j B_j \tag{2.5}$$

which is analogous to (2.3) in the single lineage case. To find the steady state for the multilineage case, we set (2.5) equal to zero

$$B_j = c(\bar{S} - \sum_k B_k)\lambda_j U_j$$

where $\lambda_j = \mu_j^{-1}$. We then sum over all values of j and replace the subscript j with k, for clarity.

$$\sum_k B_k = c(\bar{S} - \sum_k B_k) \sum_k \lambda_k U_k$$
$$\sum_k B_k = \bar{S}\frac{c\sum_k \lambda_k U_k}{1 + c\sum \lambda_k U_k}$$

Therefore, the steady state is

$$B_j = \bar{S}\frac{c\lambda_j U_j}{1 + c\sum \lambda_k U_k}$$

For example, suppose we have two T-cell populations: 'self'($j = S$) and 'foreign' ($j = F$). At QSS,

$$B_S = \bar{S}\frac{c\lambda_S U_S}{1 + c(\lambda_S U_S + \lambda_F U_F)}$$
$$B_F = \bar{S}\frac{c\lambda_F U_F}{1 + c(\lambda_S U_S + \lambda_F U_F)}$$

This leads to the differential algebraic system

$$\frac{dT_S}{dt} = (\gamma - \delta)\frac{c\lambda_S U_S}{1 + c(\lambda_S U_S + \lambda_F U_F)} - \delta U_S$$
$$\frac{dT_F}{dt} = (\gamma - \delta)\frac{c\lambda_F U_F}{1 + c(\lambda_S U_S + \lambda_F U_F)} - \delta U_F$$

$$T_S = U_S + \bar{S}\frac{c\lambda_S U_S}{1 + c(\lambda_S U_S + \lambda_F U_F)}$$
$$T_F = U_F + \bar{F}\frac{c\lambda_S U_S}{1 + c(\lambda_S U_S + \lambda_F U_F)} \tag{2.6}$$

In general we have a pair of equations for each T-cell lineage.

$$\frac{dT_j}{dt} = (\gamma - \delta)\bar{S}\frac{c\lambda_j U_j}{1 + c\sum \lambda_k U_k} - \delta U_j$$
$$T_j = U_j + \bar{S}\frac{c\lambda_j U_j}{1 + c\sum \lambda_k U_k} \tag{2.7}$$

2.2.3 Central tolerance

We include central tolerance indirectly via initial conditions. We assume that any 'self' antigen may be presented in the Thymus, but a 'foreign' antigen is not. Thus, there will be fewer self reactive than foreign reactive precursors at the start of an immune reaction, as the self reactive T-cells tend to be deleted via negative selection (Figure 2.2). However, we can relax this assumption to model situations where the self antigen is not present in the thymus or to evaluate the other mechanisms by themselves. In general, we find that changing the initial conditions has only a small effect on the model outcome.

If a T-cell encounters its antigen in the Thymus it may differentiate into a Treg instead of dying. Thus, the other effect of central tolerance is the generation of self reactive regulatory T-cells. We always assume that there are no foreign reactive Tregs.

2.2.4 Equilibria of the multilineage system

The system (2.7) represents a regulation-free immune response. The only interaction between lineages is competition for space on DCs. In this section, we show that this system exhibits competitive exclusion so that only the T-cell population that binds the most strongly (with the largest λ_j) is present at equilibrium. We can assume that each lineage has a unique λ_j, as any populations that share a λ can be treated as a single population. We also include this analysis to demonstrate how the differential-algebraic system may be analyzed using conventional techniques.

When we put (2.6) in steady state, we find that for each j, either $U_j = 0$ or

$$1 + c\sum_k \lambda_k U_k = c\lambda_j \bar{S}\frac{\gamma - \delta}{\delta}$$

As all values λ_j are unique, this condition can only be met for a single j. At each steady state, all $U_j = 0$ except for one. Thus, each lineage has an equilibrium that it dominates completely, as $T_j = 0$ if and only if $U_j = 0$. The equilibrium value is given by

$$U_{jk} = \bar{S}\frac{\gamma - \delta}{\delta} - \frac{1}{c\lambda_j}$$

To analyze the stability of the system, we must first write our DAE as a first order ODE. We have equations of the form.

$$\begin{aligned}
\frac{dT_j}{dt} &= f_j(\mathbf{U}) = -\delta U_j + (\gamma - \delta)B_j(\mathbf{U}) \\
T_j &= g_j(\mathbf{U}) = U_j + B_j(\mathbf{U}) \\
B_j(\mathbf{U}) &= \bar{S}\frac{c\lambda_j U_j}{1 + c\sum_k \lambda_k U_k}
\end{aligned}$$

where $\mathbf{U} = \{U_j\}$. If we let $\mathbf{T} = \{T_j\}$ and $\mathbf{B} = \{B_j\}$, we can rewrite the system in vector form

$$\begin{aligned}
\frac{d\mathbf{T}}{dt} &= \mathbf{f}(\mathbf{U}) = -\delta\mathbf{U} + (\gamma - \delta)\mathbf{B}(\mathbf{U}) \\
\mathbf{T} &= \mathbf{g}(\mathbf{U}) = \mathbf{U} + \mathbf{B}(\mathbf{U})
\end{aligned}$$

We then rewrite this as a single equation

$$J_g(\mathbf{U})\frac{d\mathbf{U}}{dt} = \mathbf{f}(\mathbf{U})$$

where $J_g(\mathbf{U})$ is the Jacobian of $g(\mathbf{U})$ Alternatively,

$$\begin{aligned}
\frac{d\mathbf{T}}{dt} &= \mathbf{f}(\mathbf{g}^{-1}(\mathbf{T})) \\
&= \mathbf{h}(\mathbf{T})
\end{aligned} \tag{2.8}$$

In general, we cannot find $\mathbf{g}^{-1}$, but (2.8) is useful for linearizing the system near steady states. The linearization is the Jacobian of $\mathbf{h}$ evaluated at a steady state $\mathbf{U}^* = \mathbf{g}^{-1}(\mathbf{T}^*)$.

$$\begin{aligned}
J_h(\mathbf{T}^*) &= J_f(\mathbf{g}^{-1}(\mathbf{T}^*))J_{g^{-1}}(\mathbf{U}^*) \\
&= J_f(\mathbf{U}^*)J_g(\mathbf{U}^*)^{-1}
\end{aligned}$$

where $\mathbf{f}(\mathbf{U}^*) = 0$. Both $\mathbf{U}^*$ and $J_h(\mathbf{U}^*)$ can thus be calculated without inverting $\mathbf{g}$.

We have shown that (2.7) has solutions $\mathbf{U}_0 = 0$ as well as solutions $\mathbf{U}_j$ of the form

$$U_{jk} = \begin{cases} \bar{S}\frac{\gamma-\delta}{\delta} - \frac{1}{c\lambda_k} & k = j \\ 0 & k \neq j \end{cases} \tag{2.9}$$

To calculate the stability of the equilibria, we must calculate the eigenvalues of J_h at each equilibrium. Any such eigenvalue ν must satisfy

$$|J_f - \nu J_g| = 0$$

Given that $J_f = -\delta I + (\gamma - \delta)J_B$ and $J_g = I + J_B$ where J_B is the jacobian of $\mathbf{B}(\mathbf{U})$, we have

$$\nu = \frac{(\gamma - \delta)\sigma - \delta}{1 + \sigma}$$
$$0 = |J_B(\mathbf{U}^*) - \sigma I|$$

The upper triangular structure of J_B at all values for U^* allows for the eigenvalues to be calculated along the diagonal. We find that all eigenvalues of J_h, ν, are negative only for the critical point dominated by the lineage with the highest λ_j.

2.2.5 Tolerogenic DCs

The multilineage model is equivalent to the no-Treg case discussed in [43]. We find that the antigen with the highest value for λ_j always completely dominates the competition for space on DCs. As immunogenic DC may present autoantigens, an autoreactive T-cell clone may have the highest affinity for the DC during infection. To combat this, we divide our DCs into two populations. Immunogenic DCs work as discussed above. They come from the site of infection and present both self and foreign antigens. Tolerogenic DCs come from uninfected areas of the body and so we expect them to carry mostly self antigens (see Figure 2.3). T-cells that are bound to them will die rather than proliferate.

Let B_{Ij} and B_{Tj} be the number of j T-cells bound to immunogenic and tolerogenic DCs, respectively. Then for $j = S, F$,

$$\frac{dT_S}{dt} = \gamma B_{IS} - \omega B_{TS} - \delta T_S \tag{2.10}$$
$$\frac{dT_F}{dt} = \gamma B_{IF} - \omega B_{TF} - \delta T_F \tag{2.11}$$

Each lineage has different values of μ for immunogenic and tolerogenic DC, so

$$\frac{dB_{IS}}{dt} = c(\bar{S}p_I - B_{IS} - B_{IF})U_S - \mu_{IS}B_{IS}$$
$$\frac{dB_{TS}}{dt} = c(\bar{S}(1 - p_I) - B_{TS} - B_{TF})U_S - \mu_{TS}B_{IS}$$

where p_I is the proportion of DCs that are immunogenic. Solving for each B in steady state and substituting into (2.10)

$$\begin{aligned}\frac{dT_S}{dt} &= (\gamma - \delta)\bar{S}p_I \frac{c\lambda_{IS}U_S}{1 + c(\lambda_{IS}U_S + \lambda_{I,F}U_F)} \\ &\quad - (\omega + \delta)\bar{S}(1 - p_I)\frac{c\lambda_{TS}U_S}{1 + c(\lambda_{TS}U_S + \lambda_{TF}U_F)} - \delta U_S \\ \frac{dT_F}{dt} &= (\gamma - \delta)\bar{S}p_I \frac{c\lambda_{I,F}U_F}{1 + c(\lambda_{IS}U_S + \lambda_{I,F}U_F)} \\ &\quad - (\omega + \delta)\bar{S}(1 - p_I)\frac{c\lambda_{TF}U_F}{1 + c(\lambda_{TS}U_S + \lambda_{TF}U_F)} - \delta U_F\end{aligned}$$

As before, these must be closed with the T-cell conservation equations.

$$T_S = \bar{S} p_I \frac{c\lambda_{IS} U_S}{1 + c(\lambda_{IS} U_S + \lambda_{I,F} U_F)} + \bar{S}(1 - p_I) \frac{c\lambda_{TS} U_S}{1 + c(\lambda_{TS} U_S + \lambda_{TF} U_F)} + U_S$$

$$T_F = \bar{S} p_I \frac{c\lambda_{I,F} U_F}{1 + c(\lambda_{IS} U_S + \lambda_{I,F} U_F)} + \bar{S}(1 - p_I) \frac{c\lambda_{TF} U_F}{1 + c(\lambda_{TS} U_S + \lambda_{TF} U_F)} + U_F$$

2.2.6 Regulatory T-cells

Regulatory T-cells provide an additional mechanism of tolerance independent from Tolerogenic DC. We consider two different mechanisms of action by Tregs. 'Suppressive' Tregs limit proliferation by competing for growth signals with effectors, whereas 'Killer' Tregs permanently disable effectors, rendering them anergic [78]. As Tregs act nonspecifically, the terms governing these interactions always refers to the total number of Tregs bound to a particular DC.

We assume that there is only one population of Tregs and that they share a receptor with the self reactive T-cells. The rules governing the binding and unbinding of Tregs are thus the same as for self reactive effector cells.

$$B_{IR} = \bar{S}_I \frac{\lambda_{IS} U_R}{1 + c(\lambda_{IS}(U_R + U_S) + \lambda_F U_F)} \tag{2.12}$$

$$B_{TR} = \bar{S}_T \frac{\lambda_{TS} U_R}{1 + c(\lambda_{TS}(U_R + U_S) + \lambda_F U_F)} \tag{2.13}$$

All T-cells use the growth factor IL-2 to proliferate; however, only effector T-cells produce this cytokine. We assume that IL-2 is localized around individual DCs, so it is used either by the T-cell that secreted it or T-cells bound to the same DC [60]. Let I_i be the concentration of IL-2 around dendritic cell i, α_I be the production rate of IL-2 by a single T-cell, and k_E and k_R be the IL-2 consumption rates of effectors and Tregs, respectively.

$$\frac{dI_i}{dt} = \alpha_I \#\text{effectors bound to } i - (k_E \#\text{effectors bound to } i + k_R \#\text{Tregs bound to } i) I$$

We assume that IL-2 is in equilibrium and that the effective growth rate of each cell type is linearly proportional to the amount of IL-2 it consumes. For effector cells on DC i,

$$\hat{\gamma}_i = \gamma k_E I_i^* \tag{2.14}$$

$$= \gamma \frac{k_E \#\text{effectors bound to } i}{k_E \#\text{effectors bound to } i + k_R \#\text{Tregs bound to } i} \tag{2.15}$$

This expression depends only on the ratio of k_E to k_R, so we set $k_E = 1$. Constitutive

expression of the high affinity IL-2 receptor subunit CD25 is a defining characteristic of Tregs that distinguishes them from effector T-cells experimentally. Expression of CD25 increases IL-2 affinity by roughly a factor of 100 [1]; however, it is also transiently upregulated on activated effector T-cells. Furthermore, effector T-cells, as producers, may have better access to IL-2 than Tregs, which depend on diffusion from nearby cells. Therefore, we assume that $100 > k_R > 1$, but leave the exact value as a control parameter to be determined. The expression for per capita growth is

$$\begin{aligned}\hat{\gamma} &= \gamma \frac{\#\text{Producers}}{\#\text{Consumers}} \\ &= \gamma \frac{\#\text{effectors}}{\#\text{effectors}+\#\text{Tregs}}\end{aligned}$$

The binding model tells us the expected number of effectors and Tregs to find on a DC; however, not all DC are identical. The number of effectors and Tregs follow a hypergeometric distribution [44]. Rather than use the expected per capita growth rate from that distribution (see Appendix A), we use the following heuristic argument, which produces a close approximation to the analytic result. We present the argument with only one type of DC, as the process readily extends to multiple types. Let b_E and b_R be the proportion of DC spots filled by effectors and Tregs, respectively.

$$b_E = \frac{1}{\bar{S}} \sum_{\text{type}_j=\text{Eff}} B_j \tag{2.16}$$

$$b_R = \frac{1}{\bar{S}} \sum_{\text{type}_j=\text{Treg}} B_j \tag{2.17}$$

We consider a single, fixed T-cell that is bound to a DC. The per capita growth rate depends on the number of producers and consumers of IL-2 bound to the same DC, including the cell itself. The number of IL-2 consumers is the T-cell itself plus its expected number of neighbors. The number of producers is the expected number of effector neighbors plus itself if it is an effector.

$$\#\text{Consumers} = 1 + (N_S - 1)(b_E + b_R) \tag{2.18}$$

$$\#\text{Producers (if effector)} = 1 + (N_S - 1)b_E \tag{2.19}$$

$$\#\text{Producers (if Treg)} = (N_S - 1)b_E \tag{2.20}$$

In addition to suppressing proliferation, Tregs may also indirectly kill or anergize Tregs on the same DC. They do this through a number of mechanisms often mediated via the DC itself [78]. We assume that Treg-mediated effector killing occurs according to mass action between the two cell types bound to the same DC, $\beta \frac{(N_S-1)}{N_S} b_E b_R$, as experiments

with nonlinear functions showed little difference in behavior (not shown). The parameter β controls the rate of Treg killing.

The differential equations for the Treg System are

$$\begin{aligned}\frac{dT_F}{dt} &= (\hat{\gamma}_{IE}(\mathbf{U}) - \delta)B_{IF}(\mathbf{U}) - (\hat{\gamma}_{TE}(\mathbf{U}) - \delta)B_{TF}(\mathbf{U}) - \delta U_F \\ \frac{dT_S}{dt} &= (\hat{\gamma}_{IE}(\mathbf{U}) - \delta)B_{IS}(\mathbf{U}) - (\hat{\gamma}_{TE}(\mathbf{U}) - \delta)B_{TS}(\mathbf{U}) - \delta U_S \\ \frac{dT_R}{dt} &= (\hat{\gamma}_{IR}(\mathbf{U}) - \delta)B_{IR}(\mathbf{U}) - \delta U_R\end{aligned} \tag{2.21}$$

with constraints

$$\begin{aligned}T_F &= U_F + B_{IF}(\mathbf{U}) + B_{TF}(\mathbf{U}) \\ T_S &= U_S + B_{IS}(\mathbf{U}) + B_{TS}(\mathbf{U}) \\ T_R &= U_R + B_{IR}(\mathbf{U}) + B_{TR}(\mathbf{U})\end{aligned}$$

where $\mathbf{U} = [U_F, U_S, U_R]^T$. Table 2.2 summarizes the per capita growth rates ($\hat{\gamma}$) of bound effectors and Tregs. Note that Tregs are not affected either way by tolerogenic DC.

2.2.7 Heterogeneous DC populations

Although Tregs are antigen specific, their inhibitory functions are not. The only way for an effector T-cell to avoid Tregs is to avoid binding to DCs, meaning that they also fail to proliferate. This is only a problem if we assume that all DCs are identical. If some DCs present more self antigen than others, then they will bind a greater proportion of self reactive Tregs and effector cells. Foreign reactive T-cells will bind to different dendritic cells with fewer Tregs.

To model this, we let Λ_S and Λ_F be random variables. Each DC represents an independent sample of these random variables. Let λ_{iS} and λ_{iF} be the value of Λ_S and Λ_F on DC i. $B_{i,j}$ is expected number of T-cells of type j on DC i.

$$\begin{aligned}B_{iS} &= \frac{c\lambda_{iS}U_S}{1 + c(\lambda_{iS}(U_S + U_R) + \lambda_{iF}U_F)} \\ B_{iR} &= \frac{c\lambda_{iS}U_R}{1 + c(\lambda_{iS}(U_S + U_R) + \lambda_{iF}U_F)} \\ B_{iF} &= \frac{c\lambda_{iF}U_F}{1 + c(\lambda_{iS}(U_S + U_R) + \lambda_{iF}U_F)}\end{aligned}$$

Our system now includes a summation over all DCs.

$$\frac{dT_S}{dt} = -\delta U_S + \sum_i \hat{\gamma}_{iE}B_{iS}$$

$$\frac{dT_R}{dt} = -\delta U_R + \sum_i \hat{\gamma}_{iR} B_{iR}$$
$$\frac{dT_F}{dt} = -\delta U_F + \sum_i \hat{\gamma}_{iE} B_{iF}$$

Although this allows us in principle to make every DC unique, we study a single case with just two DC categories; simulations with scaled beta-distributed λ show that the two category case captures the key behavior (results not shown). The two values for λ represent a switch like behavior for binding duration as a function of an underlying variable, such as the amount of a particular antigen to which the DC is exposed. This agrees with some experiments [36] and biophysical modeling [6].

Let $\phi_S \in [0, 1]$ be the probability that a DC collects and presents antigen S. On those DCs, the T-cell:DC interactions are stable and long lasting. On the remaining DCs, bound T-cells unbind quickly.

$$p_{\Lambda_S}(\lambda_S) = \begin{cases} \phi_S & \lambda_{\max} \\ 1 - \phi_S & \lambda_{\min} \end{cases} \tag{2.22}$$

We shall refer to this as the heterogenous case. The expected value of Λ_S is $E[\Lambda_S] = \lambda_{\min} + \phi_S(\lambda_{\max} - \lambda_{\min})$. If we ignore the variability in DCs and set $\lambda_{iS} = E[\Lambda_S]$ for each i, then this model reduces to (2.21), which we will refer to as the homogenous case. Table 2.3 explicitly defines these two cases. In the heterogenous case, we use the homogenous term for immunogenic DCs presenting foreign antigen. We do this to avoid having a large population of activated DCs that have not collected foreign antigen while still allowing the foreign antigen to be rare. This modification does not significantly change the results.

2.2.8 Outputs of the model

We wish to measure the strength of the foreign reactive immune response and the self reactive immune response. Each T-cell has three possible fates. It can become part of the immune response, be killed or deactivated, or leave and continue to circulate to other lymph nodes. The last possibility occurs if the T-cell does not make sufficient contact with a DC. We designate 'activated' T-cells to be those that have spent sufficient time bound in order for them to divide once. We call other T-cells 'naive'. Let $N_j = p_{N,j} T_j$ and $A_j = (1 - p_{N,j}) T_j$ be the number of naive and activated T-cells of type j, respectively.

Activation status has no effect on binding, unbinding, or death rates. The rate of activation is exactly the rate of proliferation, as T-cells activate upon their first division.

$$\frac{dT_j}{dt} = \text{Proliferation} - \text{Death} - \text{Leaving}$$

$$\frac{dN_j}{dt} = -p_{N,j}(\text{Proliferation} + \text{Death} + \text{Leaving})$$
$$\frac{dA_j}{dt} = 2p_{N,j}\text{Proliferation} + (1 - p_{N,j})(\text{Proliferation} - \text{Death} - \text{Leaving})$$

The 'proliferation' terms for the jth T-cell are $\sum_i \eta_{ij} B_{ij}$ where η_{ij} is the per capita growth rate with $\beta = 0$ and $\omega = 0$ (see Table 2.2). As $p_{N_j} = \frac{T_j - A_j}{T_j}$, we have

$$\frac{dA_j}{dt} = 2\frac{T_j - A_j}{T_j} \sum_i \eta_{ij} B_{ij} + \frac{A_j}{T_j}\frac{dT_j}{dt} \tag{2.23}$$

Finally, C_j is the number of activated T-cells that have left the lymph node.

$$\frac{dC_j}{dt} = \delta A_j. \tag{2.24}$$

$C_S(t_{\text{final}})$ and $C_F(t_{\text{final}})$ represent the total number of activated T-cells that have left the lymph node after t_{final} days.

2.3 Results

Our goal is not to match specific data sets, but to examine how the various mechanisms contribute to immune tolerance. An ideal model of immune tolerance should allow for a strong response to foreign antigens while avoiding or limiting a response to self. Additionally, this behavior should be robust to initial conditions as well as the relative prevalence of the antigens and level of infection.

We assume that self antigens are presented equally on immunogenic and tolerogenic DC: $\phi_S = \phi_{S,I} = \phi_{S,T}$. Foreign antigens are only presented by immunogenic DC $\phi_F = \phi_{F,I}$ and $\phi_{F,T} = 0$. We vary two parameters: the proportion of DC presenting the self antigen, ϕ_S, and the proportion of DC that are immunogenic, p_I. Changing these **situational parameters** allows us to evaluate the maintenance of tolerance to a variety of different types of self antigens, as well as different intensities of infection. We refer to four different situations, for which we choose different values of p_I and ϕ_S.

1. A rare self antigen ($\phi_S = 0.1$) that is presented primarily during infection, meaning that all relavant dendritic cells are immunogenic ($p_I = 1$). These 'cryptic' antigens are often involved in autoimmune disease [58] (Figure 2.4).
2. A more common antigen ($\phi_S = 0.5$) that is presented on immunogenic and tolerogenic DC equally ($p_I = 0.5$). (Figure 2.5)
3. A cryptic self antigen that ($p_I = 0.8$), when presented, appears on a large number of immunogenic DC ($\phi_S = 0.9$).
4. A very common self antigen ($\phi_S = 0.8$) that appears slightly more often on immuno-

genic than tolerogenic DC ($p_I = 0.6$)

These last two situations test the limits of our model (see Appendix B). In addition to changing these situational parameters, we can also change initial conditions. For all simulations, we start with a total of 1000 effector cells and, if applicable, 80 Tregs. Unless otherwise stated we will use 'even' initial conditions, with 500 self effectors and 500 foreign effectors. Occasionally, we will use 'self skewed' initial conditions with one foreign and 999 effectors and 'foreignskewed' initial conditions with 1 self and 999 foreign effectors.

Throughout the results section, we compare three different types of Tregs (absent, suppressive or killer Tregs) and two different types of DC population (homogenous or heterogenous) to give a total of six different model combinations. We can further refine the killer Treg model by varying two **control parameters**: the strength of Treg-induced effector T-cell death, β, and the relative affinity of Tregs for IL-2, k_R. We assume that these values are innate properties of the immune system and do not change in response to situational parameters.

We judge the success or failure of a particular model in a particular situation in several ways. First, we calculate the final count for each type of T-cell (see 2.2.8). We call the ratio of foreign to self in the final count the **specificity** of the response. This single number does not reveal the size of the response, so we set two additional criteria: that the number of foreign cells exceed 10000 (immunity) and that the number of self cells be less than the initial population of self cells (tolerance). We use the cut off of 10000 because it allows us to graphically distinguish between different models, not because the number holds any biological significance.

2.3.1 Heterogenous DCs improve Treg efficacy

To assess the effect of Tregs in the absence of tolerogenic DC, we first compared the models with $\phi_S = \phi_F$, $p_I = 1$ and equal initial condition (500 self and 500 foreign effectors). Figure 2.4 shows the number of activated T-cells as a function of time for each of the six models. Self and foreign reactive effector T-cells behave identically in the homogenous case. This should be expected as they have the same binding and unbinding rates to the DC and so the two populations are indistinguishable. With homogenous DC, the Tregs kill both self and foreign effectors indiscriminately but cannot wipe either out as they are dependent on the effectors for growth factor. This system exhibits a limit cycle analogous to a predator prey model.

In the heterogenous case, there are always more foreign than self T-cells, because immunogenic DC still present the foreign antigen homogenously (Table 2.3). When we

add Tregs that only compete for IL-2 (Figure 2.4E), the population tends towards 100% foreign reactive T-cells, but there is an initial window during which some self reactive T-cells are activated. The addition of killer Tregs (Figure 2.4F) decreases the number of self reactive T-cells produced to below the initial condition of 500. The Tregs also initially lower foreign reactive numbers, but this is only transient. Once the self reactive T-cells are cleared, the foreign reactive population rebounds. If we start with one self effector and 999 foreign effectors, the initial transient disappears.

2.3.2 Tolerogenic DCs favor foreign reactive responses

Without regulation by Tregs or tolerogenic DC, the population that binds most strongly to DC will dominate the response. If $\phi_S > \phi_F$, then self T-cells bind more strongly to DC on average so we expect a purely self reactive response in the absence of regulation. Figure 2.5 shows the time series when $\phi_S = 5\phi_F = 0.5$, but 50% of DC are tolerogenic. In all cases, there is a robust foreign response and essentially no self response. The addition of tolerogenic DC can change a self reactive response into a primarily foreign reactive one.

In this situation, Tregs are not required for tolerance and actually decrease the total output of foreign reactive T-cells in all cases, inhibiting the immune response. The effect is much larger for homogenous (Figure 2.5 B,C) Tregs than heterogenous (Figure 2.5 E,F) and for killer (Figure 2.5 C,F) Tregs than nonkiller Tregs (Figure 2.5 B,E).

2.3.3 A heterogenous DC population is more robust to changing immunogenicity and initial conditions

We compare the robustness of each model by changing the initial conditions and numbers of tolerogenic DC. For this experiment, we let $\phi_F = \phi_S = 0.1$. We measure the strength of the self and foreign response by counting the number of activated T-cells leaving the lymph node. Figure 2.6 shows the counts of foreign (red), self (blue dashed), and regulatory (blue dotted) T-cells as a function of the proportion of DCs that are immunogenic (p_I). In both the homogenous and heterogenous cases, foreign T-cells outnumber self T-cells if there are roughly equal numbers of immunogenic and tolerogenic DCs. With too many tolerogenic DCs, the immune response is extremely small. With too few, the immune response contains large numbers of self reactive T-cells. Killer Tregs mitigate the latter effect in the presence of heterogenous DCs. In general, greater diversity of the DC population, either via heterogeneity or intermediate p_I, increases the ratio of foreign to self T-cells.

The initial conditions, shown as pale red and blue lines in Figure 2.6, can play a large role. The bottom row of Figure 2.6, for example, has initial conditions of 999 self T-cells and one

foreign T-cell. These lopsided initial conditions skew the outcome towards autoimmunity in the homogenous case. In this case the system is bistable, so the outcome depends strongly on initial conditions. In the heterogenous case, both lineages can coexist as they each have their own spatial resource. This change from bistability to coexistence decreases the sensitivity to initial conditions.

2.3.4 Killer Tregs have the largest effect for rare self antigens and bias the system toward tolerance

So far, we have assumed that the rare antigen and self antigen overall appear at the same rate on immunogenic DC. During an immune response a self antigen may be more (or less) common than the foreign antigen. To study this condition, we vary ϕ_S and fix $\phi_F = .1$. For each set of values of the parameters ϕ_S and p_I, we calculate the specificity of the immune response and evaluate immunity and tolerance. Figure 2.7 shows the results of this experiment for each model. The darker red color corresponds to a higher specificity. The solid and dashed lines indicate boundaries of areas with tolerance and immunity, respectively. The regions marked IT are those that have both properties. For large numbers of tolerogenic DC, all models behave similarly for most parameter values. With few tolerogenic DC (high p_I) and moderate ϕ_S, the heterogenous killer Treg model performs the best according to all measures. On the other hand, this same model does not perform well compared to the others for moderate p_I and high ϕ_S. This is an example of high levels of regulation causing the immune system to 'err on the side of caution' as tolerance is achieved, but only a weak immune response. However, if we increase the prevalence of the foreign antigen, ϕ_F, then the immune response is restored even for the killer Treg model (data not shown).

2.3.5 IL-2 competition and direct killing work in synergy

To study the best combination of IL-2 competition and killing by Tregs, we vary the two control parameters k_R and β. We then evaluate the model specificity, immunity, and tolerance for the four different values of our situational parameters. Figure 2.8 shows the specificity using a color scale and divides the parameter space into regions with tolerance (T), immunity (I), and both (IT). The blue dot indicates the value of k_R and β that we chose for our simulations. For three of the four situations it lies within the IT region and for the fourth, it has both tolerance and a high degree of specificity. Although there are other parameter combinations that have a qualitatively similar outcome, we note that Tregs must have both a heightened affinity for IL-2 and an ability to kill, or mediate the killing

of, effectors.

2.4 Discussion

We have created a simple model of immune tolerance, featuring only four cell types: effector T-cells, regulatory T-cells (Tregs), and immunogenic and tolerogenic dendritic cells (DCs). T-cells bind to DCs that present their cognate antigen, proliferating when bound to immunogenic DC and apoptosing when bound to tolerogenic DC. Tregs inhibit effector cells antigen-nonspecifically by altering the microenvironment around individual DCs. Heterogeneity of antigen presentation by DCs allows Tregs to preferentially inhibit T-cells that share antigen-specificity. We sought a model that would exhibit a strong response to foreign antigens and a weak response to self antigens under a wide range of antigen expression profiles. We assume self and foreign antigens differ in two important ways. First, immunogenic DC present a mixture of self and foreign antigens, but tolerogenic DC primarily present self antigens. Second, due to presentation of the self antigen in the thymus, there will be an initial population of self reactive Tregs. We find that tolerogenic DC promote tolerance to common self antigens, whereas Tregs promote tolerance to rarer self antigens. In addition, we find that Tregs perform better when they can both actively kill effectors and inhibit their proliferation.

The different types of DC heterogeneity prevent autoimmune responses to different kinds of self antigens. Tolerogenic DC prevent immune responses to ubiquitous self antigens, as we assume that tolerogenic DC will present such antigens in large numbers. We find that immunity and tolerance are maintained in the absence of Tregs when there are significant numbers of tolerogenic DC, but that Tregs improve the specificity. Tregs are crucial for tolerating slightly less common antigens, which may appear on few tolerogenic DC. Self antigens that are primarily presented during infection fit this profile. To be effective, Tregs must be able to kill effector T-cells and DCs must present self antigen heterogenously. The model fails to tolerate extremely common antigens that are not presented on tolerogenic DC. Without Tregs, there is typically a failure of tolerance and response specificity. Response specificity can be restored by Tregs, but the result is generally an abrogated immune response.

Central tolerance plays two distinct roles in this model. First, we assume the existence of self reactive Tregs of thymic origin. Second, negative selection in the thymus reduces the number of self reactive naive T-cells. Central tolerance thus initially biases the system away from self reactivity. Our model is not generically bistable, so the initial bias is irrelevant to

the final outcome. Including any positive feedback, such as autoimmune-related pathology that can promote further self reactive T-cells through a tissue damage, could increase the importance of initial conditions and thus central tolerance.

We did not explore the dynamics of this model, such as the limit cycles in Fig. B.1. Cyclic T-cell populations have been observed in autoimmune diabetes [46]. Although the time scales are different from what we observe in our model, it seems plausible that Tregs are driving this cycle as they have been implicated in controlling the early development of the disease [15]. The limit cycle involves two populations: foreign effectors and self Tregs, so the Tregs are exerting nonspecific control. This may be an important feature of the immune system as even foreign reactive T-cells can cause cell damage, which can in turn lead to autoimmunity [27]. Therefore, it makes sense that all T-cell responses, even foreign reactive ones, should be controlled by Tregs.

The model could be extended naturally to simulate multiple infections over a period of several years with a portion of the response to one infection becoming the initial conditions for the next. This type of model could help explain epidemiological patterns in autoimmune diseases that have a lengthy progression. One such pattern is the apparent protection from multiple sclerosis when moving from high latitude to low latitude. Several studies have found that only migration during childhood significantly lowers incidence rate; however, the age of onset is typically after 30 [2, 42]. The development of MS must therefore take several decades and so any mathematical model used to study it must take this longer timescale into account.

Molecular mimicry, bystander activation and epitope spreading are common mechanisms for the initiation of autoimmune disease [27]. In molecular mimicry, the pathogen presents an antigen that is nearly identical to a self antigen. According to our model, it would not be possible to have both immunity and tolerance in this situation as the self and foreign T-cell population would be a single population that reacts to both self and foreign. However, if we also include a second foreign reactive T-cell lineage that does not also respond to self, this case is identical to those already studied. We would see an immune response only towards the foreign antigen that does not mimic self. Bystander activation is the nonspecific activation of T-cells, some of which may be self reactive, during an immune response. This could be modelled with an extremely large number of T-cells that have $\phi = 0$. A preliminary run of this situation shows that this can significantly delay an effective immune response, although we have not explored how this may lead to autoimmune disease.

Epitope spreading is implicated in numerous animal models of autoimmune disease [27]

particularly multiple sclerosis [49]. In this process, immunogenic DC present multiple self antigens in addition to the primary foreign antigen leading to an autoimmune response. This autoimmune response leads to further damage and the presentation of different self antigens, which spreads the autoimmune response to a different target. Our model explicitly addresses this issue, and we find that a sufficient number of tolerogenic DC prevent the initial spread of autoimmunity. However, we have not included immunopathology, the damage caused by the immune system itself, which could potentially allow a transient autoimmune response to become self-sustaining by decreasing the number of tolerogenic DC. Similarly, chronic inflammation can trigger autoimmune disease. For example, the chronic inflammatory disorder Crohn's Disease is a major risk factor for Ankylosing Spondylitis, a form of degenerative autoimmune arthritis [12]. In NOD mice, a model for Type 1 diabetes, viral infection speeds up disease progression only if there is already pancreatic inflammation [33].

The inverse of autoimmune disease is the tolerance of exogenous antigens. The human body provides a home to hundreds of species of commensal micro-organisms that we continuously tolerate, in addition to the many antigens that we eat and inhale. The tolerance to antigens in the gut is thought to involve tolerogenic DC and Tregs [76]. This process is conceptually similar to the tolerance of self as harmless exogenous antigens should not be accompanied by a danger signal. The main difference is that the Tregs do not differentiate in the thymus, but rather secondary lymphoid organs during a response. CD4 T-cells can differentiate into several effector subtypes including induced Tregs or iTregs. The other subtypes include Th1, Th2, and Th17. In lymphoid tissues of the gut, there may simultaneously be antigens from pathogenic bacteria, commensal bacteria, and food. These antigens may all require different types of T-cell response. For example, IgA antibody, produced during a Th2 response, keeps commensal bacteria from invading epithelial cells [52]. There have been several models of T-cell subtype differentiation [24, 72, 79], but none of them allow for distinct responses to distinct antigens. Extending any of these models to include DC heterogeneity may be sufficient to achieve this.

Immunological processes exist on a variety of scales: the molecular level of antigen recognition, the cellular level of T-cell activation and differentiation, the systemic level of an adaptive immune response and self tolerance, and even the population level of herd immunity. Mathematical models can link these levels, predicting outcomes at one based on hypotheses at another. Models that can reliably trace cellular and molecular behavior to the systemic level should prove invaluable in the treatment of immune disorders and

provide basic insight into how the immune system works. In this paper, we have evaluated a variety of cellular mechanisms thought to induce systemic tolerance. Our model allowed us to distinguish the roles played by tolerogenic DC and Tregs and even between Tregs that mediate killing of effectors and those that merely compete for resources. The distinct mechanisms provide a patchwork of partially overlapping protection, in which different components are best suited to combating different threats. Such models may help us understand the evolutionary history of the immune system. The evolutionary perspective may be key to understand much of the seemingly unnecessary complexity of the immune system.

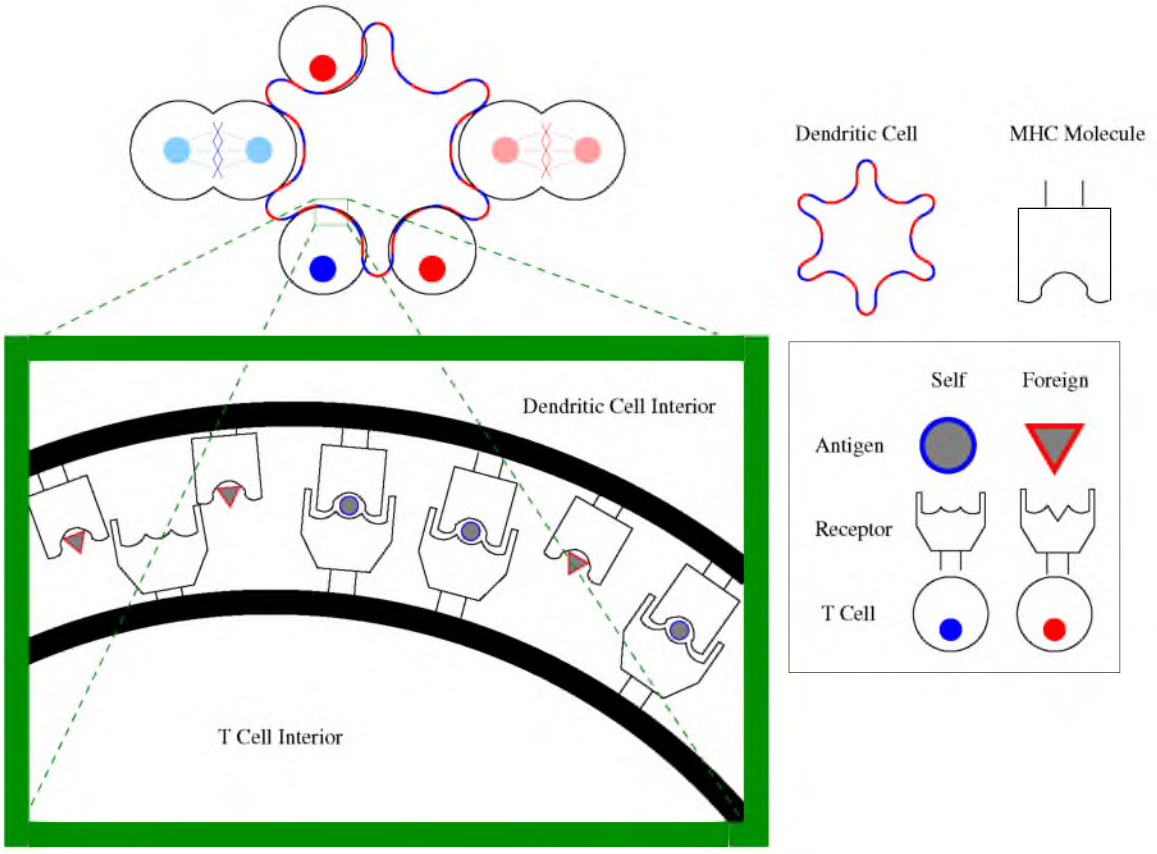

Figure 2.1: Interaction of DC with T-cell. Different T-cell lineages respond to different antigens presented on the DC surface. Zoomed in region shows the molecular interactions of receptors on the self surface. The binding affinity of self (blue) and foreign (red) T-cells is determined by the amount of complementary antigen presented on the surface of the DC. A single DC may present multiple different antigens simultaneously and therefore bind T-cells from multiple lineages.

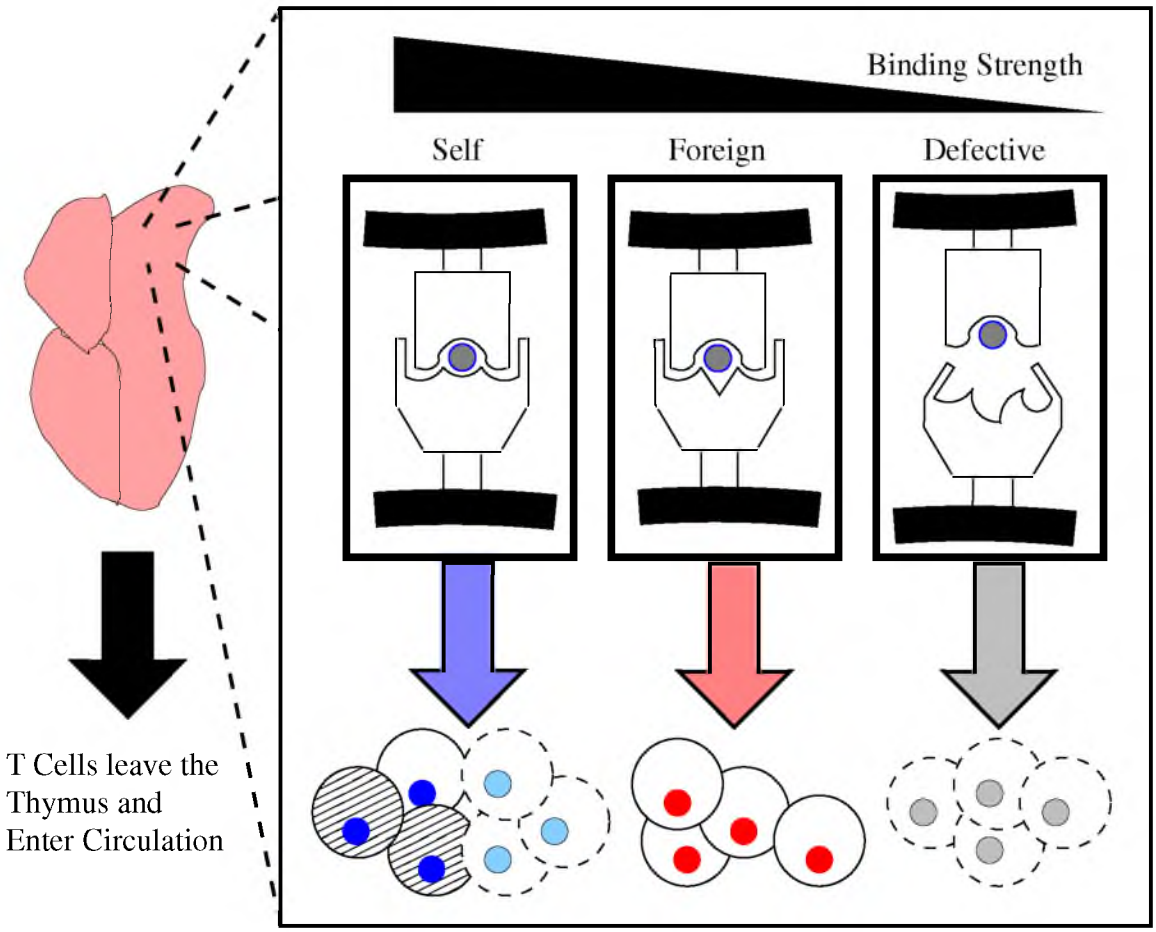

Figure 2.2: Possible outcomes of central tolerance in the thymus. All T-cell lineages bind self antigens in the thymus. Those that bind strongly are either deleted or become Tregs, with only a few mistakes entering circulation. Those that bind weakly are deleted. Those that bind with intermediate strength enter circulation as effector T-cells.

Table 2.1: Variable names and parameters values used in this chapter

Symbol	Description	Value
T_j	T-cells of type j	
U_j	T-cells of type j not bound to any lymph node	
B_{ij}	T-cells of type j bound to DC of type i	
b_E	Probability that a DC spot is occupied by an effector	
b_R	Probability that a DC spot is occupied by an Treg	
$\bar{S}_i$	Total number of spots on DC type i	
γ	Growth rate of T-cells	5 days^{-1}
δ	Leaving rate of T-cells	1 day $^{-1}$
ω	Death rate of T-cells on Tolerogenic DC	5 days^{-1}
β	Strength of Treg killing	1.2 days^{-1}cells^{-1}
k_E	Relative IL-2 affinity of effectors	1
k_R	Relative IL-2 affinity of Tregs	3
N_S	Number of T-cell binding spots per T-cell	10
N	Number of DCs	1000
p_I	Proportion of DCs which are immunogenic	0-1
c	Treg:DC binding rate	20 days^{-1} cells^{-1}
λ	Treg:DC contact duration	.0005-.05 days
ϕ_{ij}	Relative Treg:DC contact strength	0-1
t_{final}	Duration of infection	10 days

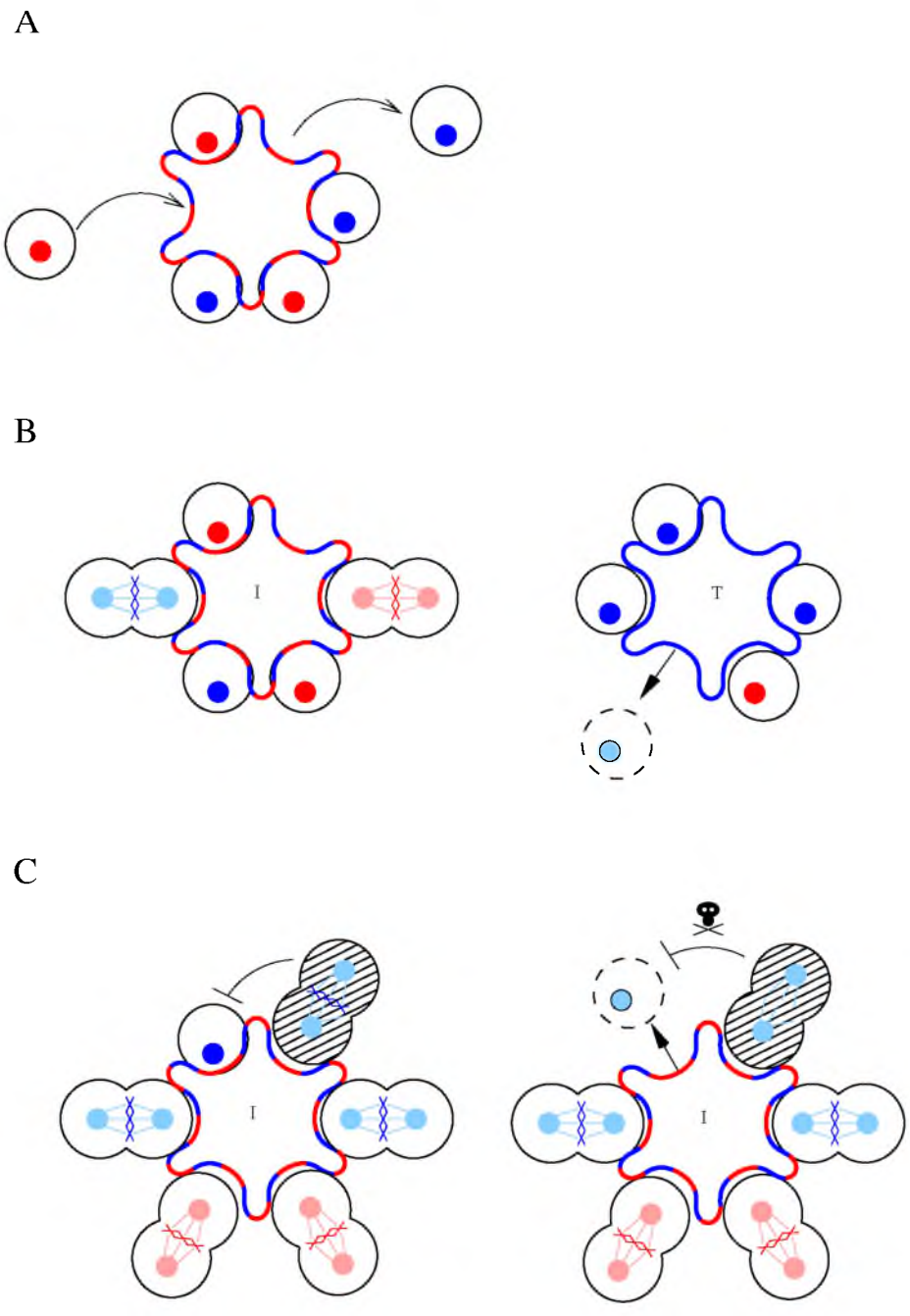

Figure 2.3: Potential outcomes of interactions between DC and T-cells. Immunogenic DC (I) carry both self and foreign, so we depict them as multicolored. Tolerogenic DC (T) carry mostly self are shown in blue. We indicate Tregs with diagonal shading. T-cells bind and unbind to spots on DCs (A). T-cells bound to immunogenic DC proliferate, and T-cells bound to tolerogenic DC deactivate (B). Suppresive Tregs prevent T-cells from proliferating, whereas killer Tregs actively kill or deactivate T-cells (C).

Table 2.2: Per Capita Growth Rates of Bound T-cells ($\hat{\gamma}$)

	Immunogenic	Tolerogenic
Effectors	$\gamma\frac{1+(N_S-1)b_{IE}}{1+(N_S-1)(b_{IE}+b_{IR})} - \beta b_{IR}(N_S-1)$	$-\omega - \beta b_{TR}(N_S-1)$
Tregs	$\gamma\frac{(N_S-1)b_{IE}}{1+(N_S-1)(b_{IE}+b_{IR})}$	0

Table 2.3: Binding affinities of self and foreign T-cells

		Immunogenic		Tolerogenic	
		Affinity	Probability	Affinity	Probability
Homogenous	Foreign	$\lambda_{\min} + \phi_{IF}(\lambda_{\max} - \lambda_{\min})$	1	$\lambda_{\min} + \phi_{TF}(\lambda_{\max} - \lambda_{\min})$	1
	Self	$\lambda_{\min} + \phi_{IS}(\lambda_{\max} - \lambda_{\min})$	1	$\lambda_{\min} + \phi_{TS}(\lambda_{\max} - \lambda_{\min})$	1
Heterogenous	Foreign	$\lambda_{\min} + \phi_{IF}(\lambda_{\max} - \lambda_{\min})$	1	$\lambda_{\max}$	ϕ_{TF}
				$\lambda_{\min}$	$1 - \phi_{TF}$
	Self	$\lambda_{\max}$	ϕ_{IS}	$\lambda_{\max}$	ϕ_{TS}
		$\lambda_{\min}$	$1 - \phi_{IS}$	$\lambda_{\min}$	$1 - \phi_{TS}$

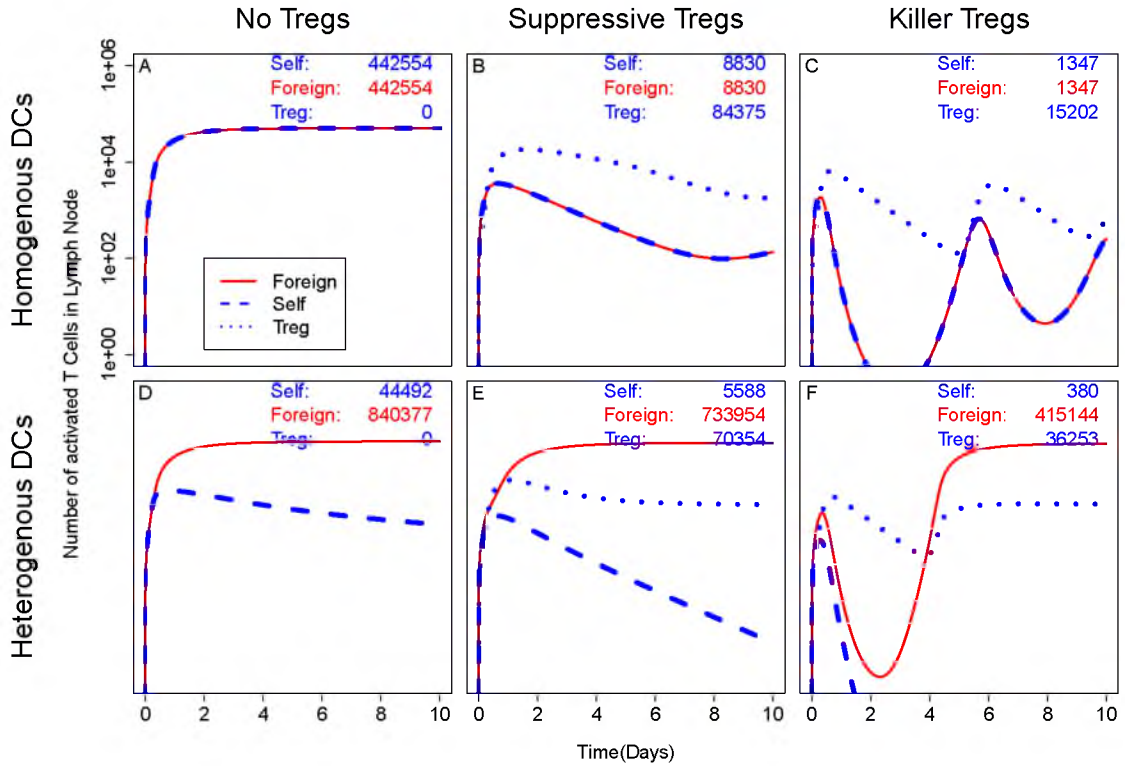

Figure 2.4: Activated T-cells versus time (days) for foreign (red), self (blue dashed), and Treg (blue dotted) in the absence of tolerogenic DC. Each panel represents a different model. The numbers in each plot represent the total number of effector cells of each type that leave the lymph node. Parameters: $\phi_S = 0.1$, $\phi_F = 0.1$, $p_I = 1$

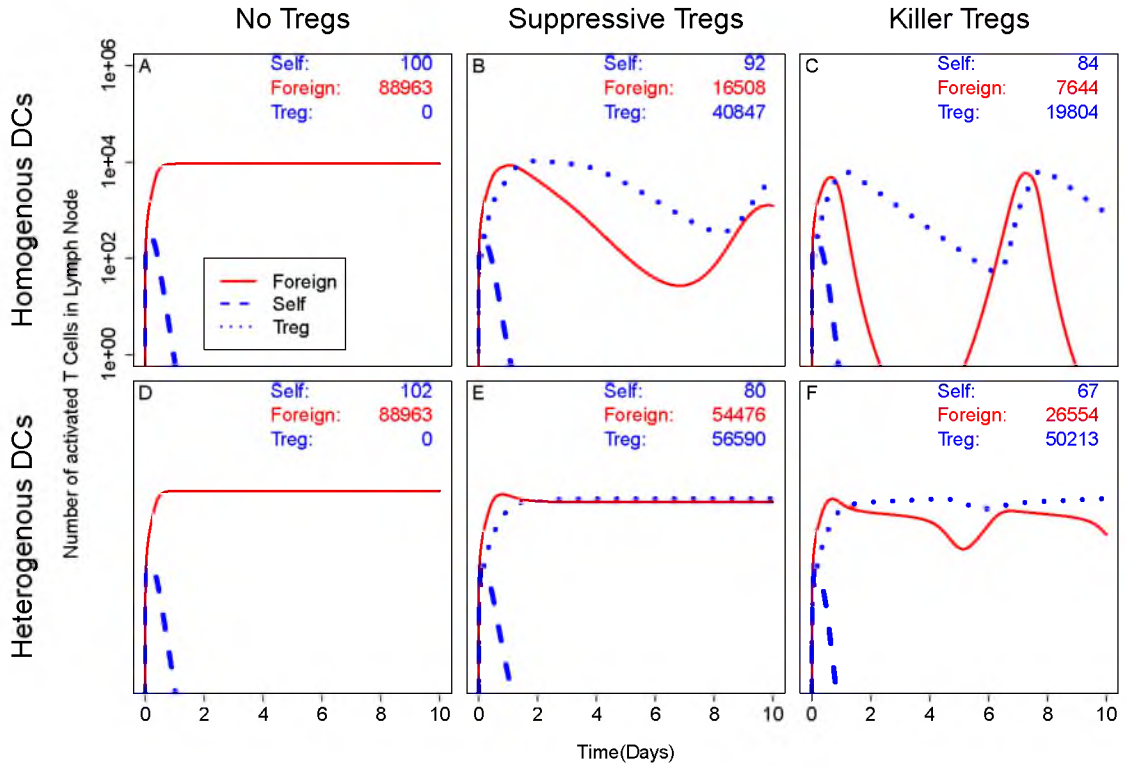

Figure 2.5: Activated T-cells versus time (days) for foreign (red), self (blue dashed), and Treg (blue dotted) with 50% of DC tolerogenic. Each panel represents a different model. The numbers in each plot represent the total number of effector cells of each type that leave the lymph node. Parameters: $\phi_S = 0.5$, $\phi_F = 0.1$, $p_I = 0.5$, $\beta = 1.25$, $k_R = 3$

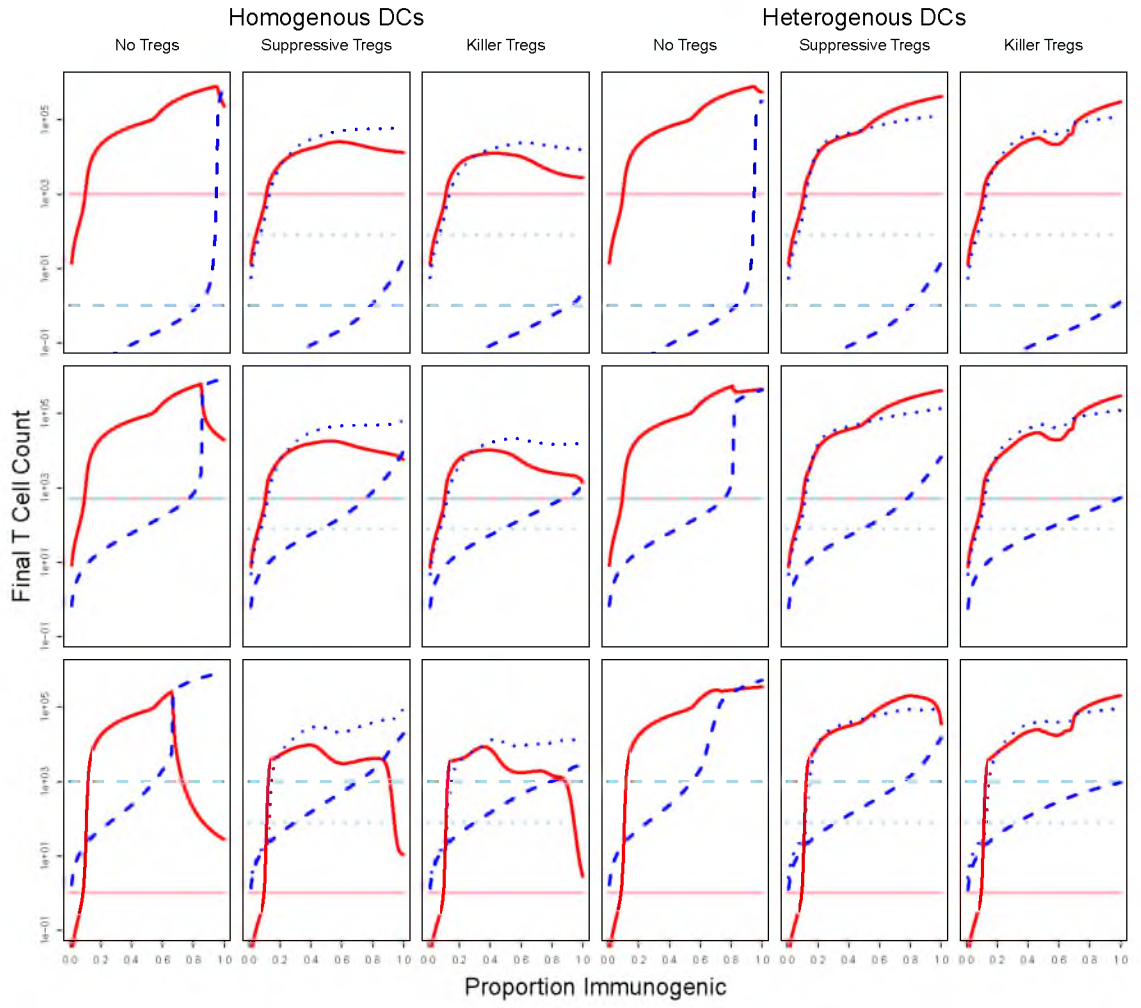

Figure 2.6: Comparison of model performance for different values of p_I (proportion immunogenic DC) and different initial T-cell counts. In each plot the vertical axis is the final number of T-cells of each type and the horizontal axis is p_I. Each column is a different model and each row a different set of initial conditions: 999f vs 1s, 500f vs 500s, 1s vs 999f. If Tregs are present then their initial condition is 80. The solid red lines represent foreign effector T-cells; the dashed and dotted blue lines represent self effector and Tregs, respectively; the corresponding tinted flat lines indicate the initial conditions for each population. Parameters: $\phi_S = 0.1$, $\phi_F = 0.1$, $\beta = 1.25$, $k_R = 3$

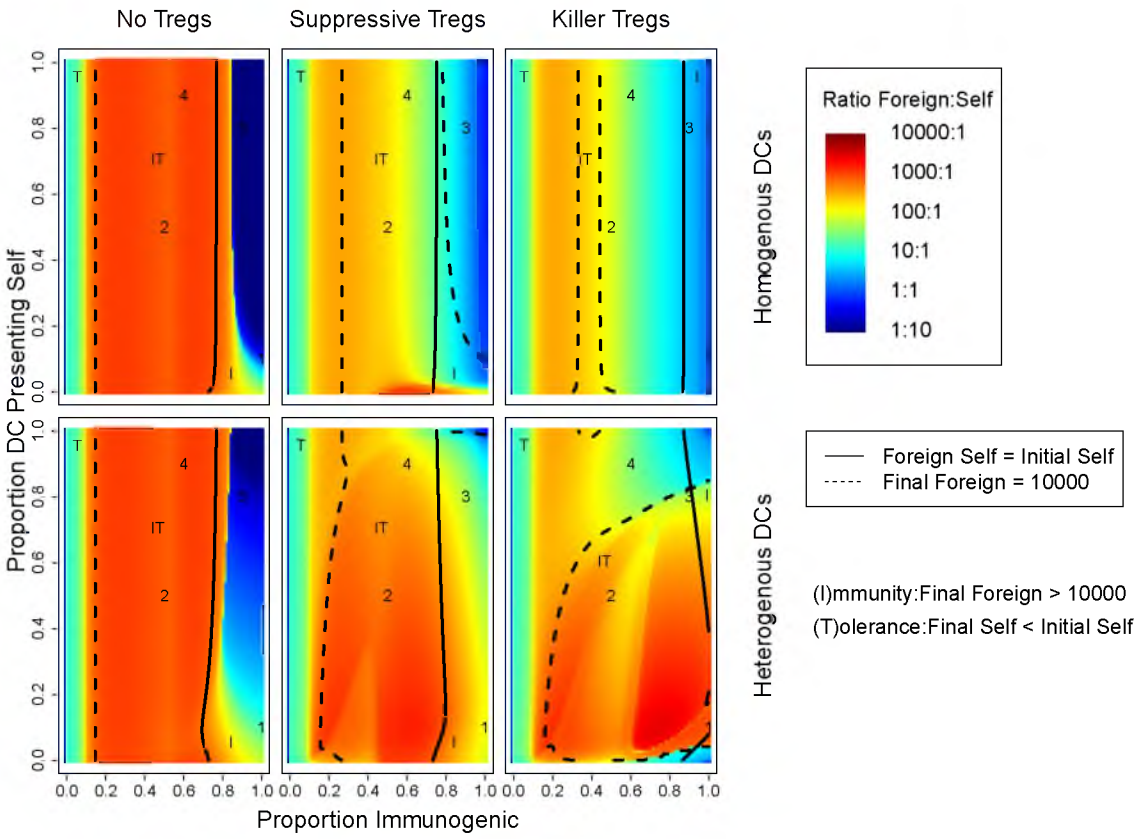

Figure 2.7: Comparison of model performance for different values of ϕ_S (self antigen presentatation by DC) and p_I (proportion DC immunogenic). Color scale represents the ratio of foreign reactive to self reactive T-cells generated during the immune response. The darker red color indicates a higher ratio of foreign to self. The dotted (foreign = 10000) and solid (self = 500) are isoclines for the final T-cell counts that delineate regions of immunity and tolerance respectively. In immune regions (I), the size of the foreign response is at least 10000 cells strong. In tolerant regions (T), the size of the self response is less than the initial number of self T-cells (500). Regions denoted IT show where both conditions are met. In blank regions, neither condition is met. Parameter values used for time series are marked 1-4. Parameters: $\phi_F = 0.1$, $\beta = 1.25$, $k_R = 3$

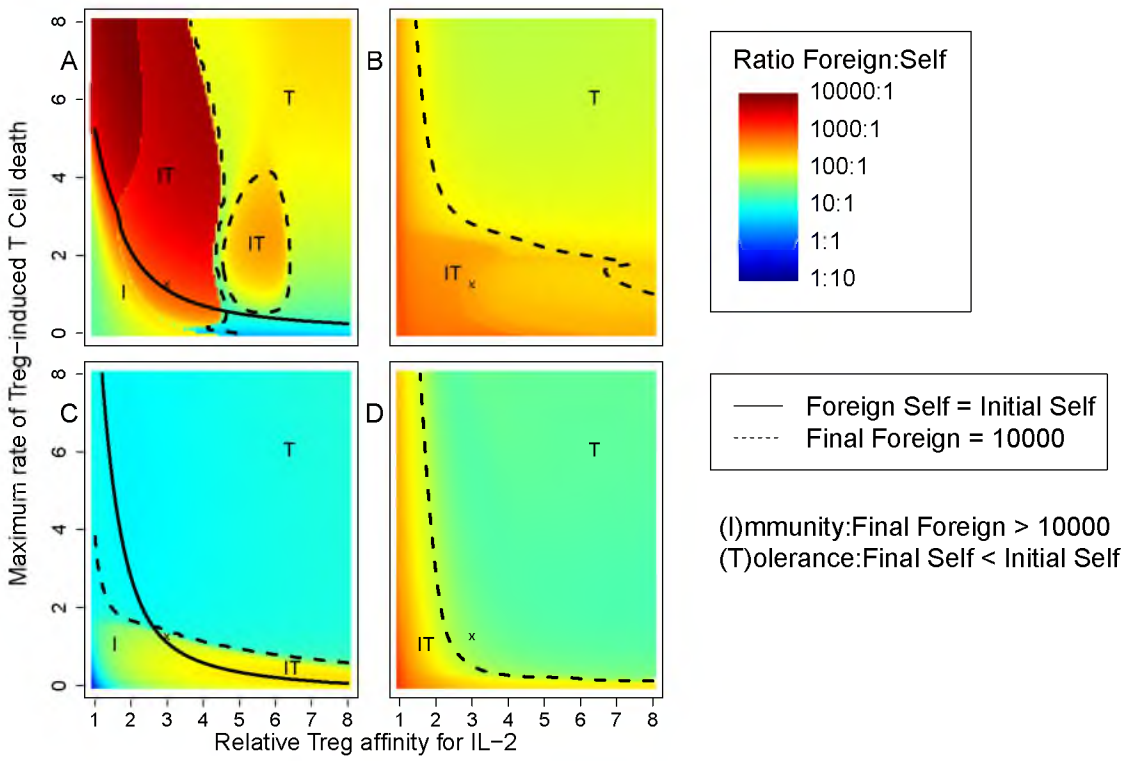

Figure 2.8: Comparison of model efficacy for different values of the Treg parameters k_R (relative affinity for IL-2) and β (strength of Treg-mediated effector killing). Each panel corresponds to a different set of situational parameters corresponding to numbers 1-4 in 2.7. Color denotes model specificity and parameter regions are divided into regions of tolerance(T), immunity(I), both (IT), and neither (blank).

CHAPTER 3

MATHEMATICAL MODEL OF TYPE 1 DIABETES IN THE NOD MOUSE

3.1 Introduction

In the previous chapter, we developed a generic model of immune regulation by Tolerogenic dendritic cells (DC) and regulatory T-cells (Tregs). We show that such regulation could prevent or limit the proliferation of self reactive T-cells under the a variety of immunological circumstances. In that model, we assume that the antigen presentation and immunogenicity of DC is constant. More importantly, we assume that it is independent of the ensuing immune response. Although this may be a reasonable assumption for a short-lived infection, it should break down when we consider a chronic disease. In this chapter, we develop a model of such a chronic disease, Type 1 diabetes, and we shift our focus from the dynamics within a lymph node to those at the site of infection, the pancreas. We investigate the role of immune-regulation in its nominal progression and in its potential treatment.

3.1.1 Biological background

Type 1 diabetes (T1D) is an autoimmune disorder in which T-cells invade the islets of langerhans within the pancreas and kill insulin producing β-cells. The nonobese diabetic or NOD mouse is an inbred mouse strain that spontaneously develops T1D. Among females, the age of onset is on average 12-16 weeks, with an incidence of 60-80%. Prior to T1D onset, at 3-4 weeks of age, immune cells such as CD4 T-cells, CD8 T-cells, and macrophages invade the islets. This infiltration, called **insulitis**, gradually becomes more severe, affecting more islets and penetrating more deeply (see Figure 3.1). It is present in all NOD mice, even those that do not develop T1D.

NOD mice exhibit multiple immune problems. For an extensive review, see [8]. Here we focus on a few key differences from the wild type, which may mimic the factors that lead to genetic susceptibility in humans. First, there is a **failure in central tolerance** as

NOD mice do not effectively present peptides from the proinsulin gene in the thymus. This leads to the generation of a population of proinsulin reactive lymphocytes, although these T-cells typically have a low affinity for their target T-cell antigen. These T-cells are the first detected in the pancreas during immunopathogenesis and eventually give way to other more reactive T-cell clones. However, the anti-proinsulin response appears to be required [25, 82]. In humans, T1D is associated with lower expression of insulin in the thymus [38]. Second, NOD mice have a **defect in the clearance of apoptotic cells**. Specifically, this is a defect in **macrophages**, an antigen nonspecific immune cell with a large number of jobs, including the clearance of dead cells and the activation of T-cells. The excess apoptotic cells can become necrotic and trigger an inflammatory response by macrophages. This defect is particularly important at the time of weaning when the pancreas undergoes structural changes and heightened apoptosis [71]. This **apoptotic wave** and subsequent inflammation initiates an immune response, and T-cells start to infiltrate the pancreas (see Table 3.1). Finally, NOD mice have a **defect in the growth and survival factor IL-2**. Despite its role as a T-cell growth factor, deficiency in IL-2 typically leads to uncontrolled growth of effector T-cells as IL-2 is required for the proliferation and survival of Tregs. Tregs can control the development of T1D in the NOD mouse for several months, and T1D is greatly accelerated in Treg-deficient NOD mice [15, 20]. Human T1D patients have impaired IL-2 signaling via a defect in the high affinity IL-2 receptor [38].

It is unclear what causes T-cells to escape the regulation of Tregs and destroy β-cells. The simplest hypothesis is that the destruction of β-cells within the islets is ongoing, but that T1D is not diagnosed until the β-cell mass reaches a critical level. However, quantification of the β-cell mass shows that it does not start to decline until 8-12 weeks of age [4], 6-10 weeks after the apoptotic wave [71]. Ablation of Tregs in 4-6-week old mice leads to rapid T1D onset [20], indicating that Tregs are required to prevent disease progression. This suggests that Tregs possibly lose effectiveness over time. This hypothesis is supported by the work of Tritt et al. [69], who find that older mice have similar numbers of Tregs, but they are less able to control T1D than those of young adult mice, and Pop et al. [55], who find that Tregs from older mice have a loss of function *in vitro*. Another possibility is that β-cells gradually lose function over time. It may be that the β-cells degranulate, losing their ability to produce insulin, [3] or simply apoptose [31, 68] in response to increased demands. Finally, the delay may be due to the time it takes for the development of a population of T-cells capable of killing β-cells. In the early stages of insulitis, the most important population of T-cells is **CD4s**, or helper T-cells, which can

activate other components of the immune sytem, but not directly kill target cells. Another population of T-cells, **CD8s** or killer T-cells, is very efficient at killing target cells, but require additional activation. In the early stages of T1D in NOD mice, the CD8 population is generally insulin-specific with a low affinity. After several weeks, high affinity CD8s, specific to islet-specific glucose-6-phosphate catalytic subunit related protein (IGRP), take their place. The destruction of β-cells corresponds to the expansion of this population [7].

Almost all NOD mice develop insulitis, and yet many do not develop T1D. Trudeau et al. [70] find signficant differences in the makeup of the CD8 T-cell population between those that get T1D and those that do not. In particular, CD8 T-cells specific for the islet antigen IGRP are at much higher levels in the 'prediabetic' mice, although they do not appear until week 8 in either group [70]. Fu et al. [26] perform MRIs of mice at different ages and find that the degree of inflammation is significantly greater in the mice destined for T1D. At 6 weeks, inflammation of the pancreas is significantly correlated with the eventual development of T1D. They also find that the mice with lower inflammation expressed higher levels of CRIg, a marker of a class of regulatory macrophages. Taken together, these studies suggest that the eventual fate of an individual mouse is predetermined at the initiation of insulitis. The nature of the insulitis of each mouse should therefore fall into at least two classes, which can be distinguished by the presence of CRIg-expressing macrophages. Islets with more severe inflammation have a greater level of β-cell turnover and therefore a greater presentation of IGRP. This ultimately leads to a greater IGRP CD8 response and T1D.

3.1.2 Prior modeling

As discussed above, the initiation of T1D requires a proinflammatory stimulus, which, in the NOD mouse, likely occurs during weaning. Nerup and colleagues [53] propose a nonmathematical description of T1D initiation, the 'Copenhagen Model', which is not specific to NOD mice. The stimulating event, such as a virus, causes minor β-cell destruction and, more importantly, releases β-cell antigens triggering an immune cascade. De Blasio et al. [18] proposed a simple model of 4 ODEs (resting and activated macrophages, β-cell antigen and T-cells) to reproduce this phenomenon. The model is intentionally generic and does not describe any particular environmental insult. They find that the activity of Macrophages is key and that the nature of the T-cell response does not drive inflammation. Maree et al. [47] expanded upon this model and incorporated the ideas of Trudeau [71]: that NOD mice have a reduced ability to clear apoptotic β-cells that then become necrotic. They find that for NOD mice, the system is bistable; the wave of apoptosis transfers the system from a resting 'healthy' state to a 'disease' state.

Regulatory T-cells play an important role of slowing the progression of T1D and other autoimmune diseases. Alexander et al. [5] study a generic model of the Treg-controlled autoimmune disease. They demonstrate that Tregs may not eliminate an autoimmune response, but can reduce it to a subclinical level. Similarly, Magombdze et al. incorporate Treg control into the framework of the Copenhagen/Maree models and find that Tregs cannot eliminate the autoimmune response, but can reduce its intensity so that the β-cell population is barely affected. See the previous chapter for a more complete review of Treg models.

Leah Keshet and colleagues have investigated the dynamics of the CD8 population in a series of papers. The time series of the IGRP CD8 population in [70] appears cyclical. Mahaffy, Keshet et al. [46] model this phenomenon using multiple T-cell compartments: 'activated' T-cells can become either effectors and memory cells (which can later become activated upon restimulation). Their model reproduces the observed cycle and the β-cells die off step-wise during each cycle until none remain. Khadra, Keshet et al. [40] investigate the competition between low-affinity and high-affinity CD8s. High-affinity CD8s kill β-cells, releasing antigens and perpetuate the immune response, whereas low-affinity CD8s simply crowd the environment. This leads, fairly robustly, to a bistable system that has a 'healthy' state with few high-affinity CD8s and a 'diseased' state with many.

3.1.3 Outline of our approach

We seek a simple model that

1. has two possible outcomes, a 'T1D' state and an 'insulitis but no T1D' state;
2. develops T1D predominantly within a narrow time window; and
3. is initially under the control of a Treg population, which it subsequently escapes.

We propose a model of T1D development that proceeds in two stages. An 'initiation' phase corresponding to the development-driven apoptosis and a 'progression' phase describing the increase in the number and reactivity of the islet-specific CD8 population. The initiation phase has two distinct outcomes corresponding to distinct stable equilibria: **mild-insulitis**, which does not lead to progression, and **severe-insulitis**, which does. These two states are characterized by differences in the makeup of the macrophage population, the ratio of infiltrating Tregs to effector T-cells, and the cytokine milieu of the islet. We show how various treatments can shift the system from the severe insulitis state to the mild. The 'progression' phase is a feedforward model. Activated macrophages stimulate the growth of the CD8 population, which in turn kill β-cells causing a rise in blood glucose. Only in

the severe insulitis state do the activated macrophages promote a sufficient growth in CD8 cells to promote T1D development.

We then validate this model by simulating various treatments of NOD mice found in the literature and comparing the results. To replicate incidence data, we must have heterogeneity in the mouse population. We generate this heterogeneity by changing the initial number of activated macrophages and the death rate due to CD8s, which we assume are quite variable. The justification for this is that they are the result of complicated processes (see [47] and [40], respectively) that can have multiple outcomes in otherwise identical organisms. We add a small amount of noise to all other parameters. We then perform a sensitivity analysis to investigate which parameters are key for the development of T1D. Specifically, we are interested in those that lead to an acceleration or delay of T1D versus those that change the incidence. Finally, we propose some further extensions and some possible experiments to further validate the model.

3.2 The initiation model

3.2.1 Activation of macrophages

Macrophages are among the first cells to infiltrate the islet in NOD mice [38], likely in response to an apoptotic wave of β-cell death during weaning (the 'apoptotic wave', see [71]). As explored in [47], NOD macrophages are inefficient at clearing these apoptotic cells, which leads to further inflammation and β-cell death. Here, we shall assume that the apoptotic wave has just passed, resulting in an initial excess of macrophages.

Tissue-resident macrophages are a type of innate immune cell, meaning non-antigen-specific, with an incredibly wide array of potential behaviors. They phagocytose other cells, act as antigen presenting cells (APCs) and control the behavior of neighboring cells, both immune and nonimmune, via the release of cytokines. They are critical in the initiation and continuation of immune responses and yet they can also act as 'custodians', clearing away debris from dead cells. These regulatory activities correlate with the expresion of the receptor CRIg on a macrophages surface. CRIg expression is promoted by the regulatory molecule IL-10 and inhibited by the inflammatory molecule IFN-γ as well as other inflammatory molecules such as arachidonic acid [30]. Importantly, the expression of CRIg by pancreatic macrophages is negatively correlated with the progression to T1D [26]. Both IL-10 and IFN-γ are **cytokines**: diffusing, extracellular molecules used for communication between cells, typically of the immune system.

We assume there are two classes of Macrophage: inflamatory macrophages (M^*), corresponding to low CRIg expression, which can stimulate the activation and proliferation of

T-cells, and regulatory macrophages (M), corresponding to high CRIg expression which act primarily as phagocytes. Macrophages can switch back and forth in response to external signals from cytokines. All macrophages enter the pancreas at a rate J in the regulatory class. They activate to become inflammatory at a basal rate a_0, but their activation rate can be greatly enhanced by IFN-γ. Likewise, inflammatory macrophages deactivate at a basal rate b_0, and their deactivation rate is enhanced by IL-10.

$$\begin{aligned}
\frac{dM^*}{dt} &= aM - bM^* - \delta M^* \\
\frac{dM}{dt} &= J - aM + bM^* - \delta M \\
a &= a_\gamma \frac{I_\gamma^2}{k_\gamma^2 + I_\gamma^2} + a_0 \\
b &= b_{10} \frac{I_{10}^2}{k_{10}^2 + I_{10}^2} + b_0
\end{aligned}$$

IFN-γ is produced by TH1 effector CD4 T-cells (T) in response to IL-12, a product of inflammatory macrophages. We let T^* denote the population of effector T-cells expressing IFN-γ. IL-10 is produced by CD4 Tregs (R). Pancreatic Tregs in NOD mice overexpress IL-10, so we assume that the entire population expresses IL-10 without the need for further stimulation.

$$\frac{dT^*}{dt} = c\frac{I_{12}^2}{k_{12}^2 + I_{12}^2}(T - T^*) - eT^* \tag{3.1}$$

$$\frac{dI_\gamma}{dt} = \alpha_\gamma T^* - \omega_\gamma I_\gamma \tag{3.2}$$

$$\frac{dI_{12}}{dt} = \alpha_{12} M^* - \omega_{12} I_{12} \tag{3.3}$$

$$\frac{dI_{10}}{dt} = \alpha_{10} R - \omega_{10} I_{10}, \tag{3.4}$$

where c is the rate at which T-cells are activated by IL-12 and e is the rate at which they revert to resting. Cytokine i is produced at a rate α_i and decays at rate ω_i. We assume that all cytokine concentrations equilibriate rapidly. Therefore, we set (3.3)-(3.4) equal to zero, and solve for the equilibrium concentrations. This yields the three-dimensional ODE:

$$\begin{aligned}
\frac{dM^*}{dt} &= -\delta_M M^* + \big(a_\gamma F(\nu_\gamma T^*) + a_0\big) M - \left(b_{10} F(\nu_{10} R) + b_0\right) M^* \\
\frac{dM}{dt} &= J - \delta_M M - \big(a_\gamma F(\nu_\gamma T^*) + a_0\big) M + \left(b_{10} F(\nu_{10} R) + b_0\right) M^* \\
\frac{dT^*}{dt} &= cF(\nu_{12} M^*)(T - T^*) - eT^*
\end{aligned} \tag{3.5}$$

where

$$F(x) = \frac{x^2}{x^2+1}$$
$$\nu_i = \alpha_i/\omega_i k_i.$$

3.2.2 Analysis of equilibria

The equilibria of (3.5) are given by

$$T^* = C(M^*_{eq})T = \frac{cF(\nu_{12}M^*_{eq})}{e + cF(\nu_{12}M^*_{eq})}T$$
$$M = \frac{J}{\delta_M} - M^*_{eq}$$
$$M^* = M^*_{eq}$$

where M^*_{eq} satisfies

$$\begin{aligned} M^*_{eq} &= \frac{J}{\delta_D}\frac{A(M^*_{eq},T)}{\delta_D + B(R) + A(M^*_{eq},T)} \\ A(M^*_{eq},T) &= a_\gamma F(\nu_\gamma T C(M^*_{eq}) + a_0 \\ B(R) &= b_{10}F(\nu_{10}R) + b_0. \end{aligned} \tag{3.6}$$

(3.6) represents a fifth degree polynomial, whose coefficients alternate signs. Therefore we expect it to have 1, 3, or 5 positive real roots. For any parameter choice, the number and value of these equilibria will depend on the state variables T and R, whose dynamics are discussed in the next section.

With our parameter values (see Table 3.2) there are either 1 or 3 solutions, depending on the values of T and R. For fixed R and small values of T, as in Figure 3.2A, there is only one solution with few inflammatory macrophages. This agrees with the observation that CD4s are required for the initiation of T1D [8]. There is also only one solution for large values of T, corresponding to large numbers of inflammatory macrophages. For intermediate values of T, there is both the inflamed and noninflamed solutions, separated by an unstable threshold solution.

3.2.3 Tregs and effectors compete in the islet

During the progession of T1D, T-cells infiltrate the pancreatic islets. Cytotoxic CD8 T-cells directly kill β-cells, but the CD4 population also plays a role by maintaining an inflammatory environment that perpetuates the immune response. The CD4 population, also called helper T-cells, is often divided into two broad categories: effector T-cells and regulatory T-cells, which respectively promote or obstruct immune responses. T1D does not develop in NOD mice in the absence of CD4 effectors. With effectors present but not

Tregs, the disease develops much faster, indicating that they also play an important role [15].

Effectors and Tregs enter the islet at a rate of α_T and α_R, respectively. Although there are other populations of antigen presenting cells in the pancreas, we assume that T-cells are dependent upon interaction with macrophages in order to proliferate. This is equivalent to assuming that other APC population numbers are correlated with those of inflammatory macrophages. The maximum per-capita growth rate should therefore occur when there are very few T-cells relative to macrophages as the competition for binding space will be minimal. The decrease in proliferation rate as T-cell numbers increase has been observed in vivo [67]. For simplicity, we model this process as a Michaelis-Menten rate with the inflammatory macrophage acting analagously to an enzyme. We let σ denote the maximum proportion of T-cells undergoing mitosis and γ denote the exponential growth rate of those dividing cells. The maximum possible growth rate of the T-cell population is therefore $\gamma\sigma$.

The IL-2-BCL-2 pathway controls apoptosis of T-cells in the islets [67]. Secreted IL-2 promotes the expression of the antiapoptotic factor BCL-2 in T-cells. Tregs are dependent upon effectors for IL-2, whereas effectors are self sufficient. NOD mice are deficient in IL-2, leading to increased turnover in Tregs but not effectors [67]. Therefore, we assume that T-cells die at a constant rate δ_{T1} but that Tregs will die at an enhanced rate $\delta_{T1} + \delta_{T2}$ in the absence of IL-2. Effectors secrete IL-2 at a rate α_2 and it is taken up by Tregs at a rate ω_2. In addition, we include an input $u(t)$ representing IL-2 treatment.

$$\begin{aligned}
\frac{dT}{dt} &= \alpha_T + \gamma_T \frac{\sigma_T M^* T}{M^* + \sigma_T T + \sigma_R R} - \delta_{T1} T \\
\frac{dR}{dt} &= \alpha_R + \gamma_R \frac{\sigma_R M^* R}{M^* + \sigma_T T + \sigma_R R} - \left(\delta_{T1} + \delta_{T2} \frac{k}{k + I_2}\right) R \\
\frac{dI_2}{dt} &= \alpha_2 T - \delta_2 I_2 - \omega_2 I_2 R + u(t)
\end{aligned}$$

Putting the cytokine concentration in steady state,

$$\begin{aligned}
\frac{dT}{dt} &= \alpha_T + \gamma_T \frac{\sigma_T M^* T}{M^* + \sigma_T T + \sigma_R R} - \delta_{T1} T \\
\frac{dR}{dt} &= \alpha_R + \gamma_R \frac{\sigma_R M^* R}{M^* + \sigma_T T + \sigma_R R} - \left(\delta_{T1} + \delta_{T2} \frac{k_R R + 1}{Q(t) + k_T T + k_R R + 1}\right) R
\end{aligned} \tag{3.7}$$

where $Q(t) = u(t)/k\delta_2$ is the scaled IL-2 treatment, $k_T = \alpha_2/k\delta_2$ the scaled IL-2 production rate and $k_R = \omega_2/\delta_2$ the scaled uptake by Tregs. Equation (3.7) and (3.5) together make up the initiation model.

3.2.4 Analysis of the initiation model

To simplify the analysis of this model, we consider the case $\alpha_T = \alpha_R = 0$ with $Q(t) = Q$. The system (3.7) then becomes

$$0 = \gamma_T \frac{\sigma_T M_{eq}^* T}{M_{eq}^* + \sigma_T T + \sigma_R R} - \delta_{T1} T$$
$$0 = \gamma_R \frac{\sigma_R M_{eq}^* R}{M_{eq}^* + \sigma_T T + \sigma_R R} - \left(\delta_{T1} + \delta_{T2} \frac{k_R R + 1}{Q + k_T T + k_R R + 1} \right) R$$

which has four solution branches: the trivial solution $T_0 = R_0 = 0$, a 'T-only' solution with

$$T_1 = \frac{\gamma_T \sigma_T - \delta_{T1}}{\sigma_T \delta_{T1}} M_{eq} \tag{3.8}$$
$$R_1 = 0 \tag{3.9}$$

an 'R-only' solution satisfying

$$T_2 = 0 \tag{3.10}$$
$$0 = \gamma_R \frac{\sigma_R M_{eq}^*}{M_{eq}^* + \sigma_R R_2} - \left(\delta_{T1} + \delta_{T2} \frac{k_R R_2 + 1}{Q + k_R R_2 + 1} \right) \tag{3.11}$$

and a 'coexistence' solution satisfying

$$0 = \gamma_T \frac{\sigma_T M_{eq}^*}{M_{eq}^* + \sigma_T T_3 + \sigma_R R_3} - \delta_{T1} \tag{3.12}$$
$$0 = \gamma_R \frac{\sigma_R M_{eq}^*}{M_{eq}^* + \sigma_T T_3 + \sigma_R R_3} - \left(\delta_{T1} + \delta_{T2} \frac{k_R R_3 + 1}{Q + k_T T_3 + k_R R_3 + 1} \right) \tag{3.13}$$

Each of these solutions exist for α_T,$\alpha_R > 0$; however, only the coexistent solution is guaranteed to remain positive. The other three solutions are positive if and only if they are stable. Recalling that M_{eq}^* represents the solution of a 5th degree polynomial whose coefficients depend on T and R, we cannot directly solve this system. However, if we view M_{eq}^* as a parameter, we can implicitly solve for R, T and a parameter of our choice to create bifurcation diagrams.

First we vary k_T (Figure 3.3A) to simulate different levels of IL-2 production by NOD mice. At the current parameter values (left dotted line), there are two stable equilibria: severe (M_1^*) and mild (M_2^*) insulitis. As k_T increases, the severe equilibrium disappears. This is observed in [62], when a wild type IL-2 gene bred into the NOD mice greatly reduces T1D.

Next we increase Q (Figure 3.3B) to simulate exogenous IL-2 treatment. The effect is similar to increasing k_T, except that the lower solution branch undergous a transcritical bifurcation (red region) and switches to the R-only equilibrium. The arrows indicate, conceptually, the trajectory of the system during treatment. The trajectory starts on the

upper branch, but is forced down onto the lower one after the saddle-node bifurcation. After treatment, the trajectory remains on the lower branch.

Finally, we vary σ_R and σ_T simultaneously while keeping them in the same proportion (Figure 3.3C). This represents treatment with anti-CD3 (which actually decreases these values to zero). The result is almost exactly the same as treatment with IL-2, with the trajectory dropping down onto the lower branch after the saddle-node bifurcation. Even though this branch is on the T-only equilibrium initially (blue region), it eventually undergoes a transcritical bifurcation to arrive at the mild insulitis equilibrium.

3.2.5 Parameter estimation

The typical lifespan of a macrophage within the pancreas is 10 days, so we let $\delta = .1$ days^{-1}[47]. The concentration of these cells in the inflamed pancreas is $1*10^7$cell/ml, which we then take to be J/δ, the total number of macrophages in our model at equilibrium [47]. The macrophage deactivation rate is $b_0 = .4$ [47]. We assume that $\alpha_T + \alpha_R$ has a similiar magnitude to the macrophage influx J. From [67], we see that Tregs initially account for 30% of the CD4 population. Therefore, we let $\alpha_R = .3J$ and $\alpha_T = .7J$. From [80], we note that IL-12 triggers IFN-γ after roughly 8 hours, and so we assume that $a_\gamma = c = 8$ days^{-1}. Also from [80], the half life of the expression of IFN-γ is about 3 hrs, so $e = 5.5$ days^{-1}.

Initially, we let $\nu_{12} = \nu_{10} = \nu_\gamma = \delta/J$. This is so that the argument passed to F would be close to 1, and so its sigmoidal behavior would be relevant. We find that with these parameters, the basin of attraction of the severe insulitis state is so small that the equilibrium cannot be reached from reasonable initial conditions. Doubling the value of ν_γ resolves this.

We let $\gamma_T = \gamma_R = 2$, which corresponds to a doubling time of 8 hours. We can directly observe $\sigma_T \approx .4$ and $\sigma_R \approx .8$ from the proliferation data in [67]. We also note that, at equilibrium, roughly 10% of effectors are dividing. Assuming that the proliferation rate matches the death rate at this point, we find that $\delta_{T1} = .2$. To fit the final parameters, we note that at equilibrium, roughly 20% of Tregs are dividing and that the ratio of Tregs to effectors is about 9 to 1 [67]. Taken together, this allows us to fit the parameters $\delta_{T2} = .8$, $k_T = 5\delta/J$ and $k_R = 20\delta/J$.

3.3 The progression model

3.3.1 CD8 T-cells

NOD mice have multiple lineages of islet specific T-cells, however, we focus on the high affinity IGRP/NRP-specific subset. We assume that these cells are generated at a

low frequency due to control by central tolerance, but that they proliferate when the islet antigen IGRP is presented with costimulation in either the Pancreatic Lymph Node or the islets themselves. Following [46], we use both a linear death term, representing normal turnover, and quadratic death term, representing autoregulation by the CD8 population.

$$\frac{dC}{dt} = \alpha_C + \left(\gamma_C \frac{M^*}{M^* + k_C} - \delta_{C1}\right) C - \delta_{C2} C^2 \tag{3.14}$$

To parameterize this system we use the data for NRP-A7 CD8 T-cells in [7]. Assuming that α_C is small and that M^* is constant from week 5 onwards. Then (3.14) becomes

$$\frac{dC}{dt} \approx A_i C - \delta_{C2} C^2 \tag{3.15}$$

$$A_i = \gamma_C \frac{M_i^*}{M_i^* + k_C} - \delta_{C1} \tag{3.16}$$

Where A_i represents the exponential growth rate of CD8 population when $M^* = M_i^*$. From the time series data, we can estimate that $\delta_{C2} = 2.6{*}10^{-6}\text{cells}^{-1}\text{days}^{-1}$and $A_2 = .13$ days^{-1}. From [70], we know that there are roughly 8 times as many NRP specific CD8 in mice that get T1D versus those that do not. This implies that $A_2 \approx 8 * A_1$. Taken together, these two relations allow us to estimate the values of $\gamma_C = .27$ days^{-1}and $k_C = .75J$. Finally, α_C remains as an important parameter controlling the timing of the expansion of the CD8 T-cells. We adjust α_C, after assigning all other parameters, so that the median onset of T1D occurs at 16 weeks. This gives $\alpha_C = .03$ cells per day.

3.3.2 Metabolic subsystem

In most experiments, a T1D diagnosis corresponds to a blood glucose level 250mg/dl (normal is 100mg/dl). Glucose controls both the proliferation rate and insulin production of beta cells. The produced insulin, in turn, stimulates the uptake of blood glucose. Topp et al. [68] modeled the insulin-glucose system with the following differential equations.

$$\frac{dG}{dt} = R_0 - (E_{G0} - S_I I)G \tag{3.17}$$

$$\frac{dI}{dt} = \sigma_I B \frac{G^2}{G^2 + G_I^2} - \delta_I I \tag{3.18}$$

As, $\delta_I \gg 1$, we assume that the insulin level I is in equilibrium.

$$\frac{dG}{dt} = R_0 - \left(E_{G0} + \frac{S_I \sigma_I}{\delta_I} B \frac{G^2}{G^2 + G_i^2}\right) G \tag{3.19}$$

To account for the increase in proliferation, we follow the work of [31] who created a highly detailed model of beta cell function. We simplify their model as

$$\frac{dB}{dt} = \left(\gamma_B \frac{G^2}{G^2 + G_{hb}^2} - \delta_B\right) B. \tag{3.20}$$

To parameterize this model we note the following. First, we observe from [63] that the number of proliferating cells reaches roughly 3%. This corresponds to a max growth rate $\gamma_B = .06$. The lifespan of a typical beta cell is 60 days [31] so $\delta_B = 1/60$. The resting population of β-cells in the absence of an immune response is $B^* = 300$, allowing us to solve for $G_{hb} = 161 mg/dl$.

In [35], untreated mice experience an increase in blood glucose from 300mg/dl to 500mg/dl in the first 2 weeks after onset. This corresponds to a decrease in β-cell mass from 24 to 4.32 in our model, a loss of roughly 12% daily. To offset compensatory growth, the immune response must remove about 16% of β-cells daily. In treated mice, on the other hand, glucose levels drop to about 200mg/dl, which is still twice the baseline level. In our model, we can only account for this by a continued immune destruction of about 2% of immune cells daily. This means that the strength of the immune response is roughly 8 times less after treatment than before. Interestingly, this prediction corresponds closely to the ratio of NRP-reactive cells found in [70] between mice that get T1D and those that do not. Taken together, we conclude that we can model β-cell death due to CD8s as mass action with a constant of $\eta_8 = 3.2 * 10^{-6}$ cells^{-1}days^{-1}.

CD4s can also kill β-cells, although this primarily happens in the absence of Tregs. We include a killing term due to CD4s, which only becomes relevant to model behavior if Tregs are either absent [15] or removed [20]. Our final β-cell equation is

$$\frac{dB}{dt} = \left(\gamma_B \frac{G^2}{G^2 + G_{hb}^2} - \delta_B - \eta_8 C - \eta_4 \frac{(s_{T4} T^*)^2}{1 + (s_{T4} T^*)^2 + (s_{R4} R)^2}\right) B. \tag{3.21}$$

3.4 Simulating treatments

In the next section, we simulate the treatments described in various papers. Table 3.3 summarizes the nature and duration of these treatments. Here we descibe the implementation of IFN-α treatment, anti-CD3 antibodies (aCD3 treatment), anti-PDL1 antibodies (aPDL1 treatment), Treg treatment, and IL-2 treatment.

According to Filippi et al. [23], treatment with IFN-α boosts PD-L1 expression. PD-L1 is a negative costimulatory molecule, so it impairs the ability of APCs to activate T-cells. We therefore set $\nu_{12} = 0$ so CD4s produce no IFN-γ, and $\gamma_C = 0$ so CD8s do not proliferate [23]. Treatment with Tregs is relatively straightforward, directly increasing the R population, which we implement by changing α_R.

Fife et al. [21] treat with aPDL1, which we assume should have the opposite effect to

IFN-α treatment. We therefore increase ν_{12} by a factor of 10 and set γ_C equal to γ_T, which is the maximum growth rate of T-cells. Anti-CD3 interferes with the interaction between T-cells and APCs. Thus, we let $\sigma_T = \sigma_R = 0$ to indicate that no division takes place. We also set $\delta_{T2} = 0$ and $\delta_{T1} = .1$, which is equivalent to the assumption that both effectors and Tregs die at the IL-2 deprived death rate of $\delta_{T1} + \delta_{T2}$ as there is no source of IL-2.

Finally, to simulate IL-2 treatment we assume that Q obeys

$$Q = Q_0 \sum_{t_i} e^{(t_i - t)\delta_Q} H(t_i - t) \tag{3.22}$$

$$H(t) = \begin{cases} t & t > 0 \\ 0 & \text{else} \end{cases} \tag{3.23}$$

where the t_is are spaced every 2 days for the duration of the treatment. This represents pulses of Q_0 that decay at a rate of δ_Q per day. This matches the treatment described in [67].

3.5 Results

3.5.1 Magnitude of initial inflammation determines T1D prognosis

As demonstrated in section 3.2.4, the intiation model (3.5) and (3.7) has two stable equilibria, representing insulitis of different severities. By changing the initial conditions, we can shift the long term behavior of the system from mild to severe insulitis and the outcome from nondiabetic to diabetic. Specifically, we hold all initial conditions constant with the exception of activated macrophages. We start each simulation at $t_0 = 14$ days, during the apoptotic wave. The initial number of activated macrophages, $M^*(t_0)$, will change depending on severity of the wave, which could vary between mice. Figure 3.4 shows time series for $M^*(t_0) = 1.6 * 10^7$cells (Figure 3.4A,B) and $M^*(t_0) = 8 * 10^6$cells (Figure 3.4C,D). When $M^*(t_0)$ is high, the CD4 and macrophage populations equilibriate relatively rapidly to the severe insulitis state (Figure 3.4A), eventually leading to T1D onset (Glucose>250mg/dl) at 16 weeks (Figure 3.4C). When $M^*(t_0)$ is low, the CD4 and macrophage populations equilibriate to the mild insulitis state (Figure 3.4C), and T1D does not develop (Figure 3.4D).

3.5.2 Simulation of mouse populations

One of the main goals of this study is to model the incidence of T1D in NOD mice under various treatments. Not all NOD mice develop T1D, and the age of onset can vary among those that do. As our ODE model is deterministic, we represent the differences

between individuals via parameter values and initial conditions. To simulate experiments with groups of N mice, we make N parameter sets, sampling each parameter from a different distribution, described below. We then replicate those parameter sets and initial conditions for each treatment, so differences between treatments are never due to stochasticity. We start each simulation at the time of the initial inflammation ($t_0 = 14$ days). Therefore, we assume that the number of activated macrophages will initially be elevated in each mouse, as our model does not include the initiating event. The initial macrophage population could be different for each mouse due to diet or differences in development. We draw this value from the normal distribution $(1.2 + \mathcal{N}(.4, 1)) * 10^7$cells. Likewise, the value η_8 is dependent on the affinity of CD8s for β-cells and is therefore the outcome of a complicated process of gene rearrangement, thymic selection, and the population dynamics of competing CD8 clones. Where specified, we generate this value from the log-normal distribution $3.2 * 10^{-13}10^{\mathcal{N}(0,1/9)}\text{days}^{-1}$. We generate all other parameters by sampling from a log-normal distribution with the means given by the base parameters and the standard deviations as 1% of those means. When we show the time series from an individual mouse, we use the parameters in Table 3.2.

3.5.3 Treatment with IL-2 increases Treg:Teff ratio and prevents T1D

Several groups [35, 67] find that treatment with exogenous IL-2 can restore the Treg population and prevent the development of T1D. We treat groups of 100 mice with 1, 5, or 11 weeks of IL-2 pulses (of 500 every 2 days). Treatment for 1 week causes a transient but significicant drop in the CD4 population and a corresponding rise in the Treg population (Figure 3.5A). This results in a very small delay in T1D, but no change in incidence. Treatment for 5 weeks, on the other hand, leads to a permanent decrease in the CD4 and inflammatory macrophage population and a permanent increase in the Treg population. This leads to a very large decrease in incidence (Figure 3.6). Treatment for 11 weeks has little marginal benefit as compared to 5 weeks. In both of these latter cases, insulitis is greatly reduced, but remains perpetually. The lower level of insulitis is insufficient, in most cases, to stimulate the growth of a killer CD8, and so T1D never occurs.

3.5.4 CD3 induced tolerance requires continued activity of PD-L1

Fife et al. [21] demonstrate that early treatment with an aCD3 prevents T1D. CD3 is a surface protein on T-cells that helps them bind to antigen presenting cells. We can represent

CD3 treatment by setting $\sigma_T = \sigma_R = 0$ to indicate that no proliferation takes place. We further modify the death rates of both effectors and Tregs to be $\delta_{T1} + \delta_{T2}$, indicating that they receive no survival signals from the IL-2-BCL pathway. Fife's group also treats some mice with a PD-L1 antibody. PD-L1 acts as a negative regulator of T-cells. We represent PD-L1 treatment by increasing ν_{12} 10-fold, corresponding to a decrease in the activation threshold of CD4 T-cells. This change means that CD4 T-cells require 10 times less IL-12 to activate and start to produce IFN-γ. We also assume that more PD-L1 dramatically increases the division rate of CD8 T-cells to the maximum rate of T-cell division γ_T.

We follow the same protocol as Fife, treating with aCD3 at 5 weeks and aPD-L1 at 17 weeks, with both treatments lasting for 2 weeks. Our results (Figure 3.7) match the key features of the experiment. With aCD3 treatment, aPD-L1 accelerates T1D among NOD mice and leads to a much higher incidence. Mice that received aCD3 alone did not develop any T1D, whereas 100% of those that also received aPD-L1 rapidly developed T1D shortly after the latter treatment.

3.5.5 Synergy between IFN-α and Tregs

Filippi et al. [23] study the role of viruses in the regulation of T1D in NOD mice. They find that the virus LCMV transiently increases PD-L1 expression. In addition, they hypothesize that the Treg population generated during the immune response may explain the decreased T1D among LCMV treated mice. To test this hypothesis, they treat mice with IFN-α, which can also increase PD-L1 expression and transfer Tregs from mice previously exposed to LCMV.

We represent the boost in PD-L1 by setting $\nu_{12} = 0$, meaning that APCs cannot activate CD4 T-cells to produce IFN-γ, and $\gamma_C = 0$, meaning that CD8 T-cells cannot divide. This is esentially the inverse of how we modeled the aPD-L1 treatment. We represent the injection of T-cells by increasing α_R for the duration of the treatment.

Like Fillipi, we find synergy between the two treatments (Figure 3.8). The administration of IFN-α by itself does not change the incidence of T1D, but it does delay the age of onset. The administration of Tregs by themselves does not change the age of onset, but does decrease incidence. The combination of both treatments decreases incidence by more than the sum of the individual treatments. All of these observations replicate Fillipi's findings. In this experiment, we used a smaller range of η_8 to bring it in line with the other parameters. Without this change, the variance is so large that it obscures the synergy.

3.5.6 CD4 and macrophage parameters affect incidence while CD8 parameters affect age of onset

To determine which parameters contribute to incidence and which to age of onset, we ran a sensitivity analysis for each parameter. First we generate 100 pairs of values of η_8 and $M^*(t_0)$, our two key parameters. Then we vary each parameter, one at a time, from 50% to 200% of its baseline value, equally spaced on a log scale, with every other parameter fixed at its baseline. For each value of the current parameter, we simulate the system using each of the 100 parameters pairs for η_8 and $M^*(t_0)$. We record if and when T1D develops in each simulation.

Figures 3.9, 3.10, and 3.11 summarize the results of the sensitivity analysis. In each panel, we vary a different parameter. The blue line shows the incidence, while the red and grey lines show the median and deciles, respectively, of the age of onset. Figure 3.9 shows parameters that primarily affect age of onset, Figure 3.10 shows those that primarily affect incidence, and Figure 3.11 shows those with strongs effects on both. In general, the parameters that describe CD4 and macrophage behavior affect only incidence and those that describe CD8 behavior affect only the age of onset. We summarize this pattern in Figure 3.12 that shows the entire model, with each arrow color-coded and scaled according to its significance. Bolder arrows have greater significance, red arrows affect primarily age of onset, blue affect incidence, and purple arrows affect both. Greyed-out arrows have little affect on the model and are confined to the metabolic processes in the model.

3.6 Discussion

In this chapter, we present a mathematical model of Type 1 diabetes (T1D) in the NOD mouse. We propose that the intensity of the apoptotic wave controls the eventual development of T1D. We further propose that the long delay between this initial inflammation and the destruction of the islets is due to the growth and maturation of the CD8 population. Therefore, the model has two components: an 'initiation' component that consists of equations governing the interaction of CD4s and macrophage populations, and a 'progression' component that describes the growth of CD8s, their killing of β-cells, and the eventual rise in blood glucose. The initiation component has two possible outcomes, defined by its stable equilibria, only one of which leads to T1D. These equilibria are distinguished by the relative activity of Tregs, effectors, and activated macrophages and their associated cytokines: IL-10, IFN-γ and IL-12.

Our model reproduces the results of several experiments on NOD mice: aCD3 treatment, aPDL1 treatment, IL-2 treatment, IFN-α treatment, and Treg treatment. All of

these treatments amount to shifting the trajectory from the basin of attraction of the severe-insulitis state to that of the mild insulitis state. A treatment that does not cause a transition can still cause a delay in insulitis. For example, IFN-α treatment alone does not decrease incidence but does delay T1D due to downstream effects that interfere with the CD8 population. When combined with adoptive transfer of Tregs, it does significantly decrease incidence. According to our model, each treatment by itself is insufficient to make the transition, and so the system returns to the severe-insulitis state once treatment is over. Conversely, treatment with aPDL1 can shift the system from mild to severe arthritis. We show that aCD3 treatment followed by aPDL1 shifts the system from severe to mild and back to severe again. The equivalence between all of these treatments suggests that the system is 'memoryless'. A mouse that has been cured with aCD3 should be similar to one cured via the transfer of Tregs or IFN-α. Fife et al. [21] found similarities between aCD3 treated mice and those that received insulin coupled splenocytes that tolerized them to the peptide. Table 3.4 summarizes the experimental results that our model can reproduce.

In our model, Tregs play two separate roles. First, Tregs prevent the killing of β-cells by CD4 T-cells. This is an assumption of the model given that Tregs have been observed to control the extent of infiltration in the islet [15, 20]. Second, Tregs can control the inflammatory state of macrophages and other APCs which in turn prevents the development of a CD8 response. Due to IL-2 deficiency in NOD mice, Tregs are at a competitive disadvantage in the islets, favoring a proinflammatory environment. In our model, this proinflammatory envinronment is manifested in the severe insulitis equilibrium. We find that a moderate increase in IL-2 production can eliminate this equilibrium. Treatment with exogenous IL-2 does not eliminate this equilibrium in the long term, but can shift the system to the mild equilibrium as the other treatments do.

It has been suggested that the Treg population loses either effectiveness [69] or population size [67] over time. Lack of IL-2 uptake by Tregs decreases BCL-2 expression and thus survival. Therefore, the IL-2 deficiency lowers the Treg:effector ratio in NOD islets relative to the spleen and lymph nodes and relative to wild type islets. However, this ratio does not decline as the mouse ages. Bleyer et al. find that it stays constant until disease onset, when it *rises* slightly [35]. In our model, the Treg:effector ratio stays constant over the progression of T1D and is not significantly different between mice that develop T1D and those that do not. This is not to say that the Treg population does not decline in NOD mice, but we need not assume it to reproduce the known phenomena. The presence of T1D-resistant mice, either naturally or following treatment by IL-2, IFN-α, or aCD3, suggests ongoing

regulation of the insulitic legion by Tregs. If the Tregs were to intrinsically decline, we would expect all of these mice to also develop T1D. Although this process may happen on a timescale longer than current experiments, it cannot be the driving force behind onset of T1D.

CD8 killer T-cells drive the eventual decline of the β-cell population. Although, in this model, CD4 T-cells also possess the capacity to destroy β-cells, they do not do so in the presence of Tregs (as in [20]). The CD8 population in our model represents the population of high affinity CD8 specific to IGRP. Trudeau et al. [70] use the size of this population to predict T1D outcome, and Amrani et al. [7] show that an increase in the average affinity of the CD8 population for IGRP correspond with disease onset. To eliminate the β-cell population, the CD8 population must kill them faster than the β-cells can divide. We estimate that at the time of disease onset, CD8 T-cells kill β-cells at a rate of roughly 16% a day, which is almost 3 times as fast as β-cells have been observed to divide. Therefore, a slight decrease in CD8 number or effectiveness is unlikely to prevent T1D development, although it can slow it. We find that CD8 related parameters primarily contribute to the age of onset instead of T1D incidence. In agreement with this, TCR8.3 NOD transgenic mice that produce only high-affinity IGRP-specific CD8 T-cells have a more rapid onset, but similiar incidence to NOD mice [74].

In this model, the treatment of the CD8 population is extremely simple. We only track a single population that grows from a very small number of precursors. In NOD mice, the CD8 population transitions from insulin specific to IGRP specific [7]. An initial response to insulin is required for T1D progression [41], but it is unclear whether this is due specifically to the activity of CD8s. It is plausible that initial low levels of β-cell death due to insulin-specific CD8s releases IGRP, which is then presented on APC triggering the switch in autoimmunity. It is also plausible that the CD8-mediated death is necessary to maintain the 'severe-insulitis' state that leads to T1D in this model. One possible experiment to elucidate the role of CD8s would be to create a transgenic line of mice on the NOD background whose CD8s lack the ability to kill β-cells. According to our simple model of CD8s, they should still develop an IGRP-specific population in the same time frame. If these NOD mice continue to produce primarily insulin-specific CD8s, that will imply that CD8-related pathology drives the progression of their own β-cell affinity.

Another simplifying assumption of our model is that the β-cell population responds only to glucose levels and only homeostatically. In fact, β-cells divide in response to islet inflammation [65]. We have ignored this phenomenon, reasoning that the immune response

results in a net decrease in β-cells. In addition, β-cells can decompensate [65] when under high demand, producing less insulin per cell. This is due in part to the degranulation of β-cells during T1D progression [3]. Including any of these phenomena will change the parameter estimates for the immune-mediated killing of β-cells. More importantly, it could alter some of the conclusions of how we expect the β-cell population to respond to treatment. For example, the inclusion of degranulated β-cells could allow for a rapid rebound after IL-2 treatment in new onset mice, as in [35], which cannot be reproduced by the one-compartment β-cell model we use.

In treating T1D in both NOD mice and humans, there are two main strategies. Administration of anti-inflammatories, such as anti-CD3, Vitamin D or omega-3s [38] can reduce insulitis and hopefully prevent the development of an autoimmune destruction. Antigen specific tolerance, such as with oral administration of insulin, aims to delete the autoreactive T-cell clones directly [38, 81]. Only the former have had successful trials among humans, but the latter represent a more specific treatment.

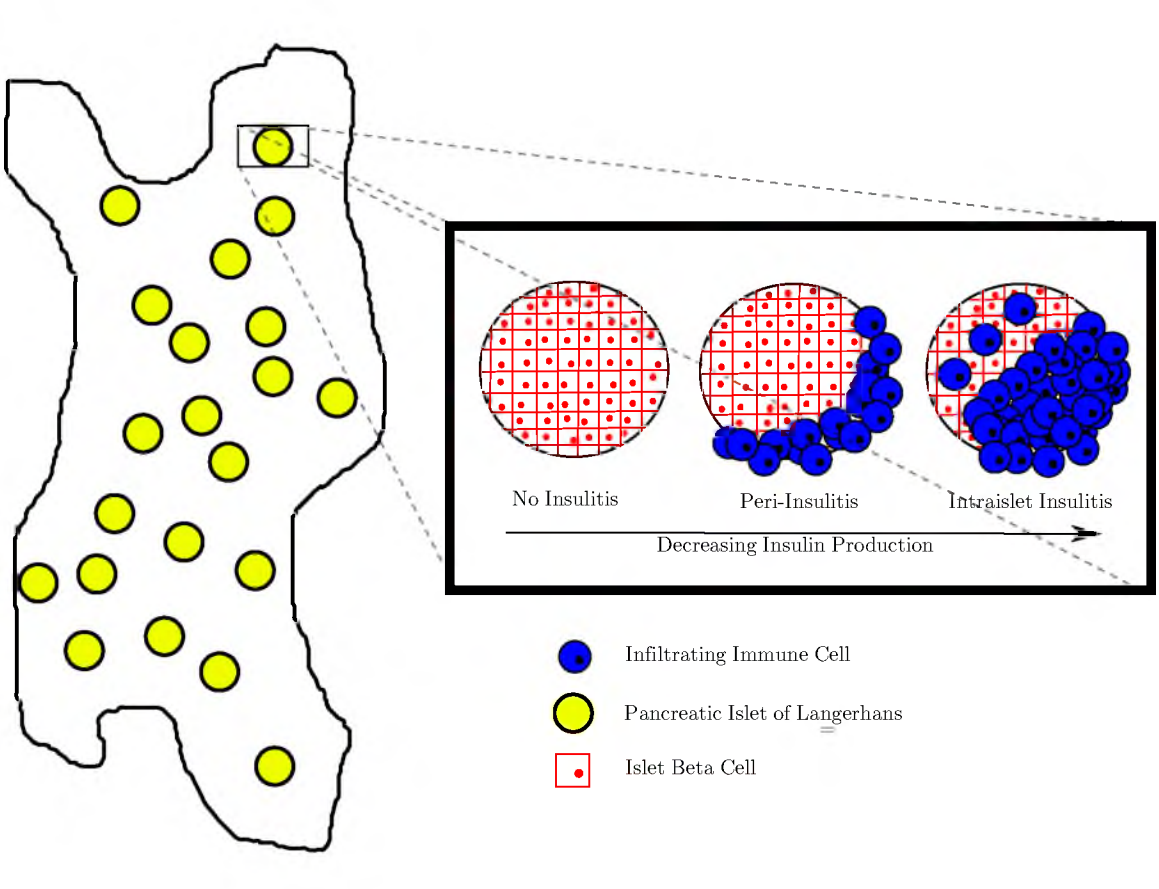

Figure 3.1: Progression of insulitis in the islets. Over time, immune cells such as T-cells and macrophages infiltrate the islets, killing β-cells and decresing insulin production.

Table 3.1: T1D progression in the NOD mouse

Time	Event	Source
9-15 days	Apoptotic Wave	[71]
18 days	T1D in Treg deficient NOD mice	[15]
3 weeks	Initiation of Insulitis	[26]
4-5 weeks	Insulin-specific CD8s dominate	[70]
4-5 weeks	Rapid T1D after ablation of Tregs	[20]
6 weeks	Differential Prognosis with MRI	[26]
6-8 weeks	Decline in Treg effectiveness	[69]
8 weeks	IGRP-specific CD8s appear	[70]
8-12 weeks	β-cell mass starts to decline	[4]
12-16 weeks	Rapid loss of β-cell mass	[4]
16 weeks	Median T1D onset	[7]

Table 3.2: Parameter values used in the model

Parameter	Description	value
J	Influx of macrophages into pancreas	1 *10^6cells
δ	Turnover of macrophages in pancreas	1 days^{-1}
a_0	Basal macrophage activation rate of macrophages	.05 days^{-1}
a_γ	Macrophage activation rate induced by IFN-γ	8 days^{-1}
b_0	Basal macrophage deactivation rate	.4 days^{-1}
b_{10}	Macrophage deactivation rate induced by IL-10	8 days^{-1}
c	CD4 activation rate by IL-12	8 days^{-1}
e	CD4 deactivation rate	5.5days^{-1}
ν_γ	Scaled IFN-γ affinity of macrophages	$2\delta/J$
ν_{10}	Scaled IL-10 affinity of macrophages	δ/J
ν_{12}	Scaled IL-12 affinity of CD4 T-cells	δ/J
α_T	Influx of effectors into islets	.7 *10^6cells
α_R	Influx of Tregs into islets	.3 *10^6cells
γ_T	Proliferation rate of effectors	2 days^{-1}
γ_R	Proliferation rate of Tregs	2 days^{-1}
σ_T	Max fraction of effectors in mitosis	.4
σ_R	Max fraction of Tregs in mitosis	.8
δ_{T1}	Basal death rate of Tregs in pancreas	.2 days^{-1}
δ_{T2}	Death rate of Tregs due to IL-2 deficiency	.8 days^{-1}
k_R	Scaled affinity of Tregs for IL-2	5 δ/J
k_T	Scaled affinity of effectors for IL-2	20 δ/J
α_C	Production of CD8s	.03
γ_C	Division rate of CD8s	.27
δ_{C1}	Death rate of CD8s	.01
δ_{C2}	Autoregulation rate of CD8s	2.6*10^{-6} cells^{-1}days^{-1}
k_C	Saturation constant for CD8 proliferation	.75 J
η_4	Rate of β-cell killing by CD4	.3
s_{T4}	Saturation constant of CD4 killing	1
s_{R4}	Control of Tregs over CD4 killing	30
η_8	Per capita rate of beta cell killing by CD8	3.2 *10^6cells
γ_B	Growth rate of beta cells	.06
G_{hb}	Glucose level for half maximal beta cell growth	161
δ_B	Death rate of beta cells	1/60
R_0	Average glucose production	864 mgdays^{-1}
E_{G0}	Basal glucose decay rate	1.44 days^{-1}
S_I	Rate of insulin-mediated glucose uptake	.72 days^{-1}/per μU
σ_I	Max insulin production rate	43.2 μUdays^{-1}per mg
δ_I	Insulin decay rate	432 days^{-1}

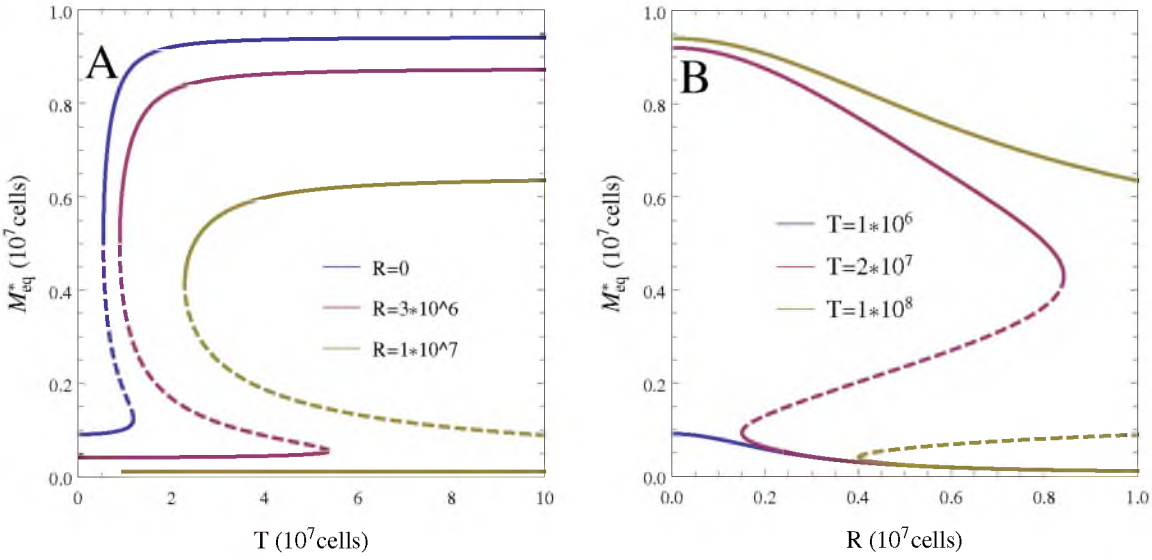

Figure 3.2: Equilibria of (3.5) with the parameters in Table 3.2.

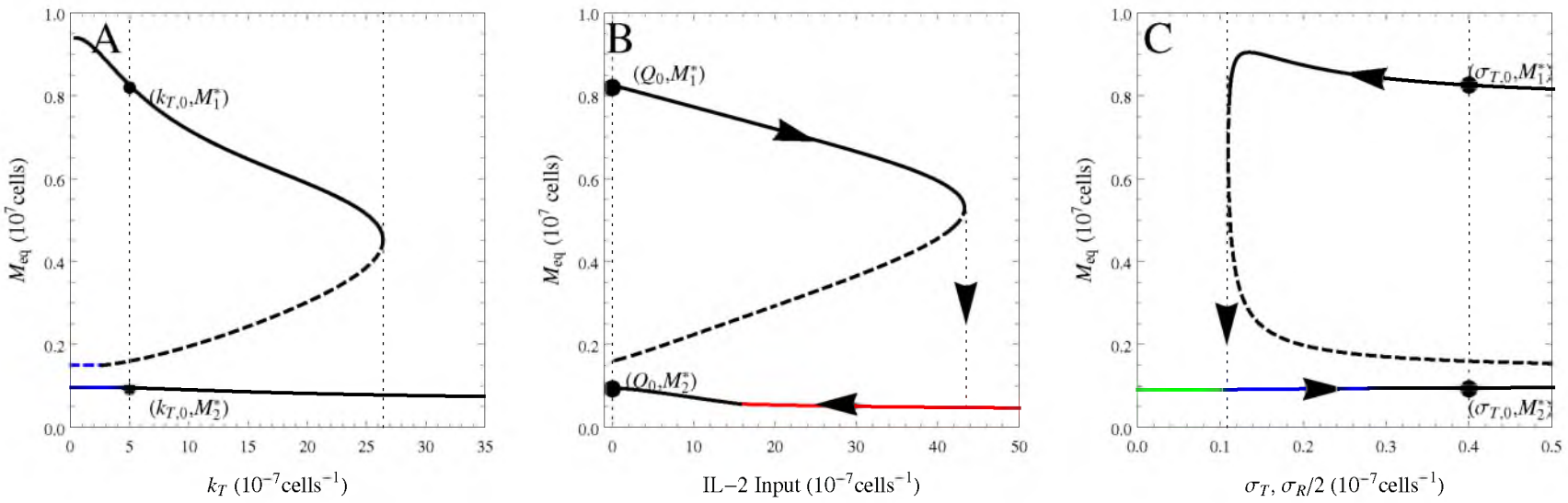

Figure 3.3: Bifurcation diagrams (A: k_T, B: Q, and C: σ_T and σ_R simultaneously) of the initiation model. Solid lines are stable states and dashed lines are unstable saddles. Black curves indicate that effectors and Tregs coexist, blue curves have only effectors, red curves only Tregs, and green curves represent the trivial solution. The arrows indicate the trajectory during IL-2 treatment (B) and anti-CD3 treatment (C). Dotted lines mark the baseline values in Table 3.2 and the locations of saddle-node bifurcations.

Table 3.3: Summary of Treatments

Treatment	Change	Timeframe
IFN-α Treatment	Day 63-77	Set $\gamma_C = \nu_{12} = 0$
Boost of Tregs	Day 77-78	Increase α_T by $15\delta/J$
anti-CD3 Treatment	Day 35-49	Set $\sigma_T = \sigma_R = \delta_{T2} = 0$ and $\delta_{T1} = 1$
anti-PDL1 Treatment	Day 119-133	Set $\gamma_C = \gamma_T$ and $\nu_{12} = 20\delta/J$
IL-2 treatment	Every two days	Pulse Q with $Q_0 = 500$ and $\delta_Q = 1\text{days}^{-1}$

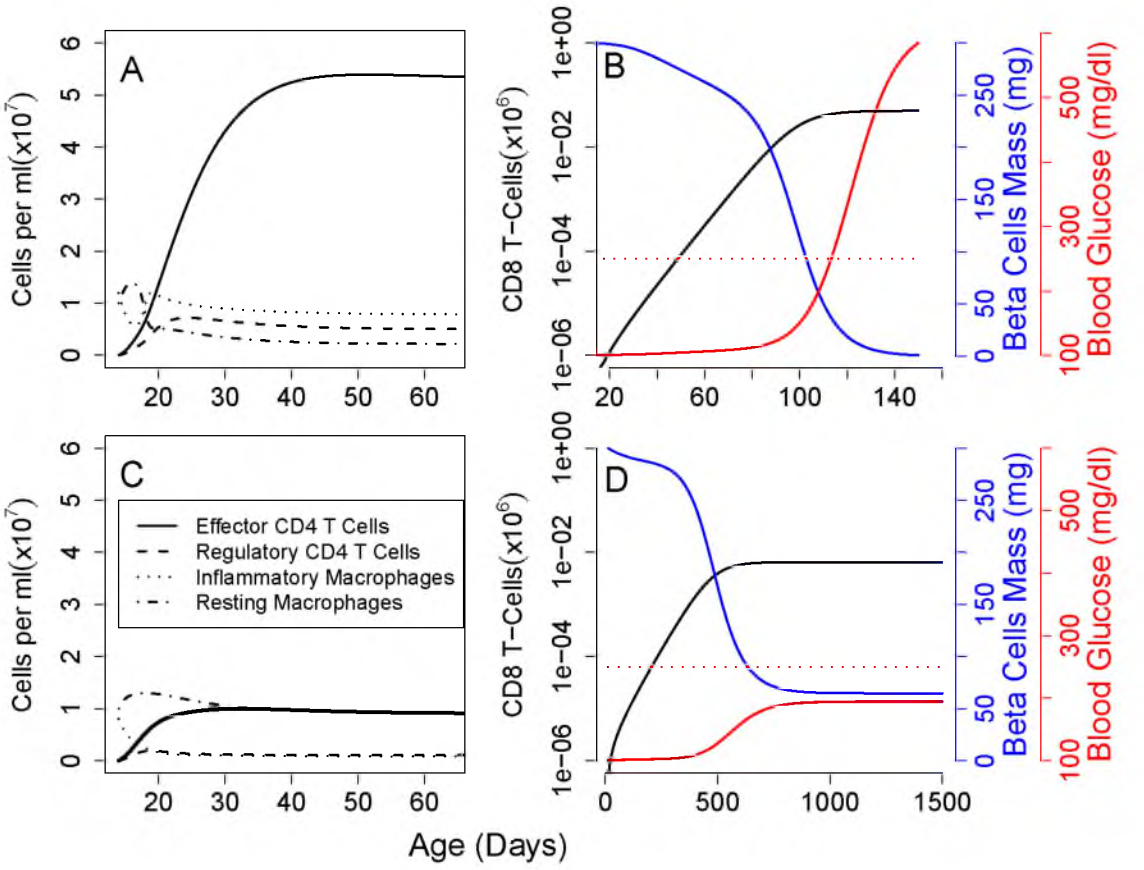

Figure 3.4: Time series with $M^*(t_0) = 1.6 * 10^7$cells (A,B) or $M^*(t_0) = 8 * 10^6$cells (C,D). Panels A and C show the CD4 and macrophage populations. Panels B and D show the CD8 population (black), β-cells (blue), blood glucose (solid red), and the glucose threshold for T1D (250mg/dl, dotted red).

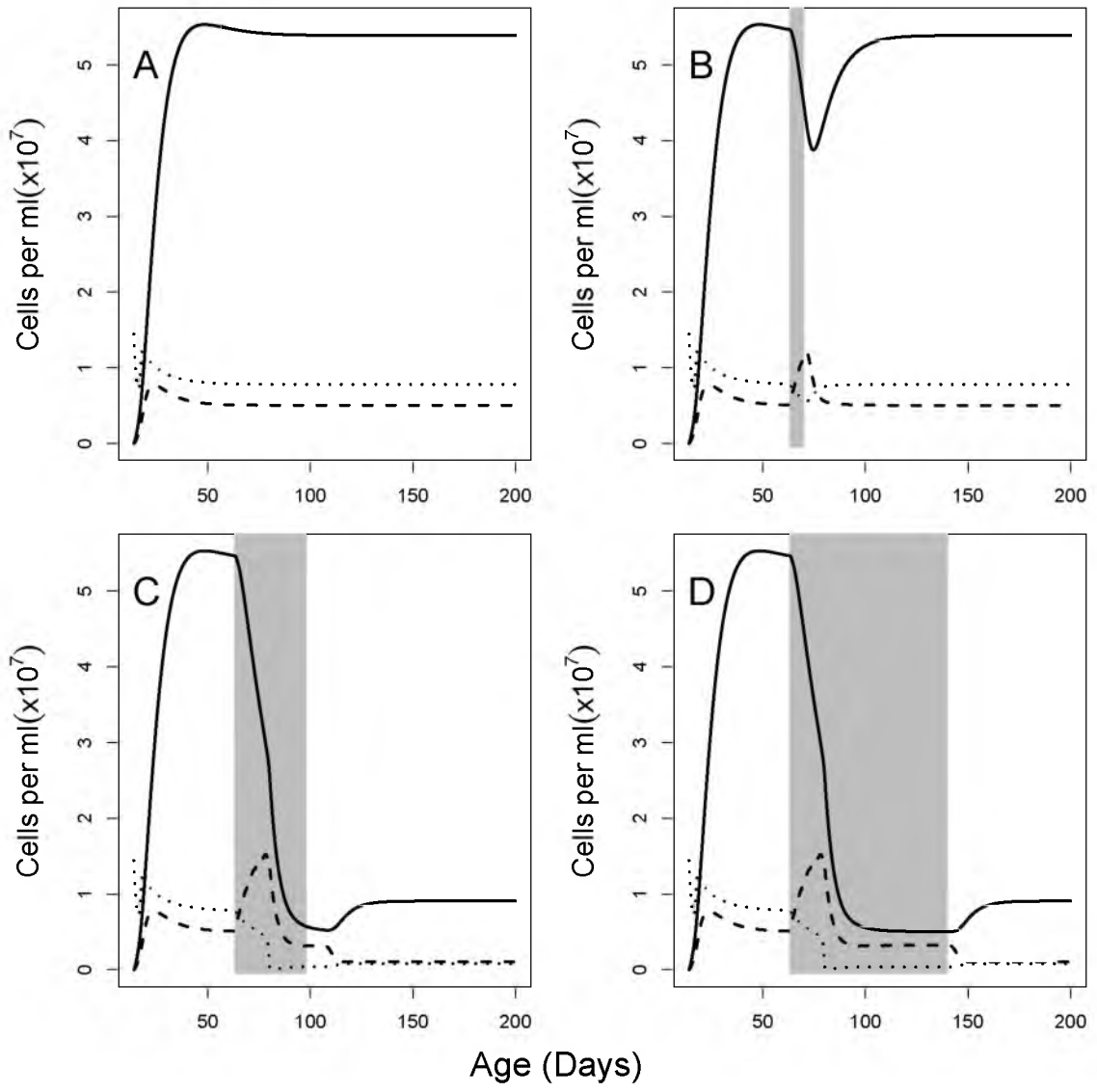

Figure 3.5: Simulation of IL-2 treatments of different lengths. Using the baseline parameters, we simulated treatment with IL-2 for 0 (Panel A), 1 (Panel B), 5 (C), or 11(D) weeks. Each panel shows the time course of the inflammatory macrophages (M^*), resting macrophages(M), effector CD4s (T), and Tregs (R). The dosage is $Q = 500$.

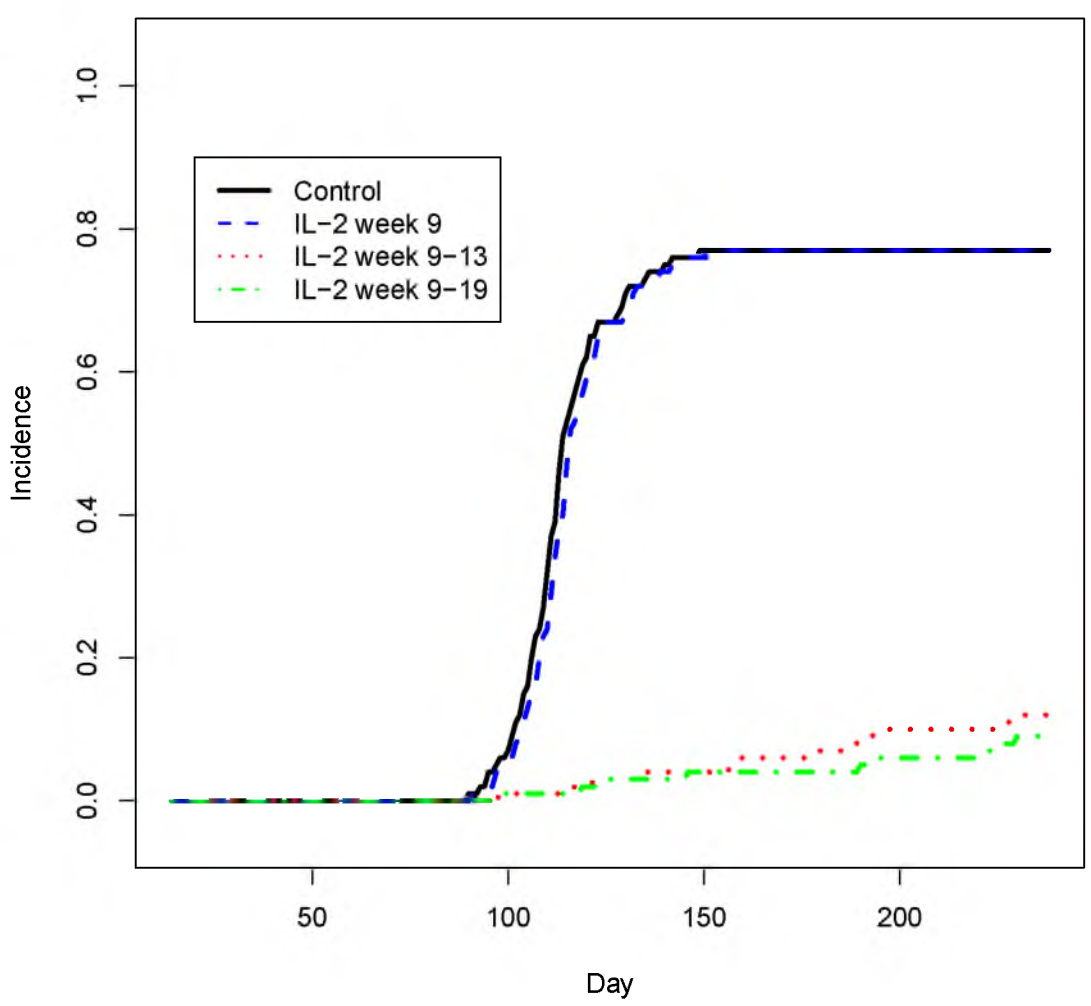

Figure 3.6: Incidence of T1D with IL-2 treatment for 0, 1, 5, or 11 weeks.

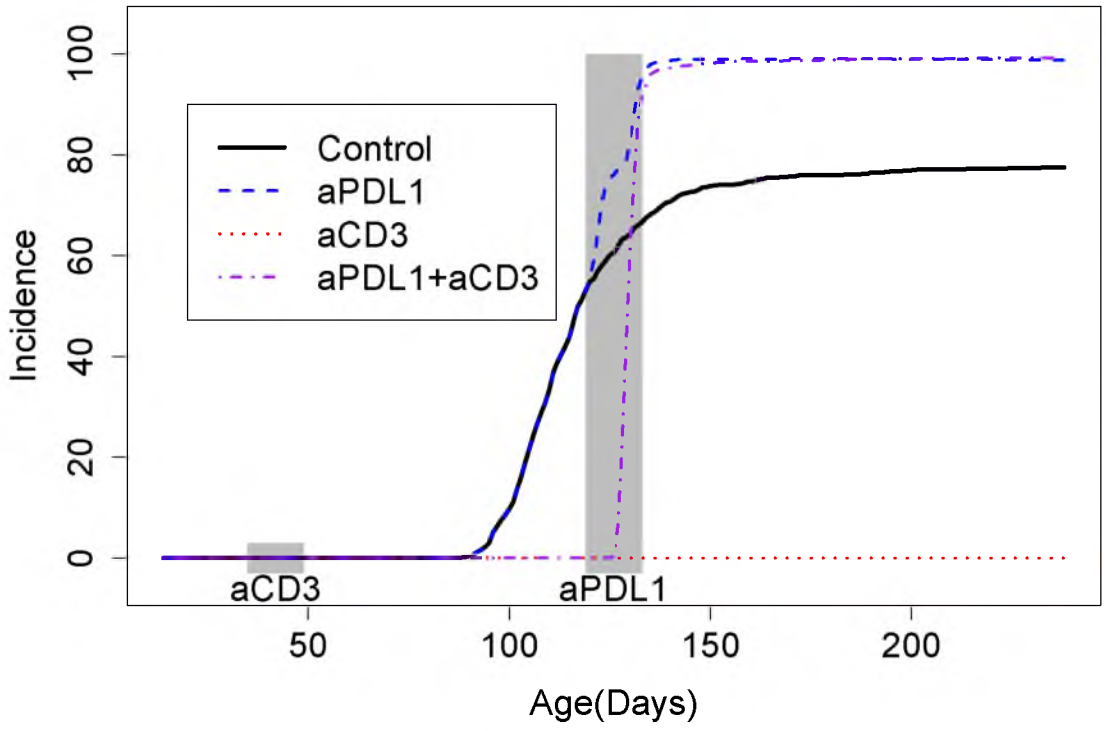

Figure 3.7: Simulation of treatment of NOD mice with aCD3 and aPDL1. We generated 100 different parameter sets ('mice') and simulated each T1D progression under four different simluated treatments. Mice received no treatment, aCD3 at 5 weeks of age, aPDL1 at 17 weeks, or both treatments. This is a replication of experiment from [21].

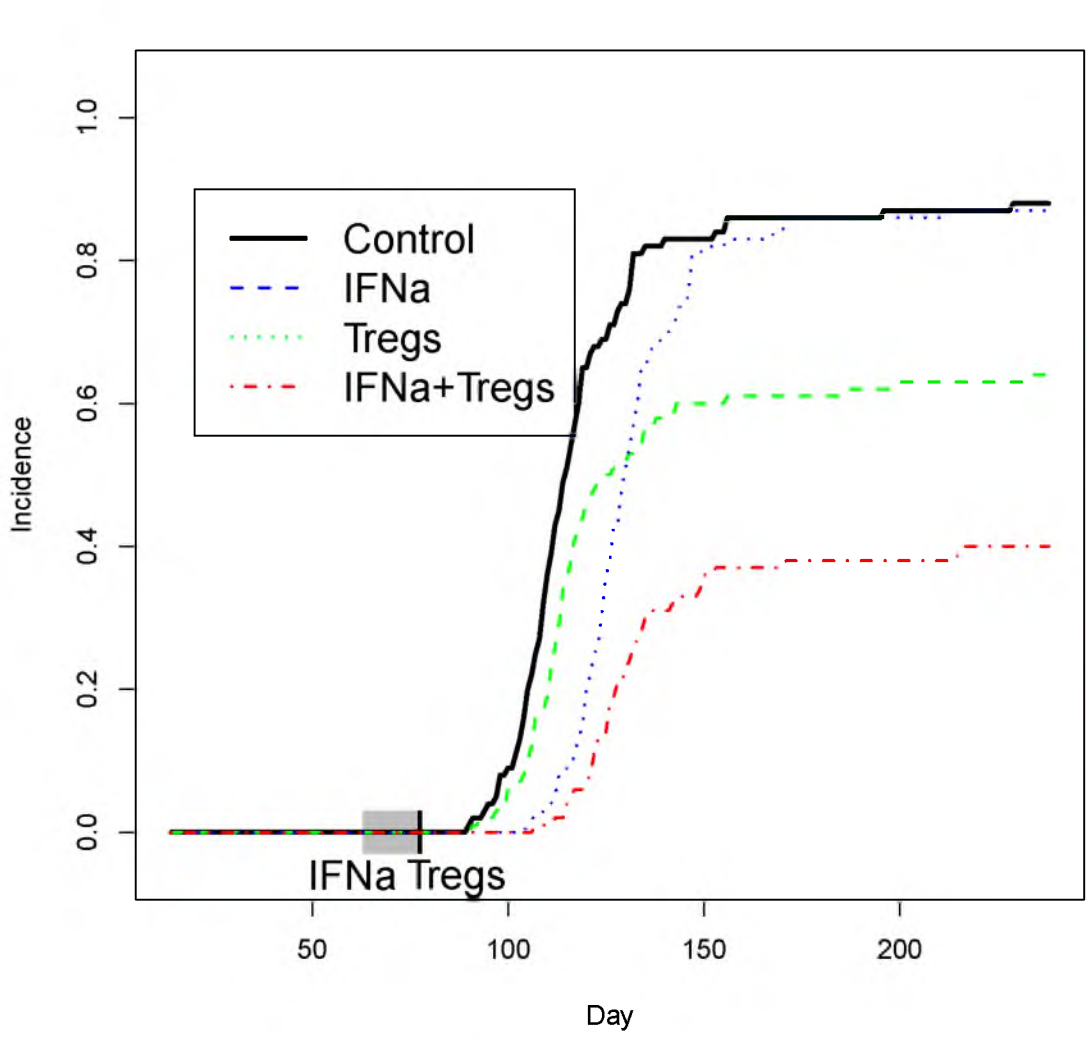

Figure 3.8: Simulation of treatment of NOD mice with IFN-α and Tregs. We generated 100 different parameter sets ('mice') and simulated each T1D progression under four different simluated treatments. Mice received no treatment, IFN-α at 9 weeks of age, Tregs at 11 weeks or both treatments. This is a replication of experiment from [23].

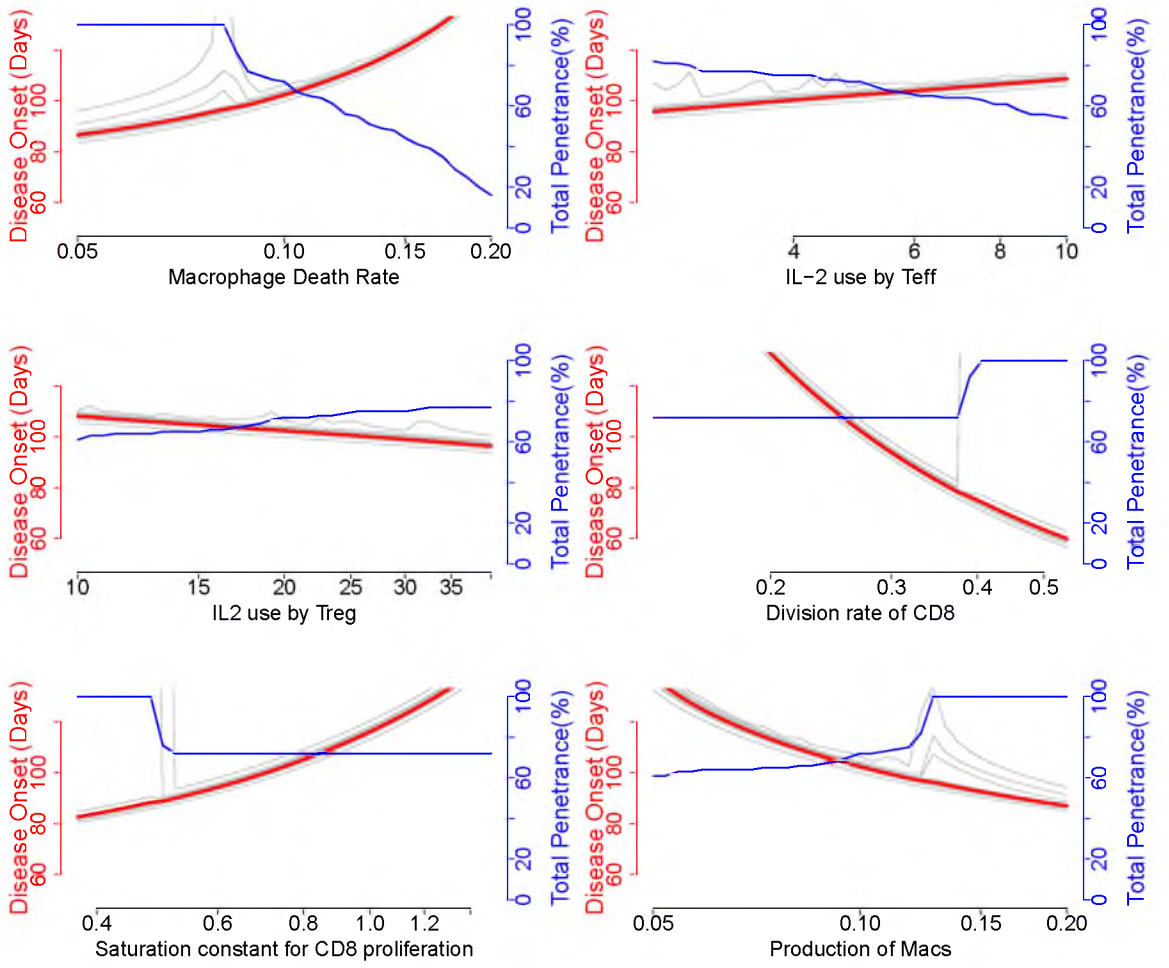

Figure 3.9: Sensitivity analysis of full model. Parameters that primarily affect age of onset. We vary an individual parameter from 50% to 200% of its baseline value. We hold each other parameter constant except for the killing rate of CD8 η_8 and the initial number of activated macrophages $M^*(t_0)$. The blue line shows the percentage of diabetic mice, by the end of 50 weeks, in the sample. The red and grey lines show the median and deciles, respectively, of the age of onset.

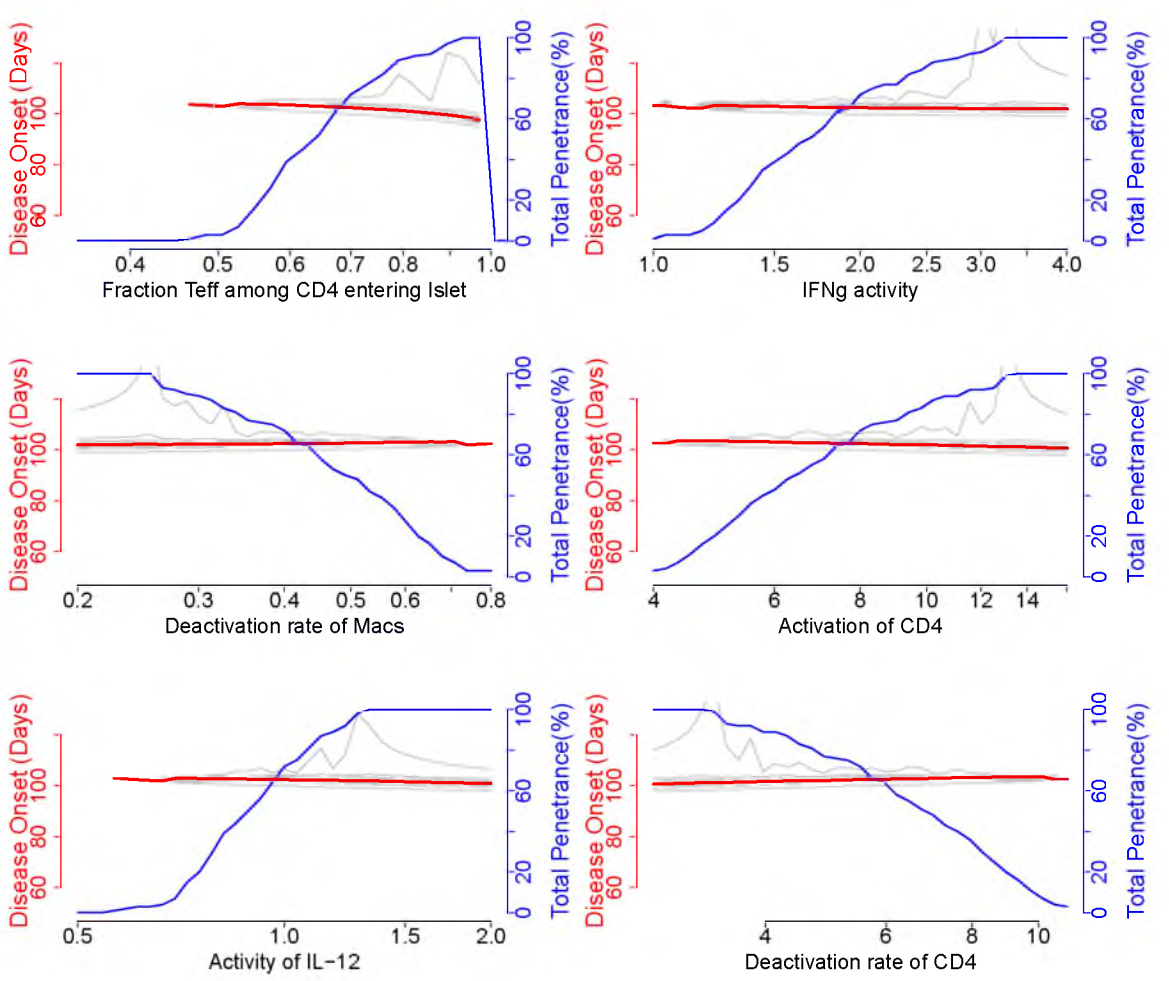

Figure 3.10: Sensitivity analysis of full model. Parameters that primarily affect incidnece. We vary an individual parameter from 50% to 200% of its baseline value. For each other parameter, we randomly sample 100 times from a normal distribution centered on the baseline value and run a seperate simulation for each parameter set. The blue line shows the percentage of diabetic mice, by the end of 50 weeks, in the sample. The red and grey lines show the median and deciles, respectively, of the age of onset.

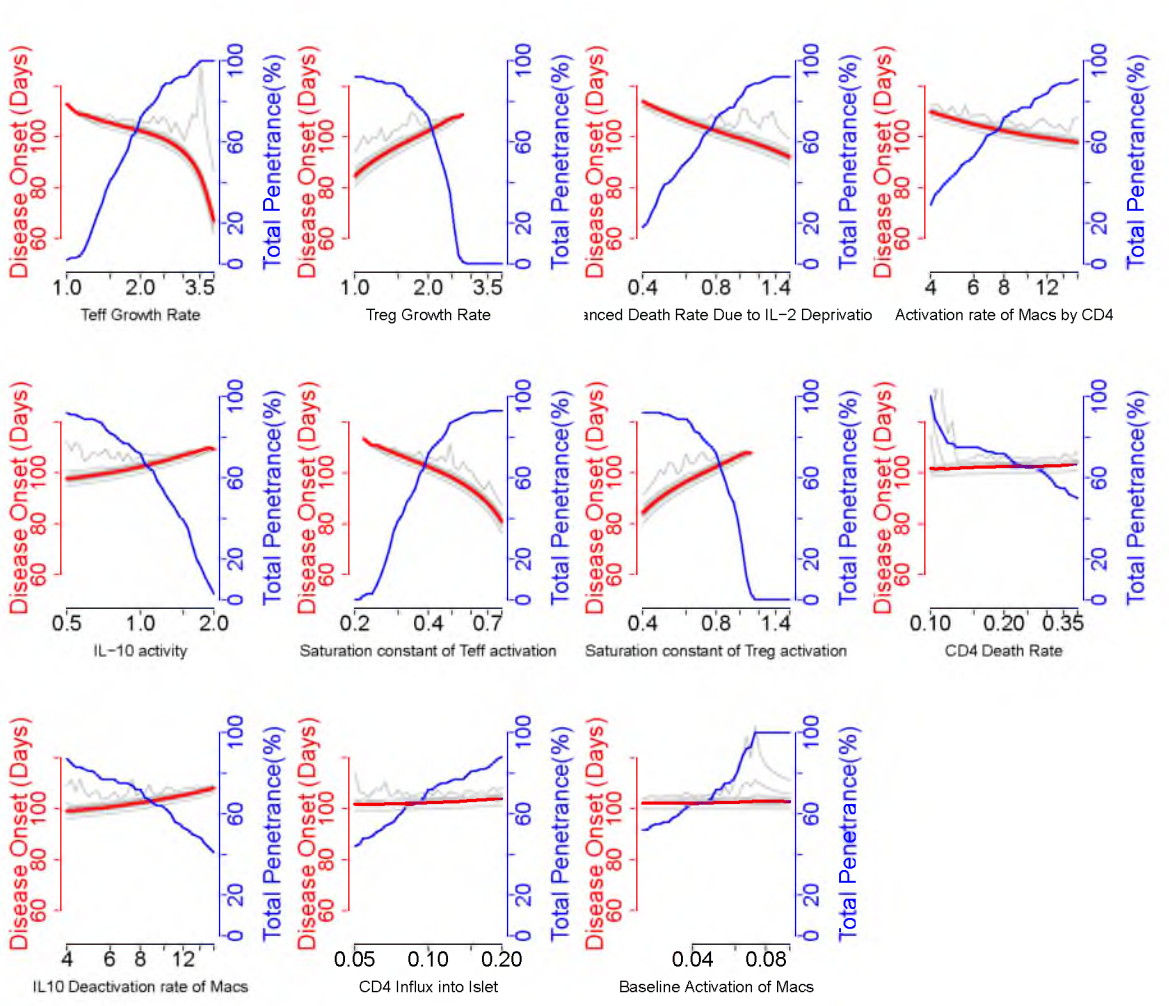

Figure 3.11: Sensitivity analysis of full model. Parameters that affect incidence and age of onset. We vary an individual parameter from 50% to 200% of its baseline value. For each other parameter, we randomly sample 100 times from a normal distribution centered on the baseline value and run a seperate simulation for each parameter set. The blue line shows the percentage of diabetic mice, by the end of 50 weeks, in the sample. The red and grey lines show the median and deciles, respectively, of the age of onset.

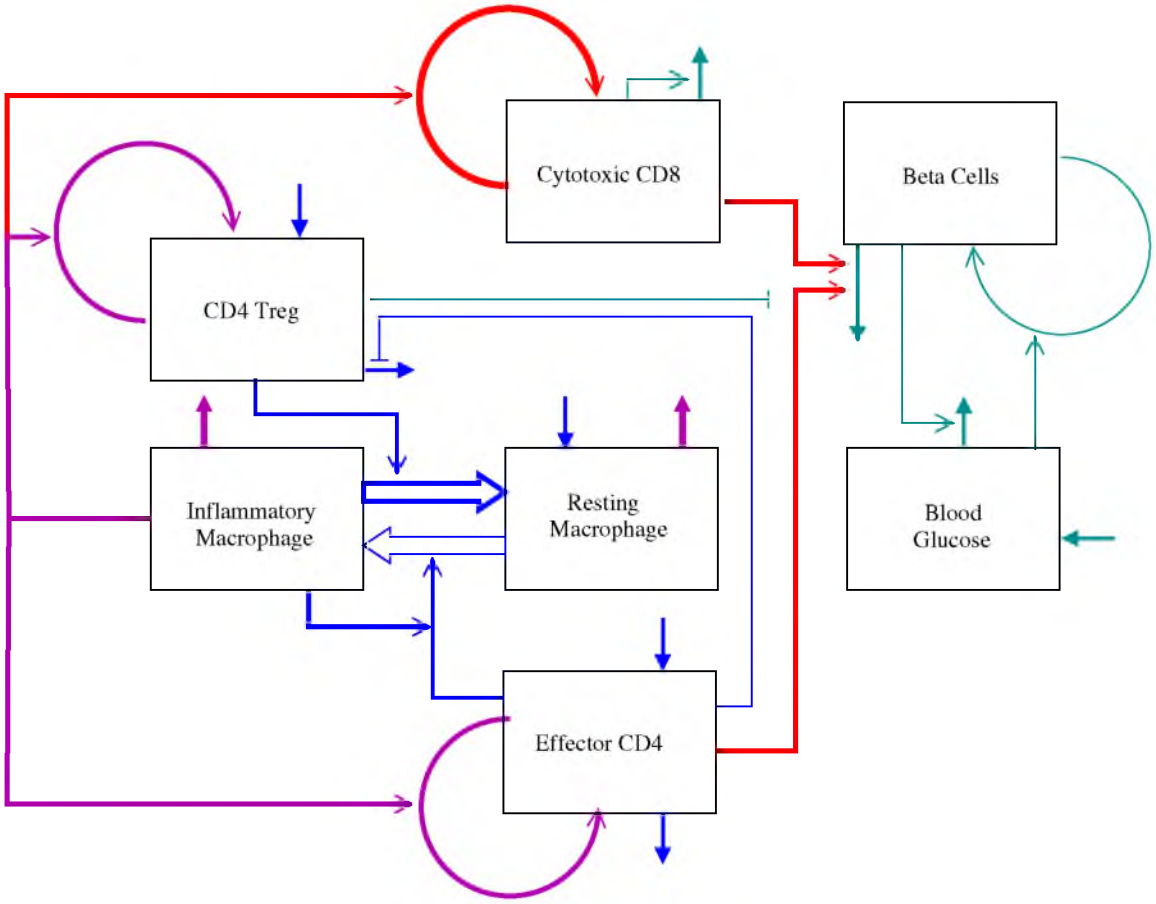

Figure 3.12: Schematic diagram summarizing the model in this chapter. Arrows are colored according to whether they affect incidence/penetrance (blue), age of onset (red), or both (purple). The strength of the effect is denoted by the arrow thickness. Arrows in dark cyan had negligible effect.

Table 3.4: Key behaviors this model can reproduce

Phenomenom	Source	Outcome
T1D at 16 weeks	[4]	Fitted
T1D in 80% of females	[8]	Fitted
T1D rapid without Tregs	[15] and [20]	
Protection from T1D with enhanced IL-2 production	[62]	
Protection from T1D with exogenous IL-2	[62]	
Protection from T1D with anti-CD3 treatment	[21]	
Protection from T1D with Treg treatment	[23]	
Delay of T1D with IFN-α treatment	[23]	
Synergy between Treg and IFN-α treatments	[23]	
NOD8.3 have faster onset, same incidence	[74]	
IGRP-specific CD8 predict outcome	[70]	
Inflammation predicts T1D months in advance	[26]	

CHAPTER 4

ACCELERATION AND DELAY OF TYPE 1 DIABETES BY VIRAL INFECTION

4.1 Introduction

The link between viral infection and the development of autoimmune disease is complex. Incidence of autoimmune diseases such as Type 1 Diabetes (T1D) are rising worldwide [28], particularly in developed nations and among those with access to modern healthcare [17]. The 'hygiene hypothesis' suggests that early childhood infection may be protective against the development of such diseases. On the other hand, viral infection is thought to act as a trigger of automimmunity in some, if not all, cases [27].

Viral infection of the NOD mouse has revealed this dichotomy in the laboratory setting. It may accelerate or delay T1D depending on the type of virus and the age of infection. The goal of this chapter is to understand the mechanisms by which viral infection can change the course of T1D.

4.1.1 Biological background

The nonobese diabetic (NOD) mouse is a useful animal model that spontaneously develops T1D. NOD mice develop a progressive insulitis or invasion of pancreatic islets by immune cells beginning at about 3-4 weeks of age. In roughly 80% of females, this leads to destruction of the β-cells and T1D onset at about 12-20 weeks [38]. Viral infection of these mice can either accelerate or delay T1D, depending not only on the virus but also the age of infection. Table 4.1 summarizes some representative experiments (see [16] for a more complete list).

Viruses can affect T1D progression in many ways. First, many viruses activate immunoregulatory processes. Infection of NOD mice with Coxsackie virus B3 (CVB3) or lymphocytic choriomeningitis virus (LCMV) can promote the development of regulatory T-cells (Tregs) and increase expression of the anti-inflammatory molecule PDL1 [23]. Artificial stimulation of Tregs and PDL1 abrogates T1D with similar effectiveness as viral

infection [23]. Viral infection can also interfere with the ongoing autoimmune response. During murine gammaherpes virus (MHV) infection, self antigen processing by dendritic cells is reduced [64].

Viruses can affect T1D progression even if they do not invade β-cells. LCMV and RRV infect cells within the pancreas, but not β-cells [23]. RRV does not even infect islet cells within the islet of Langerhans, where β-cells reside [32]. CVB4 does infect β-cells and is capable of accelerating T1D [61], suggesting that the cell type invaded determines the effect of the virus [23]. This is far from certain, however, as the type and number of infected cells is hard to study.

In general, infection early in life tends to be protective from T1D, whereas infection later in life can accelerate it. For example, infection with rotavirus (RRV) early in life delays T1D [32], whereas infection later in life accelerates it [33]. One hypothesis is that the increase of insulitis over time makes viral infection more diabetogenic. During an infection or other inflammatory event, innate immune cells called **dendritic cells** (DCs) become activated in response to either signals of damage or microbial products. These DCs can then activate antigen-specific T-cells, which fight the infection. However, there is no gurantee that the T-cells they activate have the correct specificity. For example, a virus can cause localized necrosis, leading to the release of self antigens. The DC presents these self antigens in an immunogenic manner alongside the viral antigen. We show in chapter 1 that the presence of regulatory T-cells (Tregs) and tolerogenic DC can make it more likely to generate a viral-specific immune response, but it is never guaranteed. As the mouse ages and insulitis becomes more intense, the presentation of self antigen increases. This makes it more likely that a viral infection could activate an autoimmune response. This first mechanism is known as **epitope spreading** as the immune response spreads from antigen, or epitope, to another.

The second major mechanism of T1D acceleration is **bystander activation**, the nonspecific activation of T-cells by inflammatory signals. Immune cells communicate via messenger molecules called cytokines. During an infection in the pancreas, T-cells that already reside there will, regardless of their specificity, receive many activating signals from other immune cells. The incoming signals may activate the T-cells to perform their effector function: the killing of β-cells. As insulitis progresses, more T-cells home to the pancreas, increasing the effect of bystander activation.

Viral infection early in life is often beneficial for NOD mice. One hypothesis is that viral infection generates a population of regulatory T-cells or **Tregs** [16, 56]. Although

Tregs are antigen specific, they can control other T-cells nonspecifically via cytokines as well as semispecifically, through colocalization to the same dendritic cell (see Chapter 2). The viral infection will also generate a virus-specific immune response that competes with for resources with the autoimmune response.

4.1.2 Prior modeling

We discuss much of the necessary modeling background in the prior two chapters. For more information on T1D in the NOD mouse, see Chapter 3. For more information on models of immune reuglation, see Chapter 2. Here we highlight some important concepts.

The development of T1D occurs in two stages. First, an apoptotic wave drives the initiation of insulitis [71]. Maree and Keshet show that the failure to clear necrotic cells can potentially lead to an instability of the resting state [47]. Second, the progression of insulitis results from the outgrowth of a particular population of T-cells [7]. Keshet and Khadra [40] demonstrate that competition between different high affinity and low affinity T-cells can lead to bistability. In Chapter 2, we develop a two-stage model of T1D and show that it can reproduce many results from the literature.

Viral infection may affect T1D due to immune competition or the generation of Tregs. De Boer studies the competition between T-cell populations and concludes that competition should lead to domination by the highest affinity T-cell clone [19]. In Chapter 2, we expand this model to include multiple DC populations and find that this allows multiple T-cell populations to coexist. We also show that this competitive balance depends on the presence of Tregs. Tregs can also prevent β-cell destruction within the islet [15] instead of directly inhibiting T-cell growth. Alexander et al. [5] review this mechanism of Treg activity and conclude that Tregs can make self reactive responses arbitrarily small.

In a model of multiple sclerosis treatment, De Boer and Borghans show that administration of T-cells suppresses immunopathology via the induction of Tregs [11]. In Chapter 3, we show that Tregs can act to slow but not stop T1D. Tregs invade the islets along with effector T-cells after the apoptotic wave and prevent the immediate destruction of the β-cells. Tregs and effectors coexist in one of two states: severe or mild insulitis. The former leads to T1D progression, whereas the latter does not.

4.1.3 Our approach

The goal of this study is to investigate the effect of viral infection on the timing and incidence of T1D. In particular we are interested in how the nature of the virus and the time of infection change the outcome. Viruses may affect T1D in different ways and a

mathematical model allows us to study each mechanism in isolation. The mechanisms we consider are

- virus induced inflammation of the islets, which leads to greater presentation of self antigen by immunogenic DC (epitope spreading),
- the nonspecific activation of T-cells leading to rapid β-cell destruction (bystander activation),
- competition between viral-specific T-cells and self reactive T-cells, and
- the induction of Tregs by viral-specific T-cells.

Our model has two components: an islet state model and a T-cell/DC interaction model in the pancreatic lymph node. The islet state model tracks the transition of islets between different states of infection, inflammation, and insulitis. Each islet state generates a different population of dendritic cells. For example, dendritic cells from inflamed islets are immunogenic and those from infected islets are more likely to present viral antigen. The heterogeneity of the islets is therefore crucial for accurately representing the full array of dendritic cells that traffic to the pancreatic lymph node. The T-cell/DC interaction model is a basic model of T-cell growth and death in response to the DC population emerging from the pancreas. T-cells competitively bind to DC, proliferating when bound to immunogenic DC and dying when bound to tolerogenic DC. These T-cell populations in turn then drive the transitions in the islet state model.

We find that time of infection, especially in relation to the apoptotic wave, can greatly alter the effect of viral infection on T1D. In general, we find that early infection should delay or eliminate T1D whereas later infection promotes or acceleratates it. We predict that bystander activation can cause an acceleration of T1D but decrease incidence. The combination of multiple mechanisms in a single virus can create a window of infection during which infection is beneficial.

4.2 Model description

4.2.1 Islet equations

As Diabetes progresses, Islets are gradually invaded by T-Cells, B-Cells, and inflammatory macrophages in a process called insulitis. To allow for efficient, unbiased comparisons of the extent of insulitis in different mice, pathologists group islets into distinct histological stages. We follow the same convention here, except that for the first two stages we include additional states, I_0^* and I_1^*, which differ subtly as described below.

- Stage 0 (I_0 and I_0^*): No insulitis

- Stage 1 (I_1 and I_1^*): Peri-Insulitis (Leukocytes accumulate at the periphery of the islet)
- Stage 2 (I_2): Intraislet-Insulitis (Leukocytes penetrate into the islet, covering less than 50%)
- Stage 3 (I_3): Intraislet-Insulitis (Leukocytes penetrate into the islet, covering more than 50%)
- Stage 4 (I_4): Intraislet-Insulitis (Leukocytes penetrate the entire islet)

Progression from stage 0 to stage 1 represents the initial infiltration of T-cells into an islet. We assume that T-cells can only home to islets that are inflamed and thus express the necessary adhesion molecules and chemokines. Let I_0 be the proportion of uninflamed islets and I_0^* the proportion of inflamed islets,

$$\frac{dI_0}{dt} = -\big(a + f(t)\big)I_0 + \kappa I_0^*$$
$$\frac{dI_0^*}{dt} = \big(a + f(t)\big)I_0 - \kappa I_0^*$$

Islets become inflamed at a basal rate a, but there may be additional time dependent inflammation

$$f(t) = \begin{cases} a_W & t_{w1} < t < t_{w2} \\ 0 & \text{else} \end{cases}$$

due to either a developmental program or weaning of the mice.

As with state 0, there are two classes of state 1. State I_1 are islets that have a large number of Tregs, high expression of CRIg and IL-10, low expression of IL-12 and IFNg, and low levels of beta-cell destruction. Dendritic cells within these islets remain tolerogenic when they traffic to the pancreatic lymphnode and do not promote a further immune response. I_1^* have a fewer Tregs, low expression of CRIg and IL-10, high expression of IL-12 and IFNg, and subclinical yet persistent levels of beta cell destruction, which is sufficient to drive an immune response in the pancreatic lymph node. Entry into one class or the other from the uninflamed state depends on ratio of effector to Treg cells in the periphery.

$$I_0^* \text{ to } I_1^* \text{ transition} = \beta p(T_S, R) I_0^* T_S$$
$$I_0^* \text{ to } I_1 \text{ transition} = \beta\big(1 - p(T_S, R)\big) I_0^* T_S$$
$$p(T_S, R) = \frac{(kT_S)^n}{R^n + (kT_S)^n}$$

All islets then progress through stages $1 \rightarrow 4$ at a rate that depends on T_S. We assume that progression of the disease is dependent upon a continued immune response, which gradually progresses in pathogenicity over time.

$$I_i \text{ to } I_{i+1} \text{ transition} = \rho I_i T_S$$

After reaching stage 4, islets are destroyed at a rate η. Figure 4.1 schematically represents these transitions.

In summary, the islet equations are

$$\begin{aligned}
\frac{dI_0}{dt} &= -\big(a + f(t)\big)I_0 + \kappa I_0^* \\
\frac{dI_0^*}{dt} &= \big(a + f(t)\big)I_0 - \kappa I_0^* - \beta I_0^* T_S \\
\frac{dI_1}{dt} &= \beta\big(1 - p(T_S, R)\big)I_0^* T_S - \rho I_1 T_S \\
\frac{dI_1^*}{dt} &= \beta p(T_S, R) I_0^* T_S - \rho I_1^* T_S \\
\frac{dI_2}{dt} &= \rho(I_1^* + I_1 - I_2)T_S \\
\frac{dI_3}{dt} &= \rho(I_2 - I_3)T_S \\
\frac{dI_4}{dt} &= \rho I_3 T_S - \eta I_4
\end{aligned} \tag{4.1}$$

4.2.2 Viral infection

During viral infection, infected cells and virions may be unevenly distributed throughout the pancreas. For simplicity, we assume that each islet may be infected individually, but that the inflammation state does not affect the susceptibility to infection, or the time it takes to clear the virus. To account for islets that infect the pancreas but not the islets, we divide the pancreas into 'islet zones' (Figure 4.2), which include an islet and the surrounding tissue. Let $\mathbf{I}(t) = \{I_0, I_0^*, \cdots\}$ be the vector of all uninfected states, and let $\mathbf{V}(t) = \{V_0, V_0^*, \cdots\}$ be the vector of all corresponding infected states. Then,

$$\begin{aligned}
\frac{d\mathbf{I}}{dt} &= L_I \mathbf{I} - g(t)\mathbf{I} + \delta_V \mathbf{V} \\
\frac{d\mathbf{V}}{dt} &= L_V \mathbf{V} + g(t)\mathbf{I} - \delta_V \mathbf{V}
\end{aligned}$$

where

$$g(t) = \begin{cases} r_{\max} & t_{\text{inf}} < t < t_{\text{inf}} + t_{\text{dur}} \\ 0 & \text{else} \end{cases}$$

is the infection rate. The matrix L_I represents the transition process in (4.1). The viral transition matrix, L_V, is similar to L_I but may differ in the following ways:

1. The islet inflammation rate, a, could potentially be much higher during viral infection. This depends on the nature of the virus, its tendency to elicit an immune response, and whether or not it infects islets. Therefore we define two parameters a_I and a_V

that describe this inflamation rate in infected and uninfected islets-zones.

2. The death rate of β-cells in the islets may be greater in infected areas. However, we are not considering viruses that directly kill β-cells. During an immune response, the release of cytokines can activate cells in a nonspecific way in a process called bystander activation. As discussed in the previous chapter, islets with advanced insulitis harbor a large population of potentially deadly T-cells that are kept under tight regulation by Tregs. Thus we assume that the viral infection can eliminate islets in the V_2, V_3, or V_4 classes. We define two separate killing rates η_I and η_V. The viral islet-death rate, η_V, is not only larger than η_I, but also applies to V_2 and V_3.

The full islet equations are

$$\begin{aligned}
\frac{dI_0}{dt} &= -(a_I + f(t))I_0 + \kappa I_0^* - g(t)I_0 + \delta_V V_0 \\
\frac{dI_0^*}{dt} &= (a_I + f(t))I_0 - \kappa I_0^* - \beta I_0^* T_S - g(t)I_0^* + \delta_V V_0^* \\
\frac{dI_1}{dt} &= \beta(1 - p(T_S, R))I_0^* T_S - \rho I_1 T_S - g(t)I_1 + \delta_V V_1 \\
\frac{dI_1^*}{dt} &= \beta p(T_S, R)I_0^* T_S - \rho I_1^* T_S - g(t)I_1^* + \delta_V V_1^* \\
\frac{dI_2}{dt} &= \rho(I_1^* + I_1 - I_2)T_S - g(t)I_2 + \delta_V V_2 \\
\frac{dI_3}{dt} &= \rho(I_2 - I_3)T_S - g(t)I_3 + \delta_V V_3 \\
\frac{dI_4}{dt} &= \rho I_3 T_S - \eta_I I_4 - g(t)I_4 + \delta_V V_4
\end{aligned}$$

for uninfected islets and

$$\begin{aligned}
\frac{dV_0}{dt} &= -(a_V + f(t))V_0 + \kappa V_0^* + g(t)I_0 - \delta_V V_0 \\
\frac{dV_0^*}{dt} &= (a_V + f(t))V_0 - \kappa V_0^* - \beta V_0^* T_S + g(t)I_0^* - \delta_V V_0^* \\
\frac{dV_1}{dt} &= \beta(1 - p(T_S, R))V_0^* T_S - \rho I_1 T_S + g(t)I_1 - \delta_V V_1 \\
\frac{dV_1^*}{dt} &= \beta p(T_S, R)V_0^* T_S - \rho V_1^* T_S + g(t)I_1^* - \delta_V V_1^* \\
\frac{dV_2}{dt} &= \rho(V_1^* + V_1 - V_2)T_S + g(t)I_2 - (\delta_V + \eta_V)V_2 \\
\frac{dV_3}{dt} &= \rho(V_2 - V_3)T_S + g(t)I_3 - (\delta_V + \eta_V)V_3 \\
\frac{dV_4}{dt} &= \rho V_3 T_S + g(t)I_4 - (\delta_V + \eta_V)V_4
\end{aligned}$$

for infected islets.

4.2.3 T-cell equations

In Chapter 2, we develop a model of multiple T-cell clones competing via competition for space on dendritic cells. Here, we develop a slightly simpler model that preserves the following features:

- Immunogenic DC promote T-cell proliferation, whereas Tolerogenic DC promote T-cell apoptosis or anergy.
- Dendritic cells have a finite capacity for interacting with T-cells. This limits the proliferation of T-cells and is the source of competition.
- T-cell–dendritic cell interaction is antigen specific, although a DC may present multiple antigens.
- Tregs depend on growth factors produced by effector cells to proliferate.

First, we consider a single T-cell clone, T, and two dendritic cell populations: immunogenic, D^I, and tolerogenic, D^T. These dendritic cell populations present antigen in the same way, so T interacts with them equally strongly. The T-cell clone transitions between three states, a dividing state T^*, a resting state T_0, and an anergic state T^a according to

$$\frac{dT^*}{dt} = \alpha_p C^*(T - T^* - T^a) - \omega_p T^* \tag{4.2}$$

$$\frac{dT^a}{dt} = \alpha_p C^a(T - T^* - T^a) - \omega_p T^a \tag{4.3}$$

$$C^* = \sigma D^I \tag{4.4}$$

$$C^a = \sigma D^T \tag{4.5}$$

where C^* and C^a are the numbers of contacts per day that a single T-cell has with immunogenic and tolerogenic DC, respectively. We assume that transitions between T_0, T^*, and T^a are rapid and equilibriate quickly. Therefore, we set (4.3) and (4.4) to zero. In steady state $T^* = T\frac{C^*}{k+C^*+C^a}$ and $T^a = T\frac{C^*_a}{k+C^*+C^a}$, where $k = \omega_p/\alpha_p$ is the number of contacts required per day to achieve half maximal activation. Therefore the full formula for the T-cell equation is

$$\frac{dT}{dt} = T\frac{\gamma C^* - \mu C^a}{k_p + C^a + C^*} - \delta_T T$$

This description readily expands to include multiple DC populations, indexed by i, and multiple T-cell populations, indexed by j.

$$\frac{dT_j}{dt} = T_j\frac{\gamma C^*_j - \mu C^a_j}{k_p + C^a_j + C^*_j} - \delta_T T_j$$

$$C^*_j = \sum_i \sigma_{ij} D^I_i$$

$$C_j^a = \sum_i \sigma_{ij} D_i^T$$

These equations change slightly for a Treg population. First, tolerogenic DC have no effect on Tregs. Second, Tregs depend on T-cells for growth factors. We model this with a reduced activation rate while bound to immunogenic DC. For a Treg bound to DC i, the activation rate is

$$\hat{\alpha}_i = \alpha \frac{G_i}{k_R H_i + k_I + G_i}$$
$$G_i = \text{Effectors that contact DC } i$$
$$H_i = \text{Tregs that contact DC } i.$$

The full Treg equation for Treg population R_j is

$$\frac{dR_j}{dt} = R_j \frac{\gamma C_j^R}{k_p + C_j^R} - \delta_T T_j$$
$$C_j^R = \sum_i \sigma_{ij} D_i^I \frac{G_i}{k_R H_i + k_I + G_i}$$
$$G_i = \sum_j \sigma_{ij} T_j$$
$$H_i = \sum_j \sigma_{ij} R_j$$

Rather than explicitly model the binding and unbinding of T-cells, we shall instead assume that the death rate of an individual DC is proportional to the number of contacts that it makes.

$$\frac{dD_i}{dt} = A_i(t) - \delta_D D_i - \nu \sum_j \sigma_{ij} T_j D_i \tag{4.6}$$

where σT is the rate of contacts and ν is the death rate per contact. If we assume that each DC can contact 10 T-cells simultaneously and that each interaction lasts around 10 minutes, then $\sigma T \approx 10^3$ per day. We assume that the max number of T Cells is roughly 10^6 cells (in one ml of blood); therefore, $\sigma \approx 10^{-3}$.

4.2.4 Specific immune populations

We track two populations of effector cells T_S, specific for an islet-associated self antigen S, and T_V, specific for the viral antigen V. We also consider a pool of self reactive T-cells R, which arise during the autoimmune response of T_S. We expect that, even if they are not specific for the same antigen, S, they are specific to antigens that are correlated with S in space and time and therefore likely to be presented on the same dendritic cell. These

antigens may or may not be correlated with V.

We track four types of dendritic cells.

- D_S^T Tolerogenic DC presenting S but not V. T_S binds with affinity σ_S, R with affinity σ_{SR}. T_V does not bind to these cells.
- D_S^I Immunogenic DC presenting S but not V
- D_V^I Immunogenic DC presenting V but not S. T_V binds with affinity σ_V, R with affinity σ_{VR}. T_S does not bind to these cells.
- D_B^I Immunogenic DC presenting both V and S. T_S binds with affinity σ_S, T_V with σ_V and R with the maximum of σ_{SR} and σ_{VR}.

Tolerogenic DC originate only from uninflamed islets I_0 and islets with high Treg control (I_1). Each day, A_T DC leave uninflamed islets and traffic to the pLN, with a fraction ϕ_S expressing antigen S. Immunogenic DC originate from all other classes of islets. Any DC presenting viral antigens will automatically become immunogenic. Immunogenic DC leave the islets at a rate A_I, with proportions ϕ_S and ϕ_V presenting self and viral antigens, respectively. To calculate the number of DCs that present both, we must also specify the correlation ψ. If ψ is equal or close to 1, then S and V will likely always appear together on DCs. If ψ is equal or close to -1, then S and V rarely co-occur. We can therefore view ψ to reflect which cells the virus is likely to infect. A value of $\psi = 1$ implies the virus only infects β-cells, whereas a value of $\psi = -1$ implies the virus invades cells outsides the islets. Let ϕ_B be the probability that a DC presents both antigens, then

$$\phi_B = \begin{cases} 0 & p_b < 0 \\ \phi_S & p_b > \phi_V > \phi_S \\ \phi_V & p_b > \phi_S > \phi_V \\ \phi_S + \phi_V - 1 & p_b < \phi_V + \phi_S - 1 \\ p_b & \text{otherwise} \end{cases}$$

$$p_b = \phi_S\phi_V + \psi\sqrt{(1-\phi_V)(1-\phi_S)\phi_S\phi_V}$$

$$A_{TS} = \phi_S A_T(I_0 + I_1) + A_T(\phi_S - \phi_B)(V_0 + V_1)$$

$$A_{IS} = \phi_S A_I(I_0^* + I_1^* + I_2 + I_3 + I_4) + A_I(\phi_S - \phi_B)(V_0^* + V_1^* + V_2 + V_3 + V_4)$$

$$A_{IV} = (\phi_V - \phi_B)A_I(V_0 + V_0^* + V_1 + V_1^* + V_2 + V_3 + V_4)$$

$$A_{IB} = \phi_B A_I(V_0 + V_0^* + V_1 + V_1^* + V_2 + V_3 + V_4)$$

Once inside the lymphnode, these DC interact with T-cells as described in the previous section. The full system is

$$\frac{dT_S}{dt} = \alpha_S + T_S\frac{\gamma C_S^* - \mu C_S^a}{k_p + C_S^a + C_S^*} - \delta_T T_S \tag{4.7}$$

$$\frac{dT_V}{dt} = \alpha_R + T_V \frac{\gamma C_V^*}{k_p + C_V^a} - \delta_I T_V \tag{4.8}$$

$$\frac{dR}{dt} = R\frac{\gamma C_R^*}{k_p + C_R^*} - \delta_T R \tag{4.9}$$

$$C_S^* = \sigma_S(D_S^I + D_B^I) \tag{4.10}$$

$$C_S^a = \sigma_S D_S^T \tag{4.11}$$

$$C_V^* = \sigma_V(D_V^I + D_B^I) \tag{4.12}$$

$$C_R^* = \sigma_{RS}\frac{\sigma_S T_S}{k_R\sigma_{RS}R + \sigma_S T_S + k_I} D_V^I + \sigma_{RV}\frac{\sigma_V T_V}{k_R\sigma_{RV}R + \sigma_V T_V + k_I} D_S^I \tag{4.13}$$

$$+ \sigma_{BS}\frac{\sigma_S T_S + \sigma_V T_V}{k_R\sigma_{RS}R + \sigma_S T_S + \sigma_V T_V + k_I} D_V^I \tag{4.14}$$

$$\frac{D_S^T}{dt} = A_{TS} - \delta_D D_S^T - \nu(\sigma_S T_S + \sigma_{RS}R)D_S^T \tag{4.15}$$

$$\frac{D_S^I}{dt} = A_{IS} - \delta_D D_S^I - \nu(\sigma_S T_S + \sigma_{RS}R)D_S^I \tag{4.16}$$

$$\frac{D_V^I}{dt} = A_{IV} - \delta_D D_V^I - \nu(\sigma_V T_V + \sigma_{RV}R)D_V^I \tag{4.17}$$

$$\frac{D_B^I}{dt} = A_{IB} - \delta_D D_B^I - \nu(\sigma_V T_V + \sigma_S T_S + \sigma_{RB}R)D_B^I \tag{4.18}$$

Figure 4.3 summarizes the specific immune populations schematically.

4.3 Virus-free dynamics

In the long term, the only steady state of the full system (4.1) and (4.7)-(4.18) is trivial, with no islets remaining. Thus, T1D is inevitable for a sufficiently long-lived mouse. However, the time it takes to reach this steady state can vary over several orders of magnitude. In this section, we demonstrate the apoptotic wave, though brief, can dramatically shorten the time it takes for T1D onset.

4.3.1 Analysis of islet equations

For constant $T_S \neq 0$, the only equilibrium of (4.1) is the trivial solution: $I_0 = I_0^* = I_1 = \cdots = I_3 = I_4 = 0$. Whereas if $T_S = 0$, then (4.1) is degenerate and the equilibria form a 6-dimensional subspace. For nonconstant T_S, there exist other equilibria. To see this we consider a greatly reduced system

$$\begin{aligned}
\frac{dI_3}{dt} &= -\rho I_3 T_S(t) \\
\frac{dI_4}{dt} &= \rho I_3 T_S(t) - \eta I_4 \\
I_3(0) &= 1 \\
I_4(0) &= 0
\end{aligned}$$

which has the solution

$$\begin{aligned} I_3(t) &= e^{V(t)} \\ I_4(t) &= \rho e^{-\eta t} \int_0^t e^{\eta\tau} T_S(\tau) e^{V(\tau)}\, d\tau \\ V(t) &= \rho \int_0^t T_S(\tau)\, d\tau \end{aligned}$$

As $t \to \infty$, $I_3 \to e^{V(\infty)}$ and $I_4 \to 0$. We expect a nontrivial solution if $\int_0^\infty T_s(t)\, dt$ is bounded.

Therefore, we consider the case $T_S = T_0 e^{-\delta t}$. In the limit that $t \to \infty$

$$\begin{aligned} I_0 &= \frac{\kappa}{a+\kappa} e^{-\beta T_0/\delta} \\ I_0^* &= \frac{a}{a+\kappa} e^{-\beta T_0/\delta} \\ I_1 + I_1^* &= \frac{\beta\rho e^{-\frac{T_0(\beta+\rho)}{\delta}} \left(\delta\left(e^{\frac{\rho T_0}{\delta}} - e^{\frac{\beta T_0}{\delta}}\right) + T_0(\beta-\rho)e^{\frac{\beta T_0}{\delta}}\right)}{\delta(\beta-\rho)^2} \\ I_2 &= \frac{\beta e^{-\frac{(\beta+\rho)\rho T_0}{\delta}} \left(-2\delta^2\left(e^{\frac{\rho T_0}{\delta}} - e^{\frac{\beta\rho T_0}{\delta}}\right) + (\beta-\rho)^2\rho^2 T_J^2 e^{\frac{\beta\rho T_0}{\delta}} - 2(\beta-\rho)\delta\rho T_0 e^{\frac{\beta\rho T_0}{\delta}}\right)}{2(\beta-\rho)^3\delta^2} \\ I_3 &= \frac{\beta\rho^3 e^{-\frac{T_0(\beta+\rho)}{\delta}} \left(-6\delta^3\left(e^{\frac{\beta T_0}{\delta}} - e^{\frac{\rho T_0}{\delta}}\right) + 6\delta^2 T_0(\beta-\rho)e^{\frac{\beta T_0}{\delta}}\right)}{6\delta^3(\beta-\rho)^4} \\ &\quad + \frac{\beta\rho^3 e^{-\frac{T_0(\beta+\rho)}{\delta}} \left(-3\delta T_J^2(\beta-\rho)^2 e^{\frac{\beta T_0}{\delta}} + T_0^3(\beta-\rho)^3 e^{\frac{\beta T_0}{\delta}}\right)}{6\delta^3(\beta-\rho)^4} \\ I_4 &= 0 \end{aligned}$$

Figure 4.4 shows the equilibrium distribution of islets states as a function of the initial T-cell population. We see that equilibrium changes continuously as a function of the initial condition. A larger initial T-cell population means that more islets will eventually end up with more advanced insulitis.

4.3.2 Steady state of T-cell equations

We recognize that (4.1) and (4.7)-(4.18) do not have any steady states. However, it is illustrative to consider a fixed islet population and compute the steady states of just (4.7)-(4.18). This steady state gives us information on the progression of Type 1 Diabetes. The initial invasion of the islets can take one of two forms, either mild or severe, depending on the relative population sizes of effectors and Tregs. If Tregs outnumber effectors, then most newly infiltrated islets will enter the mild insulitis state. If effectors outnumber Tregs, most enter the severe state. In the absence of infection, (4.7)-(4.18) reduce to

$$\frac{dT_S}{dt} = \alpha_S + T_S\frac{\gamma C_S^* - \mu C_S^a}{k_p + C_S^a + C_S^*} - \delta_T T_S \tag{4.19}$$

$$\frac{dR}{dt} = \alpha_R + R\frac{\gamma C_R^*}{k_p + C_R^*} - \delta_T R \tag{4.20}$$

$$\frac{dD_S^T}{dt} = \phi_S A_T I_T - \delta_D D_S^T - \nu(\sigma_S T_S + \sigma_{RS} R) D_S^T \tag{4.21}$$

$$\frac{dD_S^I}{dt} = \phi_S A_I I_I - \delta_D D_S^I - \nu(\sigma_S T_S + \sigma_{RS} R) D_S^I \tag{4.22}$$

$$C_S^* = \sigma_S D_S^I \tag{4.23}$$

$$C_S^a = \sigma_S D_S^T \tag{4.24}$$

$$C_R^* = \sigma_{RS}\frac{\sigma_S T_S}{k_R \sigma_{RS} R + \sigma_S T_S + k_I} D_S^I \tag{4.25}$$

where $I_T = I_0 + I_1$ and $I_I = I_0^* + I_1^* + I_2 + I_3 + I_4$ are the proportions of islets that export tolerogenic DC and immunogenic DC, respectively.

To analyze the equilibria of (4.19), we use the nondimensionalization shown in Table 4.2. We see that after nondimensionalization, some parameters are dominant and others negligible. In particular, the proliferation and death rates associated with T-cell-DC interaction are much larger than the normal turnover rate of T-cells. To account for these differences of scale, we make the following substitution

$$\hat{\gamma} \to g\epsilon^{-1}$$
$$\hat{\mu} \to m\epsilon^{-1}$$
$$\hat{k}_I \to k\epsilon^2$$

After substitutions, all parameters are $\mathcal{O}(1)$ except for $\epsilon \gg 1$. We use the substitution

$$X \sim \epsilon^{-1} X_{-1} + X_0 + \cdots$$
$$Y \sim \epsilon^{-1} Y_{-1} + Y_0 + \cdots$$

and solve (4.19)-(4.25) using matched asymptotic expansions. Substitution yields three different solution forms. First, if

$$\begin{aligned} I_I &< \frac{\hat{\mu}\hat{A}_T}{\hat{\gamma}\hat{A}_I} I_T \\ &= w_1 I_T \\ &\approx .1 I_T \end{aligned}$$

then the only positive solutions have $X_{-1} = X_0 = Y_{-1} = 0$. The lowest order nonzero terms, X_1 and Y_0, satisfy

$$0 = 1 + \hat{A}_I I_I + \hat{A}_T I_T + \hat{\alpha}_R Y_0 + (\hat{\gamma}\hat{A}_I I_I - \hat{\mu}\hat{A}_T I_T) X_1 \tag{4.26}$$

$$0 = \hat{A}_I \hat{\alpha}_S \hat{\sigma}_{RS} I_I X_1 + \hat{\alpha}_R k_R (1 + \hat{\alpha}_R) Y_0 (1 - Y_0) \tag{4.27}$$

which has a unique positive solution. Thus, if anergy from tolerogenic DCs outweighs proliferation from immunogenic ones, then the T_S population will be very small. More importantly, we find that $R \gg T_S$, indicating that almost every islet will enter the mild insulitis state, I_1, as opposed to the severe insulitis state I_1^*. This means that I_I will rise slowly. However, it will still rise as our solution T_S does not tend to zero.

The second solution type occurs when $I_I > w_1 I_T$ and

$$\begin{aligned} I_I &< \frac{1}{1 - \hat{\sigma}_{RS}} \frac{\hat{\mu}\hat{A}_T}{\hat{\gamma}\hat{A}_I} I_T \\ &= w_2 I_T \\ &= .35 I_T \end{aligned}$$

indicating intermediate numbers of immunogenic DC. Under these circumstances, both X and Y are $\mathcal{O}(\epsilon^{-1})$:

$$\begin{aligned} X &\sim \epsilon^{-1} \frac{k_R(\hat{\gamma}\hat{A}_I I_I - \hat{\mu}\hat{A}_T I_T)^2}{\hat{\alpha}_R(\hat{\gamma}\hat{A}_I I_I(k_R + \hat{\sigma}_{RV} - 1) + \hat{\mu}\hat{A}_T I_T(1 - k_R))} \\ Y &\sim \epsilon^{-1} \frac{k_R(\hat{\gamma}\hat{A}_I I_I - \hat{\mu}\hat{A}_T I_T)(-\hat{\gamma}\hat{A}_I I_I + \hat{\mu}\hat{A}_T I_T + \hat{\gamma}\hat{A}_I I_I \sigma_{RS})}{\hat{\alpha}_R(\hat{\gamma}\hat{A}_I I_I(k_R + \hat{\sigma}_{RV} - 1) + \hat{\mu}\hat{A}_T I_T(1 - k_R))} \end{aligned}$$

As T_S and R have the same order, we expect that significant numbers of islets will enter both the severe and mild states. The higher absolute number of T_S cells means that these islets will also progress faster to the latter stages, which only produce immunogenic DC.

Finally, if $I_I > w_2 I_T$, the Treg population cannot compete with the effector population and Y drops to a lower order of magnitude

$$\begin{aligned} X &\sim \epsilon^{-1} \frac{k_R(\hat{\gamma}\hat{A}_I I_I - \hat{\mu}\hat{A}_T I_T)}{\hat{\alpha}_R} \\ Y &\sim \frac{\hat{\mu}\hat{A}_T I_T - \hat{\gamma}\hat{A}_I I_I}{-\hat{\gamma}\hat{A}_I I_I + \hat{\mu}\hat{A}_T I_T + \hat{\gamma}\hat{A}_I I_I \sigma_{RS}} \end{aligned}$$

As $X \gg Y$, virtually all newly infiltrated islets will enter the severe insulitis state.

4.3.3 Effect of the apoptotic wave on T1D progression

The numbers of immunogenic and tolerogenic DC entering the pancreatic lymph node presenting self antigen (I_I and I_T) are the key values driving T1D progression. To examine how these values change we apply our nondimensionalization to (4.1) and make the following substitution

$$\hat{\beta} \to \epsilon b$$

$$\hat{\rho} \to \epsilon r$$

This substitution ensures that all parameters are now close to one except for $\epsilon \gg 1$. After substitution, we recover the following

$$\begin{aligned}
\frac{dI_0^T}{dt} &= -\epsilon b \frac{\hat{a}}{\hat{a}+\hat{\kappa}} X I_0^T \\
\frac{dI_1^*}{dt} &= \epsilon X \left(b \frac{\hat{a}}{\hat{a}+\hat{\kappa}} B(X/Y) I_0^T - r I_1^* \right) \\
\frac{dI_1}{dt} &= \epsilon X \left(b \frac{\hat{a}}{\hat{a}+\hat{\kappa}} (1 - B(X/Y)) I_0^T - r I_1 \right) \\
\frac{dI_2}{dt} &= \epsilon r X (I_1 + I_1^* - I_2) \\
\frac{dI_3}{dt} &= \epsilon r X (I_2 - I_3) \\
\frac{dI_4}{dt} &= \epsilon X (r I_3 - \eta I_4) \\
I_0 &= \frac{\hat{\kappa}}{\hat{a}+\hat{\kappa}} I_0^T \\
I_0^* &= \frac{\hat{a}}{\hat{a}+\hat{\kappa}} I_0^T
\end{aligned}$$

where I_0^T is the total number of uninfiltrated islets. Initially, all islets are uninfiltrated ($I_0^T = 1$), so $I_I = \frac{\hat{\kappa}}{\hat{a}} I_T$. For our parameter choices, this implies that $I_I < w_1 I_T$. Therefore, X is initially $\mathcal{O}(\epsilon)$, and Y is $\mathcal{O}(1)$ so $B(X/Y)$ is $\mathcal{O}(\epsilon^2)$. Thus, the transition from I_0 to I_1 will be extremely slow: $\mathcal{O}(\epsilon^4)$.

The apoptotic wave greatly increases a temporarily and thus modifies the DC population. In the previous section we showed that if roughly 9% or more of all islets become inflamed, then X is $\mathcal{O}(\epsilon^{-1})$ and Y is $\mathcal{O}(1)$or $\mathcal{O}(\epsilon^{-1})$. In either case, all transition rates in the islet model become $\mathcal{O}(1)$. If sufficient number of islets are infiltrated by T-cells during the apoptotic wave, then DC originating from those islets can continue to drive the T-cell population even after the wave ends, resulting eventually in T1D (Figure 4.5). However, if the wave is too brief or its magnitude too small, then most of the islet population remains uninfiltrated (Figure 4.6). The DC population then reverts to the prewave state and T1D progression is slow. Table 4.3 lists the parameters used for simulation.

4.4 Viral infection

We expect that viral infection will have fundamentally different effects whether it occurs before, during or after the apoptotic wave. Not only that, viral infection could affect T1D progression by several mechanisms simultaneously, in particular,

- Viral infection of the pancreas can lead to inflammation in the islets and the generation of more immunogenic DC. In essence, infection acts as a second apoptotic wave. We implement this with ($a_V > a_I$).
- Viral infection can lead to bystander activation of T-cells already within islets. This could rapidly precipate T1D, but also be protective in the long term by eliminating the most inflamed islets. We implement this with ($\eta_V > \eta_I$)
- Viral-specific T-cells can compete with self reactive T-cells in the lymph node. For simplicity we let $\phi_V = \phi_S = .5$. The T-cell populations compete when $\psi = 1$ and do not compete when $\psi = -1$.
- Viral-specific T-cells can stimulate the growth of Tregs, which in turn limits the growth of self reactive T-cells. We implement this with $\sigma_{RV} > 0$.

To reduce the total number of cases, we shall only analyze these properties in isolation.

4.4.1 Virus-induced inflammation aids T1D progression

If the only effect of the viral infection is to induce inflammation, then the forms of (4.19) still apply. The DC inputs I_T and I_I do change, as the balance between I_0 and I_0^* shifts. In the absence of infection, the solution of (4.1) approaches a stable manifold with $I_0^*/I_0 = a_I/\kappa$. During infection, if we assume that $a_V \gg a_I$, then

$$I_0^* \approx \frac{a_V g}{\kappa(a_V + \delta_V + \kappa + g)}$$

where δ_V is the rate of viral clearnace and g is the infection rate. Virus induced inflammation could therefore increase I_I above the critical thresholds of either $w_1 I_T$ or $w_2 I_T$. In this way, the viral infection is similar to the apoptotic wave. Such a viral infection has less impact in older mice as fewer islets are uninfiltrated and thus susceptible to virus-induced inflammation. Figure 4.7 shows the effect of this type of infection on I_I, I_T (panels A, C), insulitis, and insulin production (panel B, D). Infection at both 0 (A, B) and 60 (C, D) days accelerates T1D compared to uninfected mice (shown by grey lines), but the effect is stronger in the earlier case. Figure 4.8B shows the effect of viral infection at different ages on incidence and age of onset. Viral infection generally speeds progression, except where it overlaps with the apoptotic wave (shown in grey) when it is redundant and has little effect.

4.4.2 Bystander activation inhibits T1D progression

We assume, based on the histological data in [61], that bystander activation only affects islets with level-2 insulitis or above. Therefore, it is not a significant factor for young mice with little insulitis. If a sufficient number of islets have advanced insulitis, then their

destruction may precipitate rapid T1D. However, if T1D is not immediate, our analysis suggests that T1D is avoided altogether. The mechanism for this is a reduction in I_I without a corresponding reduction in I_T. More plainly, bystander activation selectively eliminates islets that are the source of immunogenic DC presenting self. Figure 4.9 shows the effect of this type of infection on the islet population (panels A, C, E), insulitis, and insulin production (panel B, D, F). We group the islet population into no insulitis (black), stage 1 insulitis (red), and stage 2-4 insulitis (blue). Infection at 0 days (A, B) has no effect compared to the uninfected case. At 60 days (C, D), there are sufficient islets with advanced insulitis that infection makes a significant difference. The elimination of these islets does cause a sudden drop in insulin production, but it does not precipitate insulitis. In fact, disease progress is significantly slowed. By 100 days (E, F), there is a sufficiently large number of islets at stage 2 or greater that their destruction immediately precipitates T1D. Figure 4.8C shows the effect of infection at different ages on incidence and age of onset. Infection early in life has little effect, but infection from 3-8 weeks completely eliminates T1D. Later infection may accelerate T1D, but the incidence is still lower than in the absence of infection.

4.4.3 Competition of viral and self reactive T-cells

During infection, the presence of viral-specific T-cells in the pancreatic lymph node can interfere with the growth of self reactive T-cells by competing for space on DCs. Unlike the previous cases, this mechanism substantially changes the form of the solution for X and Y. To study this case we use the substitution

$$\hat{\gamma} \to g\epsilon^{-1}$$
$$\hat{\mu} \to m\epsilon^{-1}$$
$$\hat{k}_I \to k\epsilon^{2}$$
$$\hat{\alpha}_V \to \hat{a}\hat{\alpha}_S\epsilon^{-1}$$

and seek solutions to lowest order in ϵ.

We consider a virus with $\psi = 1$ and $\phi_V = \phi_S$. With these parameters, all DCs from infected islets present both viral antigen and the self antigen, S, or no relevant antigens, i.e., $\phi_B = \phi_V = \phi_S$. The viral reactive T-cells dominate the interaction with DCs from infected islets, as $\sigma_V > \sigma_S$. Therefore, to first order in ϵ the dynamics of self reactive T-cells are determined by DCs migrating from uninfected islets. In the absence of infection, the nondimensionalized self reactive T-cell population, X, is $\mathcal{O}(\epsilon^1)$ if $I_I < w_1 I_T$ and $\mathcal{O}(\epsilon^{-1})$ if

$I_I > w_1 I_T$. This still holds true during infection with a competitive virus. Suppose that, prior to infection, the number of inflamed and uninflamed islets are given by $I_{I,u}$ and $I_{T,u}$, respectively. Then during infection,

$$\begin{aligned} I_I &= \nu I_{I,u} \\ I_T &= \nu I_{T,u} \\ \nu &= \frac{\delta_V}{g(t) + \delta_V} \end{aligned} \tag{4.28}$$

where $g(t)$ is the infection rate and δ_V is the rate that the virus is cleared from an islet. The ratio of I_I to I_T does not change, as we assume that the inflammation rate, a, is not modified by infection.

The impact of infection by a competitive virus is subtle. When $I_I < w_1 I_T$, $X \sim \epsilon X_1$ and $Y \sim Y_0$ regardless of the level of infection; however, the values of X_1 and Y_0 may change. The equations defining X_1 and Y_0 are derived by substituting (4.28) into (4.26)-(4.27).

$$X_1 = \frac{1 + \nu \hat{A}_I I_{I,u} + \nu \hat{A}_T I_{T,u}}{\hat{\gamma} \hat{A}_I \nu I_{I,u} - \hat{\mu} \hat{A}_T \nu I_{T,u}} \tag{4.29}$$

$$0 = \hat{A}_I \hat{\alpha}_S \hat{\sigma}_{RS} \nu I_{I,u} X_1 + \hat{\alpha}_R k_R (1 + \hat{\alpha}_R) Y_0 (1 - Y_0) \tag{4.30}$$

We are interested in how a decrease in the proportion of uninfected islets, ν, changes the ratio of $J = X_1/Y_0$. Therefore we make the substitution $X_1 = JY_0$ into (4.30) and differentiate with respect to ν. We find that

$$\frac{\partial J}{\partial \nu} = -\frac{J(1 + \hat{\alpha}_R Y_0)\big(\hat{A}_I \hat{\alpha}_S \gamma I_{I,u} (\hat{A}_I I_{I,u} + \hat{A}_T I_{T,u}) \nu^2 \hat{\sigma}_{RS} J + \hat{\alpha}_R k_R (1 + \hat{\alpha}_R Y_0)^2\big)}{\hat{\alpha}_R \nu \chi} \tag{4.31}$$

$$\chi = k_R (1 + \hat{A}_I I_{I,u} \nu + \hat{A}_T I_{T,u} \nu) + \big(\hat{\alpha}_R k_R (3 + 2\hat{A}_I I_{I,u} \nu + 2\hat{A}_T I_{T,u} \nu) \tag{4.32}$$

$$+ \hat{A}_I \hat{\alpha}_S \gamma I_{I,u} (\hat{A}_I I_{I,u} + \hat{A}_T I_{T,u}) \nu^2 \hat{\sigma}_{RS} J\big) Y_0 \tag{4.33}$$

$$+ \hat{\alpha}_R^2 k_R (3 + \hat{A}_I I_{I,u} q + \hat{A}_T I_{T,u} q) Y_0^2 + \hat{\alpha}_R^3 k_R Y_0^3 \tag{4.34}$$

which is strictly negative. This means that as more islets become infected and ν decreases, the ratio of self effectors to Tregs will increase. This is because the tolerogenic nature of the DCs migrating from these islets has a net negative effect on the self effector population. Therefore any infection by this type of virus, at a time prior to widespread insulitis, is likely to speed progression slightly. Infection at 20 days, shortly after the end of the apoptotic wave, is an example of this (Figure 4.10C, D). Although the T-cell populations is elevated, there has not yet been sufficient time for the development of insulitis in many islets. Viral infection at this time provides a sufficent boost to the T_S population to speed T1D onset and increase incidence.

Infection by a competitive virus can speed progression when tolerogenic DC outnumber immunogenic DC. This condition is generally met in young NOD mice, except for during the apoptotic wave when viral infection interferes with the instigation of the immune response. Although the impact of viral infection on the solutions of X and Y is small, the effect on T1D progression can be quite large. Infection at 6 days (Figure 4.10A and B), which perfectly overlaps the apoptotic wave, reduces the self reactive T-cell population by about 50%. This is enough to completely prevent T1D progression. Thus, viral infection can prevent T1D early in life, accelerates it in young adulthood, and has little effect later on 4.8D.

Finally, in the case that the entire pancreas is infected then

$$X = \frac{\hat{a}\hat{\alpha}_S + \hat{\gamma}\hat{\sigma}_V \hat{A}_I}{\hat{a}\hat{\alpha}_S + \gamma(\hat{\sigma}_V - 1)\hat{A}_I}$$
$$Y = 1$$
$$Z = \frac{\hat{a}\hat{a}_S + \hat{\gamma}\hat{\sigma}_V \hat{A}_I}{\hat{a}\hat{\alpha}_S}$$

This solution does not depend on I_T or I_I, which are now both zero. We find that the solution for both X and Y is now $\mathcal{O}(1)$. If prior to infection, $I_{I,u} < w_1 I_{T,u}$, then this dramatically increases the rate of islet invasion and insulitis progression. However, if $I_{I,u} > w_1 I_{T,u}$ prior to infection, then this should slow progression, but only for the duration of infection. If a viral infection of this kind takes place during the apoptotic wave, then the wave will become 'invisible' to the T-cell population, not affecting it at all.

4.4.4 Virus-induced regulatory T-cells

The last viral mechanism that we consider is the induction of Tregs. We have so far assumed that the regulatory T-cell population reacts to the same antigen, S, as the self reactive population or, equivalently, to an antigen that is present on the same DC as S. Under these conditions, if viral infection increases Treg proliferation, then it necessarily will boost self reactive T-cells as well, the case we studied in the last section. Here, we suppose that it is possible for the viral infection to stimulate the growth of the Treg population without also stimulating the self reactive population. In other words, we are assuming that Tregs respond to a distinct antigen from S, but one that is still often associated with it. In practice, this means that we set $\sigma_{RV} > 0$, meaning that Tregs can bind to DC that present V without S.

Viral infection prior to the apoptotic wave boosts the Treg population and prevents the development of T1D (Figure 4.8E, Figure 4.11A, B). As with competition, the perturbation

of the immune populations is subtle (the unperturbed system is shown in grey). If $I_I < w_1 I_T$, then X_1 and Y_0 now satisfy

$$0 = \frac{1 + \hat{A}_I I_I + \hat{A}_T I_T + \hat{\alpha}_R Y_0 + (\hat{\gamma}\hat{A}_I I_I - \hat{\mu}\hat{A}_T I_T) X_1}{1 + \hat{A}_I I_I + \hat{A}_T I_T + \hat{\alpha}_R Y_0}$$

$$0 = 1 + \frac{\hat{\gamma}\hat{A}_I I_I \hat{\alpha}_S \hat{\sigma}_{RS}}{\hat{\alpha}_R k_R (\hat{\alpha}_R + Y_0)} X_1 + \left(-1 + \frac{\hat{\gamma}\hat{A}_I I_V \hat{\sigma}_{RV}}{\hat{\gamma}\hat{A}_I I_V \hat{\sigma}_V + \hat{a}\hat{\alpha}_S} \right) Y_0$$

where I_V is the total number of infected islets. We assume that $\sigma_V > \sigma_{RV}$, so the solution of Y_0 remains bounded. The total number of Tregs is only increased slightly by infection at day 0 (Figure 4.11A), but this is enough to change the course of T1D development. Infection at day 30 also delays T1D, but the effect is only transient as I_I has already crossed the critical threshold.

4.5 Discussion

We develop a mathematical model of T1D progression in the NOD mouse. The model has two components: an islet transition model that tracks inflammation, insulitis, and infection and an immune model that tracks populations of T-cells and dendritic cells. We use this model to study the effect of viral infection on the age of onset and incidence of T1D. We consider four different mechanisms by which viruses could potentially affect T1D progression: virus induced inflammation, bystander activation of self reactive T-cells, direct competition with self T-cells, and the induction of regulatory T-cells.

The timing of infection can dramatically alter the progression of T1D. A developmental change in pancreatic morphology leads to a temporary increase in β-cell turnover in adolescent mice, the 'apoptotic wave'. Infection taking place before, during, or after the wave can have dramatically different results. Figure 4.8 summarizes how age of onset and disease incidence change as the time of infection changes. Inflammation due to viral infection generally increases incidence and accelerates onset (Figure 4.8B). Bystander activation can, counterintuitively, completely eliminate T1D at some ages, but accelerates T1D later in life (Figure 4.8C). Viral competition can either delay or accelerate T1D depending on whether the infection occurs before or after the apoptotic wave (Figure 4.8D). Finally, Treg-induction always delays T1D slightly, but the effect is strongest when infection is prior to the apoptotic wave (Figure 4.8E).

Bystander activation is the nonspecific activation of T-cells during an immune response. In the context of this model, viral infection activates self reactive T-cells that have already infiltrated the islets and causes an accelerated destruction of the resident β-cells. We show that if this does not precipitate T1D immediately, then it is unlikely to occur after infection

as the infiltrated islets are required to prolong the immune response. Infection of NOD mice with CVB4 at 8 weeks causes about 60% of mice to develop T1D within 2 weeks, but none after that [61]. Control mice had a median age of onset of 13 weeks, but the incidence was greater than 90%. The pattern is similar, if not quite as strong, among NOD mice infected with rotavirus at 12 weeks of age. These mice had dramatically accelerated T1D, but similar incidence rates as uninfected mice. Rotavirus infection at this age, unlike in infant mice, does not spread to the pancreas, suggesting antigen nonspecific effects. Mice with strong immune responses, as measured by antiviral antibodies, either developed T1D within 2 weeks of infection or not at all. Our model is in close agreement with these results.

Even in cases where viral infection prevents T1D, insulitis still persists. This is true experimentally [32, 77] and in our model. Whether and to what extent the degree of insulitis changes is unclear. Our model provides a detailed description of the severity of insulitis and how it changes over time. A more careful parameterization of the model and possibly a distinction between different mechanisms may be possible should more detailed insulitis data become available.

There is no single mechanism that can explain the effects that viruses have on T1D. Many viruses delay T1D onset or reduce its incidence (see Table 4.1), and our model shows that multiple mechanisms can reproduce this behavior. Filippi et al. [23] found that transfer of Tregs from virally infected mice to uninfected mice could also transfer some of the protection from T1D, providing strong support to the idea that the boost in Tregs is key. On the other hand Smith et al. concluded that the delay induced by murine gammaherpes virus was not dependent on Tregs, but rather on the reduced processing of antigen by DC [64]. Our model does predict, however, that different mechanisms produce different profiles of incidence and age of onset as a function of age. For example, if a virus boosts Tregs, then as long as it can still establish infection, then it should not matter much when the infection happens between the apoptotic wave and the onset of T1D. On the other hand, if the primary mechanism is competition, then the effect will only be significant if the infection is early in life. It should also be possible to constrain the model by attempting to directly measure some of the control parateters. For example, ψ represents the correlation between self antigen and viral antigen on DC. Its value can be inferred from knowledge of which cells the virus invades.

We have demonstrated that a single virus can either accelerate or delay T1D depending on the age of infection. In general, infection at a young age is protective, whereas infection later can quickly lead to T1D. In humans, it is thought that insulitis must already be

present before a viral infection can precipitate T1D [16]. Exposure at a younger age could theoretically generate a population of regulatory T-cells that protects against disease development. The first exposure to a novel enterovirus is likely to result in a more extensive infection and increased inflammation due to a lack of protective immunity. If the infection rate is decreased, then the first exposure may be delayed to an age with more extensive insulitis and thus a greater risk of diabetes. Another possibility is that lower infection rates in a population decreases the immunity among newborns due to the loss of protective maternal antibodies. The incidence of Type 1 Diabetes in a population is negatively correlated with the presence of maternal antibodies to enterovirus [75].

Table 4.1: Summary of selected experimental viral infection of the NOD mouse

Infection	Result	Source
2 days/T3A	Delay/Decrease in incidence	[77]
5 days/RRV	Decrease in incidence	[32]
4-6 weeks/RRV	Delay/Decrease in incidence	[32]
4-7 weeks/MHV68	No effect	[64]
6 weeks/CVB4	No effect	[61]
8 weeks/CVB4	Acceleration/Decrease in incidence	[61]
8-9 weeks/MHV68	Delay/Decrease in incidence	[64]
9 weeks/LCMV	Delay/Decrease in incidence	[23]
9 weeks/CVB3	Delay/Decrease in incidence	[23]
12 weeks/RRV	Acceleration/Increase in incidence	[33]

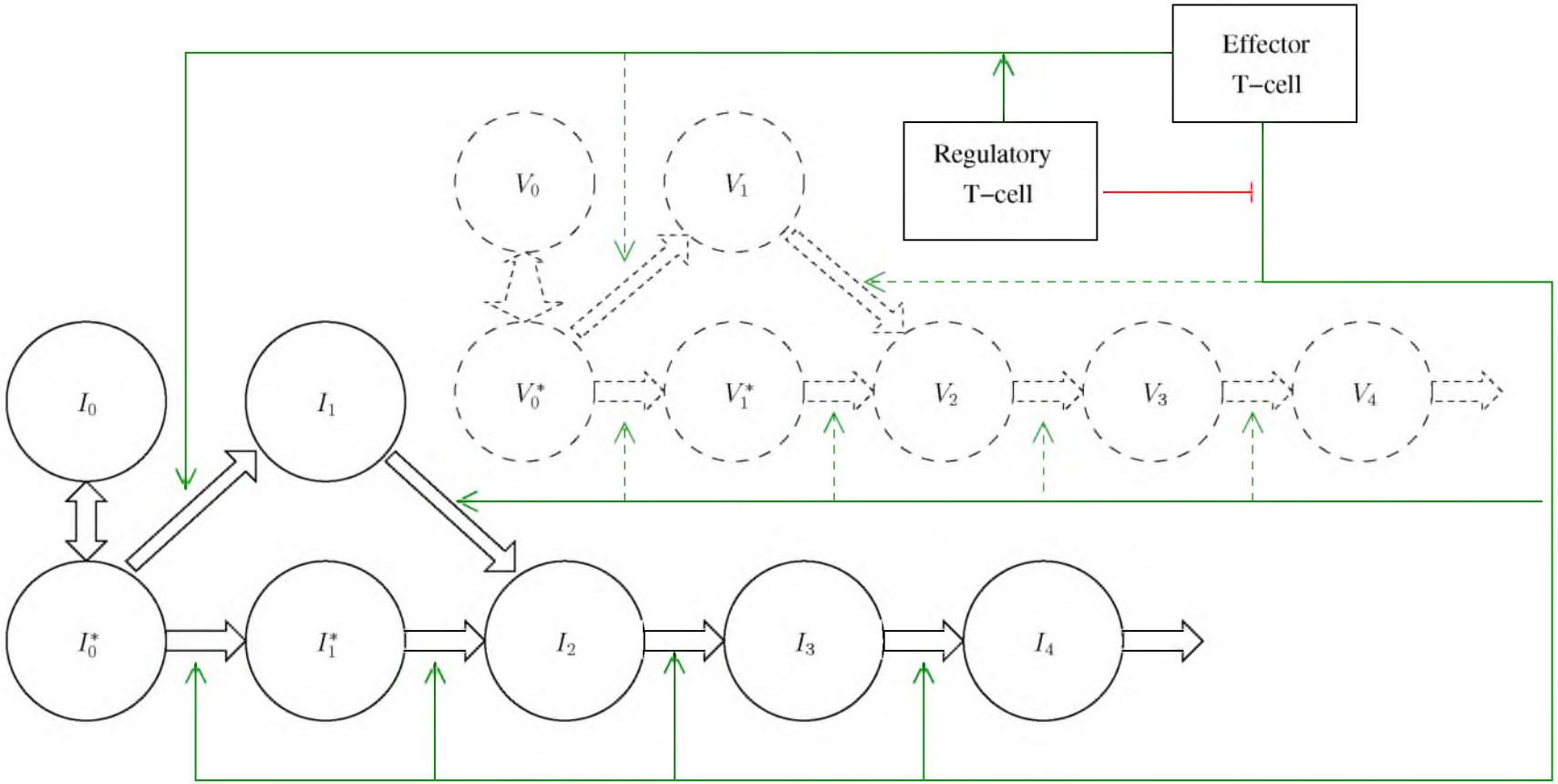

Figure 4.1: The islet transition model

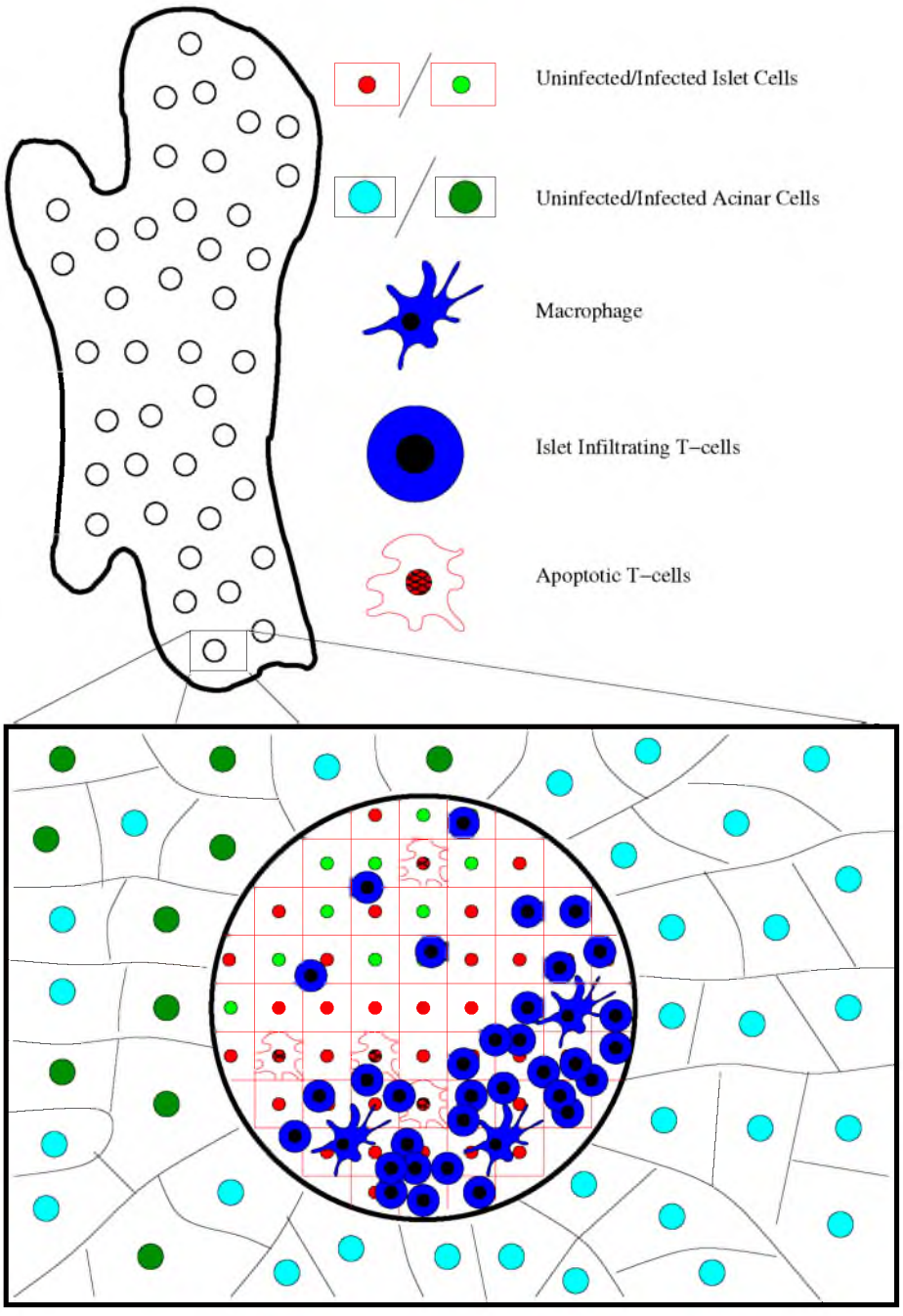

Figure 4.2: An individual 'islet zone' consists of the islet and the surrounding exocrine pancreatic tissue. T-cells and macrophages invade the islets, causing apoptosis. Viruses may infect the islets themselves or neighboring cells.

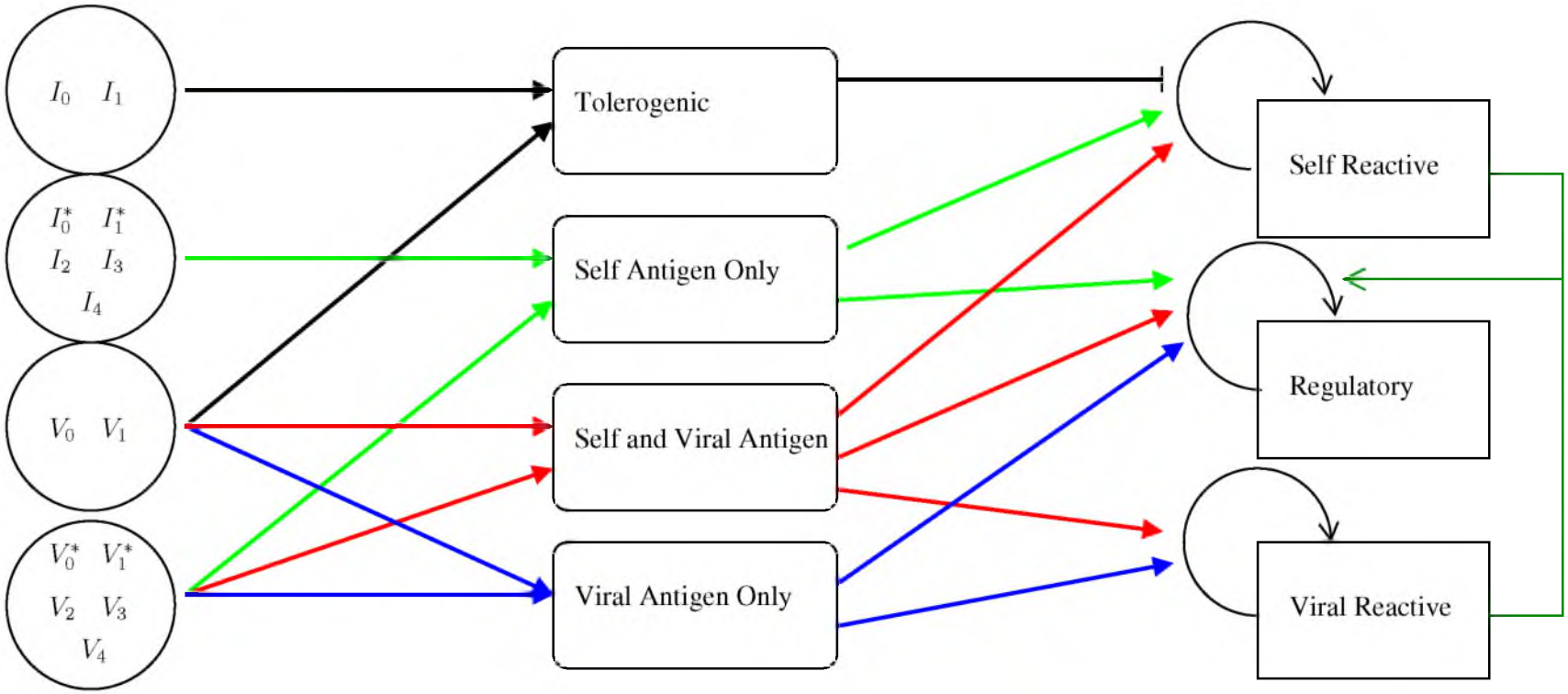

Figure 4.3: Schematic of the islet classes, DC populations, and T-cell populations. We categorize islets based on inflammation, infection, and insulitis. These attributes determine which populations of dendritic cells they produce. Dendritic cells then stimulate the growth of T-cell populations of the appropriate specificity. Arrows starting and ending at a particular DC class are color-coded for ease of reading.

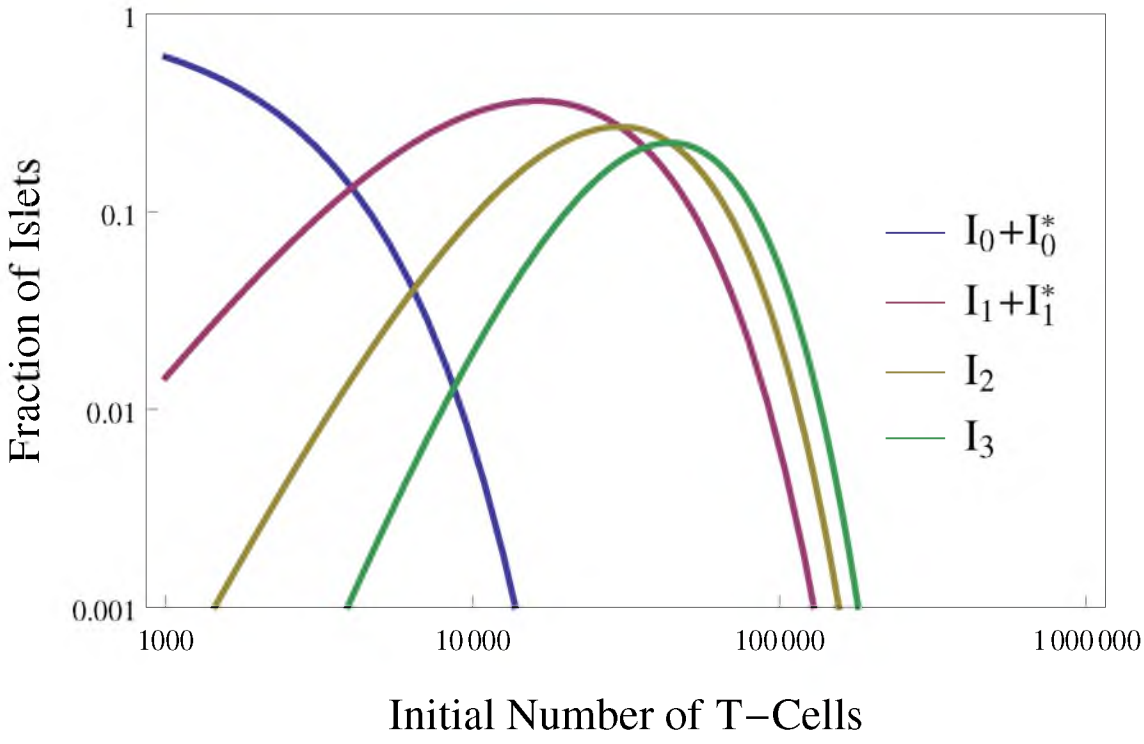

Figure 4.4: Equilibrium distribution of the islet population resulting from an exponentially decaying T-cell population (decay rate .01 per day). The fraction of islets in each stage of insulitis depends on the initial T-cell population size.

Table 4.2: Nondimensionalized parameters

X	$\frac{\delta_T}{\alpha_S} T_S$	$10^{-3} T_S$
Y	$\frac{\delta_T}{\alpha_R} T_R$	$2 * 10^{-4} T_R$
Z	$\frac{\delta_T}{\alpha_V} T_V$	$10^{-5} T_V$
τ	$\delta_T t$	.1 t
A_I	$\frac{\sigma_S}{k_p \delta_D} A_I$	1.4
$\hat{A}_T$	$\frac{\sigma_S}{k_p \delta_D} A_T$	.14
$\hat{\alpha}_R$	$\frac{\alpha_R \sigma_{RS} \nu}{\delta_D \delta_T}$	.25
$\hat{\alpha}_S$	$\frac{\alpha_S \sigma_S \nu}{\delta_D \delta_T}$	.07
$\hat{\alpha}_V$	$\frac{\alpha_V \sigma_V \nu}{\delta_D \delta_T}$	10
ϵ	$\frac{\delta_T}{\gamma}$	.02
m	$\frac{\mu}{\gamma}$	1
$\hat{\sigma_V}$	$\frac{\sigma_V}{\sigma_S}$	1.43
$\hat{\sigma}_{RV}$	$\frac{\sigma_{RV}}{\sigma_S}$	$0 - .714$
$\hat{\sigma}_{RS}$	$\frac{\sigma_{RS}}{\sigma_S}$	.714
$\hat{\sigma}_{RB}$	$\max\{\hat{\sigma}_{RS}, \hat{\sigma}_{RV}\}$	.714
$\hat{k}_I$	$k_I \nu / \delta_D$	.001
$\hat{\beta}$	$\beta \alpha_T / \delta_T^2$	.05
$\hat{\rho}$	$\rho \alpha_T / \delta_T^2$	$7.14 * 10^{-3}$
$\hat{a}$	a / δ_T	.2
$\hat{\kappa}$	κ / δ_T	5

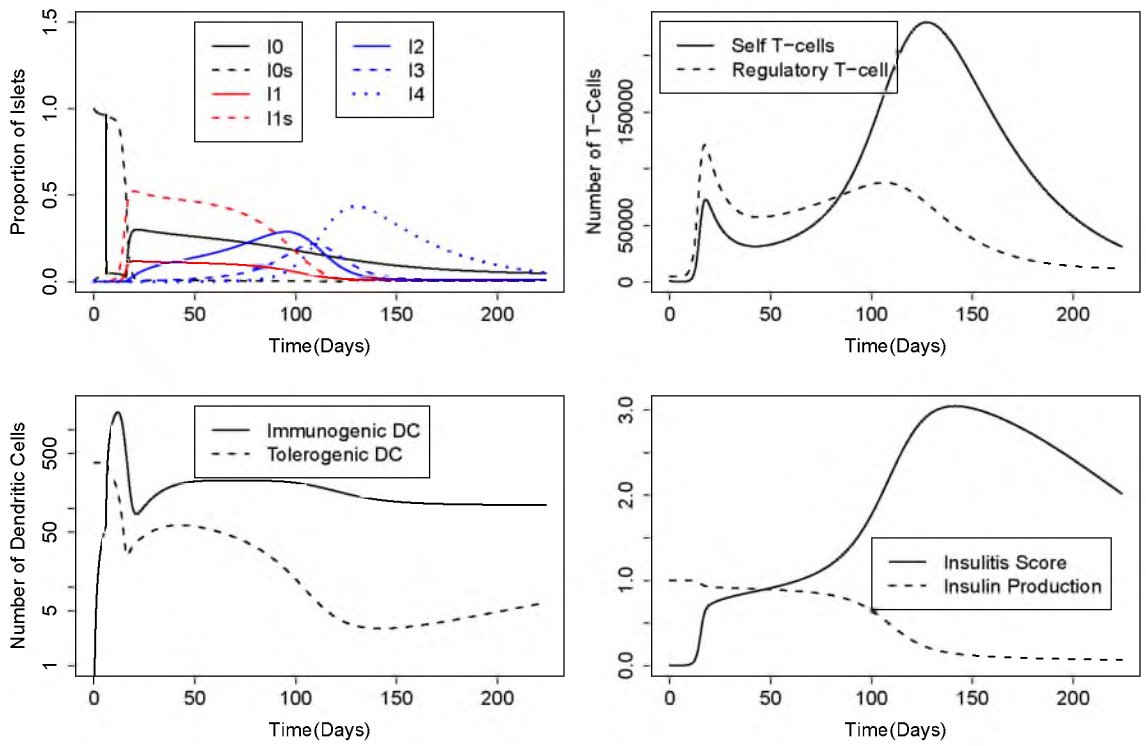

Figure 4.5: Time series of the full model with parameters in Table 4.3. The apoptotic wave lasts from day 6 to 16.

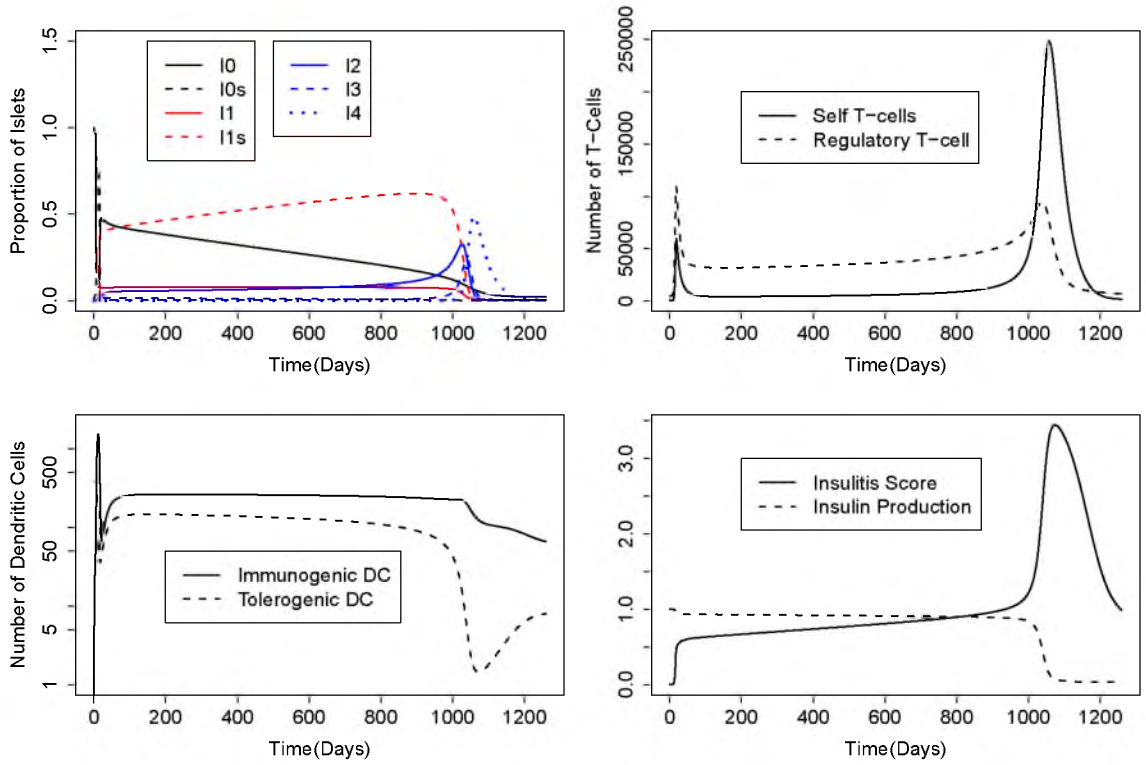

Figure 4.6: Time series of the virus-free model with parameters in Table 4.3 except that $a_W = 2.5$. The apoptotic wave lasts from day 6 to day 16.

Table 4.3: Parameter values used in the model

Symbol	Description	Value
I_i	Uninfected islets in state i	
V_i	Infected islets in state i	
T_S	Self reactive T-cells	
T_V	Viral reactive T-cells	
R	Regulatory T-cells	
D_S^T	Tolerogenic DC presenting self antigen S	
D_S^I	Immunogenic DC presenting self antigen S	
D_V^I	Immunogenic DC presenting viral antigen	
D_B^I	Immunogenic DC presenting viral antigen and S	
$F(T/R)$	Probability of severe insulitis	
$f(t)$	Inflammation rate due to development	
$g(t)$	Infection rate of islets	
γ	Growth rate of T-cells	5 days^{-1}
μ	Death rate of T-cells due to tolerogenic DC	5 days^{-1}
δ_T	Death rate of T-cells	.1 days^{-1}
k_I	D	.1 days^{-1}
k_R	D	.1 days^{-1}
k_p	Daily Contacts required for Growth	50
σ_S	Contact rate between T_S and D_S^T	.007 days^{-1} cells^{-1}
σ_V	Contact rate between T_V and D_V^T	.01 days^{-1} cells^{-1}
σ_{RS}	Contact rate between T_R and D_S^T	.005 days^{-1} cells^{-1}
σ_{RV}	Contact rate between T_R and D_V^T	$0 - .005$ days^{-1} cells^{-1}
α_S	Thymic production rate of T_S	100 cells days^{-1}
α_R	Thymic production rate of T_R	500 cells days^{-1}
α_V	Thymic production rate of T_V	10000 cells days^{-1}
δ_V	Clearance rate of virus	1 days^{-1}
a_I	Inflammation rate in infected cells	.02 days^{-1}
a_W	Inflammation rate during apoptotic wave	1 days^{-1}
t_{w1}	Start of apoptotic wave	6 days
t_{w2}	End of apoptotic wave	16 days
κ	Rate that inflammation resolves	
η_I	Death rate of uninfected islets	.03 days^{-1}
β	Invasion rate of T-cells	
ρ	Progression rate of insulitis	
a_V	Inflammation rate in uninfected cells	(.02-10) days^{-1}
t_{inf}	Time of infection	0-100 days
t_{dur}	Duration of infection	10 days
η_V	Death rate of infected islets	(.03-10) days^{-1}

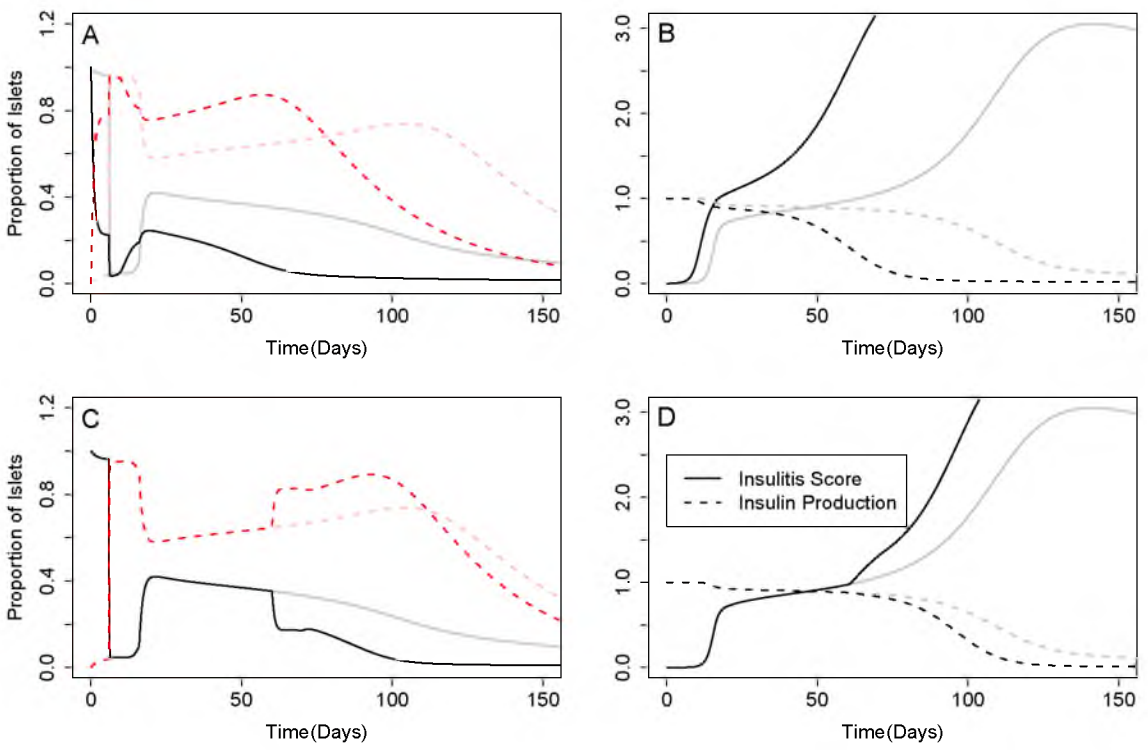

Figure 4.7: Time series of infection with a virus with inflammatory properties at age 0 (A, B) and 60 days (C, D). Panels A and C show the number of islets producing immunogenic versus tolerogenic DC. Panels B and D show the insulin production and average insulitis score. The greyed out lines show the virus-free dynamics for comparison.

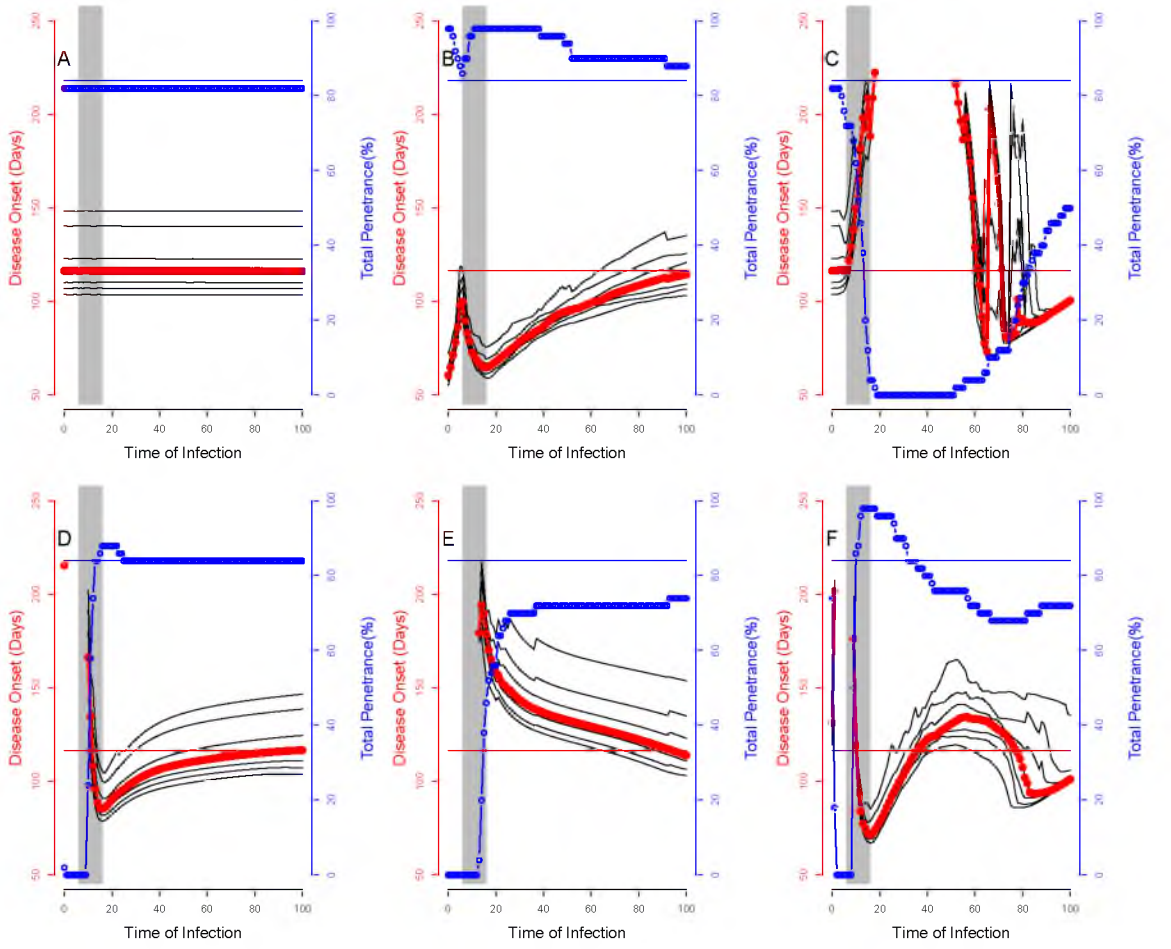

Figure 4.8: Age of onset and incidence of T1D when infected by different viruses. The apoptotic wave is marked in grey. The virus free behavior is shown by the thin red and blue lines. The black curves denote deciles of the age of onset. A: Control virus ($\phi_V = .5$, $a_V = .02$, $\eta_V = .03$, $C = -1$ and $\sigma_{RV} = 0$). B: Inflammatory virus (same parameters as A, except $a_V = 10$). C: Bystander activation virus (same parameters as A, except $\eta_V = 10$). D: Competitive virus (same parameters as A, except $C = 1$). E: Treg-inducing virus (same parameters as A, except $\sigma_{RV} = .005$). F: All-of-the-above virus ($a_V = 10$, $\eta_V = 10$, $C = 1$ and $\sigma_{RV} = .005$).

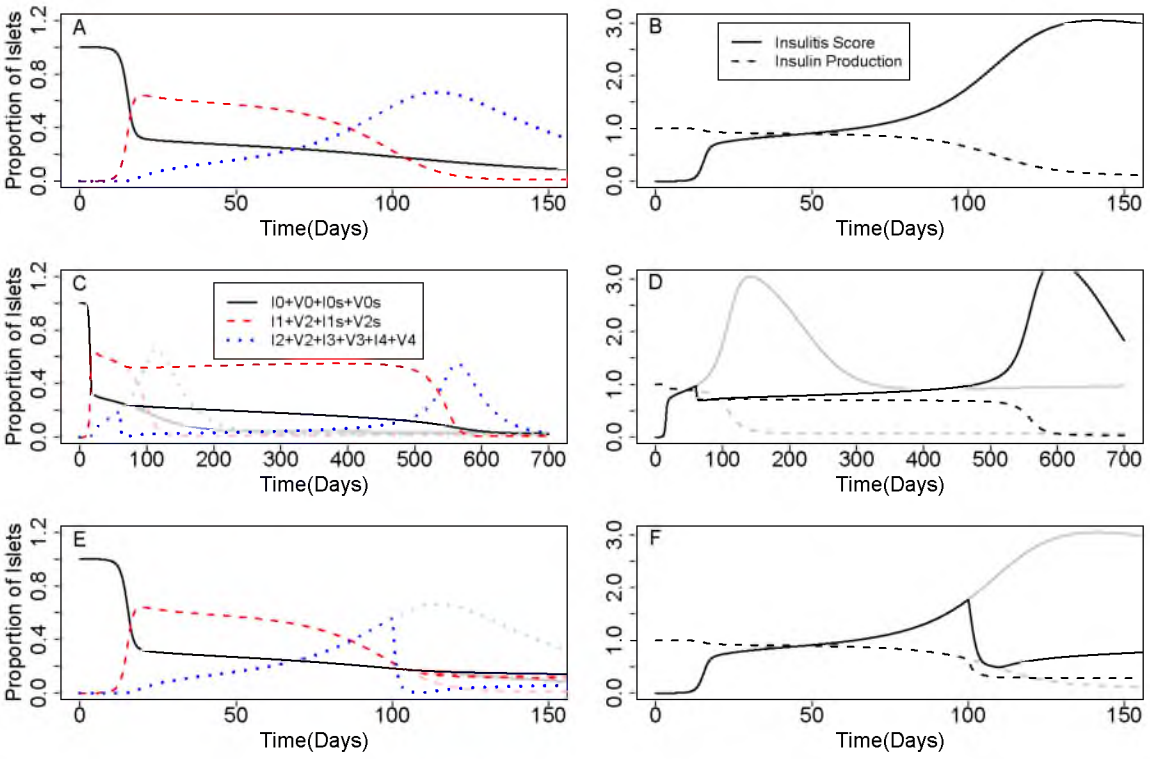

Figure 4.9: Time series of infection with a virus that promotes bystander activation at age 0 (A, B), 60 days (C, D) and 100 days (E, F). Panels A, C, and E show the number of islets with no insulitis, stage-1 insulitis or stage 2–4 insulitis. Bystander activation only affects islets in stages 2–4. Panels B, D, and F show the insulin production and average insulitis score. The greyed out lines show the virus-free dynamics for comparison.

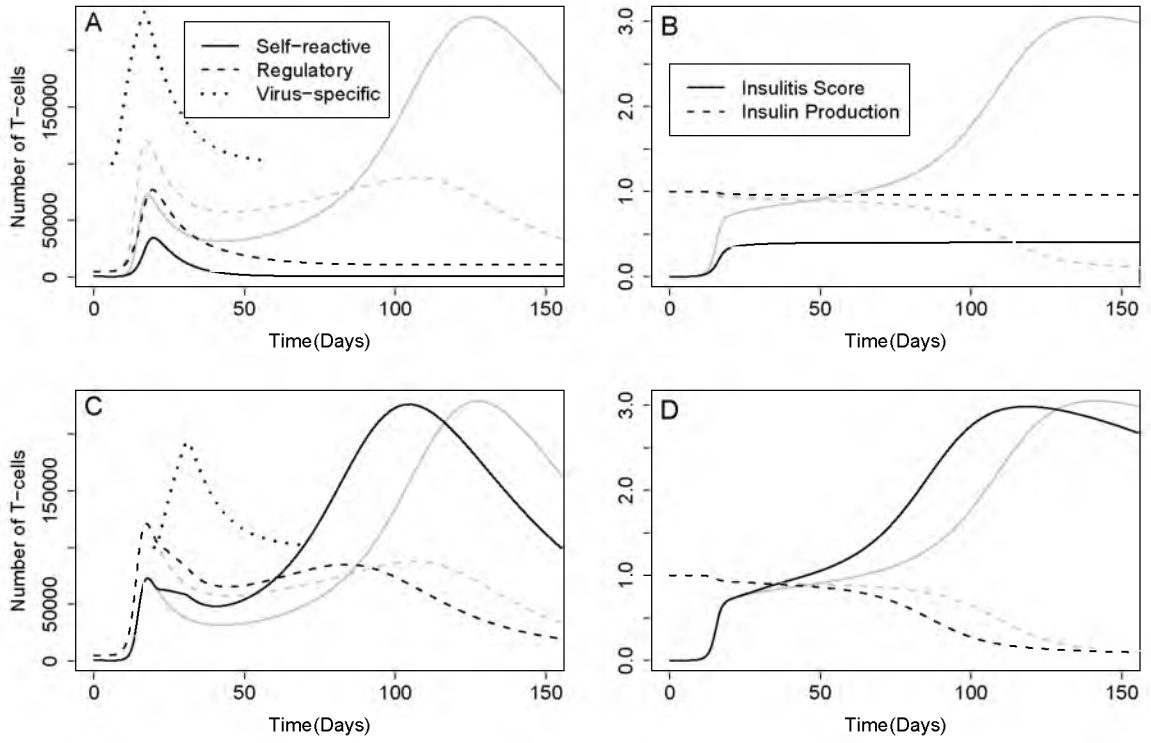

Figure 4.10: Time series of infection with a virus that competes with self reactive T-cells at day 6 (A, B) and day 20 (C, D). Panels A and C show the number of self reactive, regulatory and virus-specific T-cells. Panels B and D show the insulin production and average insulitis score. The greyed out lines show the virus-free dynamics for comparison.

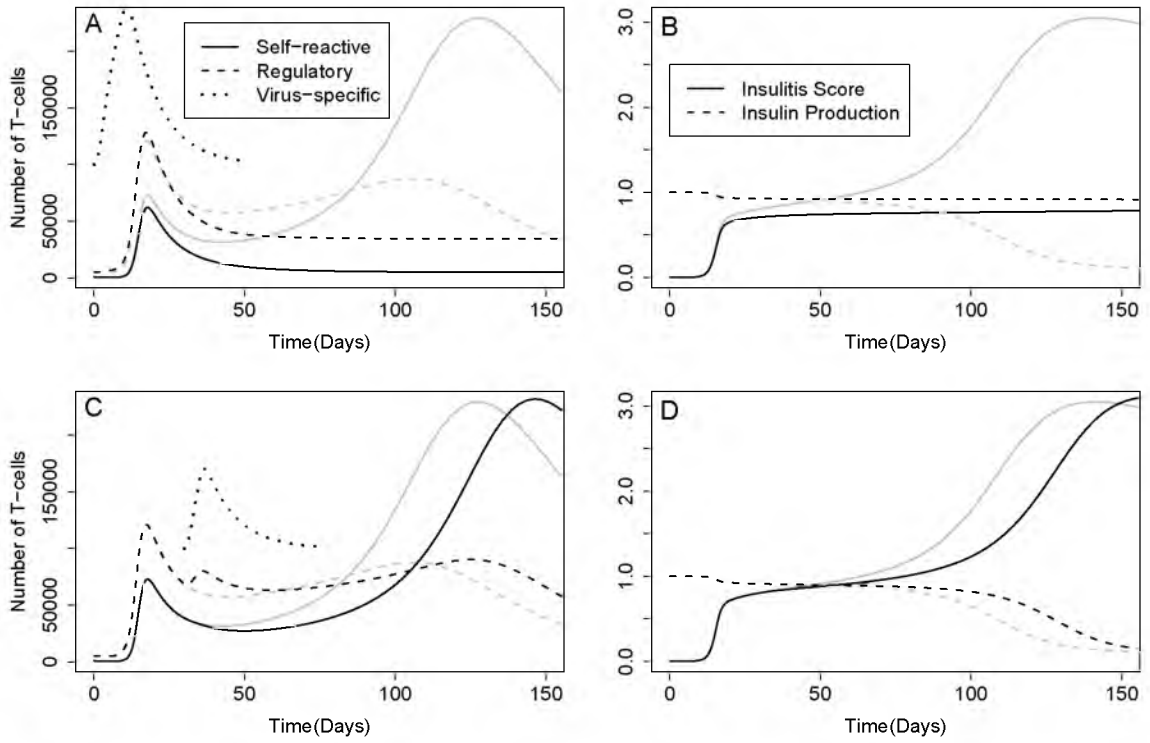

Figure 4.11: Time series after infection with a virus that promotes Treg proliferation at day 0 (A, B) and day 30 (C, D). Panels A and C show the number of self reactive, regulatory and virus-specific T-cells. Bystander activation only affects islets in stages 2-4. Panels B and D show the insulin production and average insulitis score. The greyed out lines show the virus-free dynamics for comparison.

CHAPTER 5

THE ROLE OF INTRINSIC NOISE IN AUTOIMMUNE DISEASE

5.1 Introduction

Immune regulation consists of many overlapping, redundant mechanisms such as central tolerance, tolerogenic DC, and Tregs. In the first chapter, we show that these mechanisms combine to form a robust control system that can reliably generate responses to foreign antigens and avoid responses to self antigens.

The NOD mouse has defects in each of these control mechanisms and spontaneously develops Type 1 Diabetes. These defects have analogs in human patients. However, although each NOD mouse shares these defects, not all mice develop Type 1 Diabetes. In Chapters 3 and 4 we develop a deterministic model and represent different mice via small changes in parameter values.

Here, we consider the stochasticity that may arise intrinsically from immune interactions. We demonstrate that a stochastic model predicts the onset of autoimmune diseaseas under conditions where a deterministic model predicts perpetual health. We also investigate how intrinsic stochasticity can account for differences between individuals.

5.1.1 Biological Background

At the heart of our prior models is the interaction between individual cells, particularly T-cells and DCs. Our description of these processes with ordinary differential equations makes the assumption that each T-cell and DC behaves uniformly. For example, if a T-cell enters a lymph node containing 1200 immunogenic DC and 1800 tolerogenic DC, then our differential equation model suggests that the T-cell should somehow interact with all of them, or at least a representative sample. In fact, as T-cells interact with DCs they become progressively less motile. This makes it likely that an individual T-cell will interact multiple times with the same DC or small group of DCs [50]. Therefore, we expect that the interactions of individual T-cells within a lymph node will be highly variable.

The interaction between T-cells and DC is a two way process. After binding to an immunogenic or tolerogenic DC, a T-cell will proliferate or anergize, respectively. T-cells can also change the behavior of DCs, both directly, via intercellular signalling, and indirectly, via tissue damage. For example, stimulation of CD40 on macrophages by CD40L can induce an immunogenic phenotype under circumstances that would typically produce tolerogenic DC [66]. The CD40 coreceptor, CD40L, is present on activated CD4 T-cells [1]. T-cells can also generate immunogenic DC indirectly by killing their target cells [34].

5.1.2 Prior modeling

Autoimmune responses drive the release of self antigens providing positive feedback, but also eliminate target cells, providing negative feedback. Iwami et al. [37] demonstrates that this combination of positive and negative feedback can deterministically produce many interesting dynamics. First, the system may be bistable with one 'healthy' state and one 'diseased' state. Second, the system may have only a single, 'diseased' state, but there may be an arbitrarily long transient to reach it. This is the case if there is still a 'ghost' of the healthy equilibrium that slows down the trajectory as it passes by. Finally, these feedbacks with different parameters can produce stable oscillations.

Stochastic models can often have different results from their deterministic analogs. Alexander et al. [5] develop a model of feedback between self reactive T-cells, self antigen, and immunogenic DCs. The self reactive T-cell population is controlled by a regulatory T-cell population. According to their analysis, the addition of Tregs can never eliminate the chronically autoimmune state. Tregs can, however, lower the number of self reactive T-cells present in this state to an arbitrarily low number. The stochastic system behaves quite differently in that the self reactive T-cell population always vanishes given enough time. As the trivial equilibrium is unstable, this is an example of Keizer's paradox [73]. Alexander et al. show that Tregs can eliminate the autoimmune response, before the development of a significant response.

5.1.3 Our approach

We propose an extremely simple model of immune regulation. Tolerogenic DCs eliminate self reactive T-cells, whereas immunogenic DCs stimulate their proliferation. Initially, the tolerogenic DCs outnumber the immunogenic DCs, but as the T-cell population increases, the balance shifts toward immunogenic DCs. Based on this simple mechanism, we write down a deterministic ODE model and demonstrate that it is bistable.

We then develop the analogous stochastic model of our deterministic system. The

stochastic model is fully summarized by a master equation, which we approximate with a Fokker-Planck equation. Finally, we use the Fokker-Planck equation to calculate the mean first passage time as a function of parameters. We show that under certain parameter conditions, the deterministic model predicts that the system stays in the healthy state, whereas the stochastic model predicts the development of autoimmune disease.

5.2 Deterministic model

We consider a system of very limited regulation. Let T be the number of T-cells that respond to a self antigen, A. Self reactive T-cells are produced by the thymus at a low rate, α_T. The T-cells turn over slowly at a rate δ_T. They divide upon contact with an immunogenic DC presenting A, S_I, and anergize/apoptose when they come into contact with a tolerogenic DC presenting A, S_T. When interacting with any other DC, S_0, they divide at a rate γ_h,

$$\frac{dT}{dt} = \alpha_T - \delta_T T + (\gamma S_I - \omega S_T + C)\frac{k}{T+k}T$$

where $C = \gamma_h S_0$ is the effective homeostatic growth rate. We assume that these growth rates saturate for large T, as binding space is limited. This prevents the solution from becoming unbounded, but the term does not affect dynamics much as we let $k \gg \frac{\alpha_T}{\delta_T}$.

Let α_D be the number of DCs presenting A generated daily, and let q be the proportion that are immunogenic, where

$$q = \frac{q_0 + mT}{1 + mT}$$

We call q_0 the baseline level of immunogenicity. This baseline represents ongoing inflammation or infection not due to the immunopathology of the self reactive T-cell population. T-cells increase the proportion of immunogenic DC. The equations for the DC population are therefore

$$\frac{dS_I}{dt} = \alpha_D p - \delta_D S_I$$
$$\frac{dS_T}{dt} = \alpha_D (1-p) - \delta_D S_T$$

In the deterministic system $S = S_I + S_T = \alpha_D/\delta_D$ is constant. Therefore we define $H = S_I - S_T$ and note that

$$\frac{dH}{dt} = \alpha_D(2p-1) - \delta_D H$$
$$\frac{dT}{dt} = \alpha_T - \delta_T T + \left(\gamma\frac{S+H}{2} - \omega\frac{S-H}{2} + C\right)\frac{k}{T+k}T$$

5.2.1 Nondimensionalized model

We perform the following nondimensionalization

$$\tau = \delta_T t$$
$$x = \alpha_T T/\delta_T$$
$$y = \alpha_D H/\delta_D$$

which yields the following system

$$x' = 1 - x + (g\frac{1+y}{2} - w\frac{1-y}{2})\frac{k}{x+k} \tag{5.1}$$
$$y' = \frac{1}{\epsilon}(2p - 1 - y) \tag{5.2}$$
$$p = \frac{q_0 + \mu x}{1 + \mu x} \tag{5.3}$$

Table 5.1 summarizes the nondimensionalization, which introduces three small parameters. First, $\epsilon \ll 1$ represents the ratio between DC turnover and T-cell turnover. Although T-cells can proliferate rapidly during an infection, naive and memory T-cells can be quite long-lived. We therefore assume that the turnover rate of the DC populations is about 10 times faster than that of T-cells. We also introduce two other small parameters, h_1 and h_2, which are the inverse of the population sizes of T-cells and DCs, respectively. These parameters determine the size of population fluctuations, which are insignificant for large enough populations.

5.2.2 Analysis of the deterministic model

The deterministic model has three equilibria where

$$y^* = 2\frac{q_0 + \mu x^*}{1 + \mu x^*} - 1$$

and x^* satisfies

$$-\kappa - \kappa q_0 x^*(\gamma + \omega) + \mu x^{*3} - x^{*2}(\gamma\kappa\mu - \kappa\mu + \mu - 1) + x^*(\kappa(-\mu) + \kappa\omega + \kappa - 1) = 0 \tag{5.4}$$

which has either one or three solutions. The largest solution, which we denote x_f^*, represents a 'disease' or 'final' state. From Table 5.1, we see that $\kappa \gg 1$. Therefore, $\frac{\kappa}{\kappa+x} \sim 1$ unless x has a similar order to κ. To find solutions on this order, we subsitute $x_f^* = x_\kappa \kappa$ and find that

$$x_\kappa \sim (\gamma + c - 1)$$

This solution exists provided that $\gamma + c > 1$, i.e., the maximum proliferation rate of T-cells exceeds their turnover rate, which we assume to be true.

To find the other potential solutions, we let $\frac{\kappa}{\kappa+x} = 1$ and perform the substitution

$$x \sim \mu^{-1} x_{-1} + x_0$$

since $\mu \ll 1$. We find two additional solutions: a healthy solution, x_i, with order 1 and a 'barrier' solution, x_b, with order μ^{-1}:

$$x_i \sim \frac{1}{1 + \omega(1 - q_0) - \gamma q_0 - c}$$
$$x_b \sim \mu^{-1} \frac{1 + \omega(1 - q_0) - \gamma q_0 - c}{\gamma + c - 1}$$

These solutions exist provided that $q_0 < \omega/(\gamma + \omega)$ and μ is sufficiently small (Figure 5.1).

5.3 Stochastic model

5.3.1 Discrete Jump Process

We track three state variables $\mathbf{U} = [S_I\, S_T\, T]^T$ and simulate their dynamics using the gillespie algorithm [29]. We define a transition $\mathbf{L}_i^{\pm}$ to be a column vector of length three with the ith entry ± 1 and all other entries zero. The associated propensity function $W_i^{\pm} dt$ defines the probability that a given transition will occur during an interval dt. At each time step, we

1. calculate the propensities $\mathbf{W}$ for each transition $\mathbf{L}$. Let λ be the total sum of all propensities,
2. choose a time step Δt from an exponential distribution with mean λ,
3. choose a transition, $\mathbf{L}^*$ by sampling from $\mathbf{L}$ with probabilities given by $\mathbf{W}/\lambda$, and
4. update the system:

$$\mathbf{U}_k = \mathbf{U}_{k-1} + \mathbf{L}^* \tag{5.5}$$
$$t_k = t_{k-1} + \Delta t \tag{5.6}$$

We run this algorithm until $T > \delta_T x_f / \alpha_T$, the dimensionalized diseased state, $t > t_{\max} =$ 1000 years, or $k > k_{\max} = 10^9$, whichever comes first.

5.3.2 Master Equation

To analyze this system, we once again perform the change of variables

$$S_I = \frac{S + H}{2} \tag{5.7}$$
$$S_T = \frac{S - H}{2} \tag{5.8}$$

and consider S to be approximately constant. Let $p_{ij}(t)$ be the probability that $T = i$ and $H = j$ at time t. The full master equation for p is

$$\begin{aligned}
\frac{dp_{ij}}{dt} &= \mathcal{D}_i^{(+)}\{F_{ij}^{(+)}p_{ij}\} + \mathcal{D}_i^{(-)}\{F_{ij}^{(-)}p_{ij}\} + \mathcal{D}_j^{(+)}\{G_{ij}^{(+)}p_{ij}\} + \mathcal{D}_j^{(-)}\{G_{ij}^{(-)}p_{ij}\} \\
F_{ij}^{(+)} &= \delta_T i + \omega\frac{S-j}{2}\frac{k}{i+k}i \\
F_{ij}^{(-)} &= \alpha_T + \gamma\frac{S+j}{2}\frac{k}{i+k}i + c\frac{k}{i+k}i \\
G_{ij}^{(+)} &= \delta_D(S+j)/2 + \alpha_D(1-q_i) \\
G_{ij}^{(-)} &= \delta_D(S-j)/2 + \alpha_D q_i \\
q_i &= \frac{q_0 + im}{1+im} \\
\mathcal{D}^{(+)}\{a_i\} &= a_{i+1} - a_i \\
\mathcal{D}^{(-)}\{a_i\} &= a_{i-1} - a_i
\end{aligned} \tag{5.9}$$

where $F^{(+)}, F^{(-)}, G^{(+)}$, and $G^{(-)}$ are propensity functions for our reduced model. For example, $F^{(+)}\,dt$ is the probability that the T-cell population decreases by one cell during a timestep of size dt. We wish to approximate this with a Fokker-Planck equation taking advantage of the large numbers of cells involved. Applying the same nondimensionalization as in (5.3) and Table 5.1, we have

$$\begin{aligned}
f^{(+)}(x) &= \left(x + \omega\frac{1-y}{2}\frac{kx}{x+k}\right) \\
f^{(-)}(x) &= \left(1 + \gamma\frac{1+y}{2}\frac{kx}{x+k} + c\frac{kx}{x+k}\right) \\
g^{(+)}(x) &= \epsilon^{-1}\left(\frac{1+y}{2} + 1 - q(x)\right) \\
g^{(-)}(x) &= \epsilon^{-1}\left(\frac{1-y}{2} + q(x)\right)
\end{aligned}$$

We can now convert the discrete operators into differential operators

$$\begin{aligned}
\mathcal{D}^{(+)}\{a(x)\} &= a(x+h) - a(x) \\
&\approx ha_x(x) + \frac{h^2}{2}a_{xx}(x) \\
\mathcal{D}^{(-)}\{a(x)\} &\approx -ha_x(x) + \frac{h^2}{2}a_{xx}(x)
\end{aligned} \tag{5.10}$$

To greatly simplify the analysis, we now assume that the growth rate from immunogenic DC matches the death rate due to tolerogenic DC, i.e., $\gamma = \omega$. Applying (5.3) and (5.10) to (5.9) yields the nondimensionalized PDE,

$$\frac{\partial p}{\partial \tau} = \Big[\Big(f^{(+)} - f^{(-)}\Big)p\Big]_x + \frac{h_1}{2}\Big[\big(f^{(-)} + f^{(+)}\big)p\Big]_{xx}$$

$$
\begin{aligned}
&+\Big[\big(g^{(+)}-g^{(-)}\big)p\Big]_y+\frac{h_2}{2}\Big[\big(g^{(-)}+g^{(+)}\big)p\Big]_{yy}+h.o.t.\\
&=\Big[\big(f_1(x)+f_2(x)y\big)p\Big]_x+\Big[h_1f_3(x)p\Big]_{xx}\\
&+\epsilon^{-1}\Big[\big(g_1(y)+g_2(x)\big)p\Big]_y+\epsilon^{-1}\Big[h_2p\Big]_{yy}+h.o.t.\\
f_1(x)&=x-1-c\frac{kx}{k+x}\\
f_2(x)&=-\gamma\frac{kx}{k+x}\\
f_3(x)&=x+1+\gamma\frac{kx}{k+x}\\
g_1(y)&=y\\
g_2(x)&=2q(x)-1
\end{aligned}
$$

which we can write compactly as

$$\frac{\partial p}{\partial t}=\frac{1}{\epsilon}L_1p+L_2p \tag{5.11}$$

where L_1 and L_2 are both linear differential operators. The factor of ϵ^{-1} suggests that p should be close to the nullspace of L_1. To see this more clearly, we project our PDE onto this nullspace, which is the Gaussian

$$\rho(x,y)=\sqrt{\frac{2\pi}{h_2}}e^{-\frac{y+1-2q(x)}{2h_2}} \tag{5.12}$$

The orthogonal projection, P, onto $\rho(x,y)$ is

$$P(\cdot)=<\mathbf{1},\cdot>\rho \tag{5.13}$$

where $<\cdot,\cdot>$ is the L^2 inner product and $\mathbf{1}$ is a function that is 1 for all y. We define $u=P(p)$ and $v=p-P(p)$. Projecting (5.11) yields

$$
\begin{aligned}
\frac{\partial u}{\partial \tau}\rho&=P(L_2p)\\
&=<\mathbf{1},\Big[f_1(x)+f_2(x)y)p\Big]_x+\Big[h_1f_3(x)p\Big]_{xx}>\rho\\
&=\Big(\Big[f_1(x)<\mathbf{1},p>+f_2(x)<y,p>\Big]_x+\Big[h_1f_3(x)<\mathbf{1},p>\Big]_{xx}\Big)\rho \qquad (5.14)\\
\frac{\partial u}{\partial \tau}&=\Big[f_1(x)u+f_2(x)<y,p>\Big]_x+\Big[h_1f_3(x)u\Big]_{xx}\\
&=\Big[f_1(x)u+f_2(x)(ur_1(x)+<y,v>)\Big]_x+\Big[h_1f_3(x)u\Big]_{xx}
\end{aligned}
$$

where $r_1(x)=<y,\rho>=2q(x)-1$ is the first moment of ρ. To close the system, we must compute $<y,v>$, the first moment of the orthogonal complement. To do this, we must first find the orthogonal complement of (5.11)

$$\begin{aligned}\frac{\partial v}{\partial \tau} &= \epsilon^{-1} L_1 p + L_2 p - P(L_2 p) \\ &= \epsilon^{-1} L_1 v + L_2 p - P(L_2 p)\end{aligned}$$

We see that to zeroth order $v \sim 0$; therefore, we substitute in $v = \epsilon v_1$. To lowest order,

$$\begin{aligned}-L_1 v_1 &= L_2(u\rho) - P(L_2(u\rho)) \\ &= \Big[f_1(x)u\rho + f_2(x)yu\rho\Big]_x + \Big[h_1 f_3(x)u\rho\Big]_{xx} \\ &- \Big(\Big[f_1(x)u + f_2(x) < y, \rho > u\Big]_x + \Big[h_1 f_3(x)u\Big]_{xx}\Big)\,\rho\end{aligned}$$

We note that $< y, L_1 v_1 >= - < y, v_1 >$. Therefore

$$\begin{aligned}< y, v_1 > &= \Big[f_1 u r_1 + f_2 u r_2\Big]_x + \frac{1}{2}\Big[h_1 f_3 u r_1\Big]_{xx} \\ &- \Big[f_1 u + f_2 r_1 u\Big]_x r_1 - \frac{h_1}{2}\Big[f_3 u\Big]_{xx} r_1 \\ &= f_1 r_1' u + h_2\Big[f_2 u\Big]_x + f_2 u r_1 r_1' \\ &+ \frac{h_1}{2}\Big[f_3 u r_1'\Big]_x + \frac{h_1}{2}\Big[f_3 u\Big]_x r_1'\end{aligned} \tag{5.15}$$

where $r_2 =< y^2, \rho >= h_2$ is the second moment of ρ.

We can finally write our system as a one dimensional Fokker-Planck equation by substituting (5.15) into (5.14)

$$\begin{aligned}\frac{\partial u}{\partial \tau} &= -\big[a(x)u\big]_x + \frac{1}{2}\big[d(x)u\big]_{xx} \\ a(x) &= f_1 + f_2 r_1 + \epsilon(f_2 f_1 r_1'(x) + f_2^2 r_1 r_1') \\ &+ \epsilon h_1(r_1' f_2 f_3' + \frac{1}{2} f_3 f_2 r_1'') \\ &+ \epsilon h_2 f_2 f_2' \\ 2d(x) &= h_1 f_3 + \epsilon(h_2 f_2^2 + h_1 f_3 f_2 r_1)\end{aligned}$$

where $a(x)$ and $d(x)$ are the advection and diffusion rates, respectively. To lowest order, the advection rate matches the deterministic model, with y in steady state. This is equivalent to finding a solution in the nullspace of L_2. We can see each term in the diffusion rate is preceded by one of our small parameters ϵ, h_1 or h_2. The identity of the lowest order term depends on the relative sizes of these small parameters.

- When the T-cell population size is quite small, then diffusion is dominated by the inherent noise in the T-cell birth-death process ($h_1 \gg \epsilon h_2 x$). The diffusion rate is

$$d_T(x) \approx \frac{h_1}{2}\,(1 + (1 + \gamma + c)x) \tag{5.16}$$

- When the T-cell population increases, then the diffusion is dominated by noise in the

DC population ($h_1 \ll \epsilon h_2 x$).

$$d_D(x) \approx \epsilon \frac{h_2}{2} \gamma^2 x^2 \tag{5.17}$$

We have modeled the noise in the DC population as the result of small population size, but it could be due to infection or be driven by other components of the immune system that we have not modeled. For the purpose of our analysis, it is sufficient to assume that Y has mean $r_1(x)$ and variance h_2.

5.4 Computing first passage times

Our primary interest is computing the time it takes for the system to travel from $T = 0$ to $T = x_f$. We denote this mean first passage time W. We follow the work of [29] in this section. We calculate the mean first passage time using the following system

$$W_1''(x) = 2a(x)W_1'(x)/d(x) - 2/d(x) \tag{5.18}$$

where $W_1'(0) = W_1(0) = 0$ and $-W_1(x_f)$ is the time for the system to travel from $x = 0$ to $x = x_f$. We can also calculate the second moment of the first passage time

$$W_2''(x) = 2a(x)W_2(x)'/d(x) + 4W_1(x)/d(x)$$

with $W_2(0) = W_2'(0)$. The variance can be calculated as $-W_2(x_f) - W_1^2(x_f)$. This approximation is much faster to calculate than a full stochastic simulation of the system, particularly for large system sizes. Figure 5.2 compares the mean first passage time calculated with (5.18) (solid lines) to the average of repeated stochastic simulations of the birth-death process (dashed lines) as a function of q_0, the baseline inflammation. We vary m, which measures the ability of T-cells to induce the generation of immunogenic DC, and α_D, the production rate of DC. Note that when we vary α_D, we also change g to keep the nondimensionalized γ the same. This means that change in α_D corresponds only to a change in the variance of the DC population. The mean first passage time dramatically increases as q_0 decreases, and there is a marked turning point that roughly corresponds to where the deterministic system no longer reaches x_f. This threshold changes with m, but does not depend on the variance of the DC population, which is only relevant for the stochastic system.

If the barrier equilibrium, x_b, does not exist, then the deterministic system tends towards the disease state deterministically (Figure 5.3A-C, dashed lines). If the parameters are such that x_b and x_i do not exist but there are still points at which $a(x)$ is very nearly zero, then we say that there are two 'ghost' equilibria. We see that both the deterministic and stochastic

system pause as they pass by the ghost equilibria. The stochastic system (solid black line) can, on average, jump over the barrier slightly faster then the deterministic system (dashed black line) (Figure 5.3A-C). Individual simulations of the stochastic system (Figure 5.3A-C, red, blue, and yellow) pause at the ghost barrier for variable lengths of time, but afterwards behave similarly to each other and the deterministic system.

If the barrier equilibrium does exist, along with the disease free state x_i, then the deterministic system remains disease free for all time (Figure 5.3D-F, dashed lines). The stochastic system behaves similarly to the prior case, pausing as it crosses the barrier, then growing rapidly afterwards (Figure 5.3, solid line). Individual runs also look quite similar to the prior case. However, if the simulation remains near x_i for an extended period of time, we see that the T-cell population can drop to zero (Figure 5.3D, yellow line). The T-cell population is replenished by the thymus in this model. Without this thymic input, when the T-cell population reaches zero it would not transition back to one and so would never reach the disease state, x_f.

The stochastic transition from the disease free state x_i to the disease state x_f has two stages. First, the system must escape from a potential well near x_i to the boundary or threshold state x_b. The time it takes for this process should have a large variance. Second, there is the low variance transition from x_b to x_f, where advection dominates over diffusion. This second step is similar in stochastic and deterministic systems; therefore we expect it to have a low variance. To visualize this, we approximate the distribution of W with a γ-distribution that has the same mean and variance.

$$\text{Prob}\{W = w\} \approx \frac{1}{\Gamma(k)\theta^k} w^{k-1} e^{-w/\theta} \tag{5.19}$$

$$k = -\frac{W_1(x_f)^2}{W_1(x_f)^2 + W_2(x_f)} \tag{5.20}$$

$$\theta = \frac{W_1(x_f)^2 + W_2(x_f)}{W_1(x_f)} \tag{5.21}$$

When the mean and standard deviation of W are equal, then the γ-distribution approximation reduces to an exponential distribution. The mode of the distribution then approaches zero, implying that the peak age of onset should be at birth. If the standard deviation is less than the mean, then the probability density function has a nonzero mode, predicting a peak age of onset later in life.

The height of the peak increases when we increase the basal inflammation rate. If the basal inflammation rate is low, then the mean age of onset is very large, but the variance is also high, so there is no distinct peak in the probability density function (Figure 5.4, black

line). As we increase q_0 the peak becomes more defined, and the size of the right hand tail decreases (Figure 5.4, red and blue lines).

5.5 Discussion

We propose and analyze a simple model of the growth of self reactive T-cells over the life of an individual. In particular, we analyze the role of stochastic fluctuation in disease progression. The T-cells and immunogenic dendritic cells (DCs) have mutual positive feedback, creating a bistable system under certain parameter conditions, with one 'healthy' stable steady state and one 'diseased' stable steady state separated by an unstable 'threshold' state. Stochastic fluctuation allows the system to jump from one stable steady-state to another.

Using a separation of time scales and a large system approximation, we reduce the stochastic model to a one-dimensional Fokker-Planck equation. We then derive a system of ODEs to calculate the mean and variance of the time required to jump from the healthy state to the disease state. This approximation has good agreement with the full stochastic simulation and is far faster to calculate.

Type 1 Diabetes is typically diagnosed during childhood, although the incidence increases with age until about age ten [39]. These type of incidence curves are typically interpreted to indicate a multiple-hit disease progression [9]. In the case of T1D, it has been hypothesized that viral infections are required [22]. Our model can be described as 'one hit+delay', where the hit is the escape from the potential well of the healthy state. We model this as due to the intrinsic noise of the system, without any external stimulation, in a similar fashion to mutation of an oncogene in cancer development. Despite only requiring one hit, we can still produce an incidence curve with the observed qualitative behavior.

In this paper we have only considered intrinsic noise, driven largely by small population size. This may be reasonable in the case of self reactive T-cells, but is probably far from accurate for DCs. In fact, we expect that the number of immunogenic and tolerogenic DCs should largely be driven by infection or any other proinflammatory event. Although these events may be stochastic in nature, they do not arise inherently from small population size, as we have modeled here. However, our analysis reveals that no matter what stochastic process controls the DC population, our approximation of mean first passage time depends only on its mean and variance. Therefore, driving the population with an external, noisy 'infection' function should have the same effect as altering parameters that already exist in the model.

Our model suggests that greater levels of inflammation should inevitably drive autoimmune disease, which runs counter to the hygiene hypothesis. There is compelling evidence that decreased infection in childhood actually increases the incidence of T1D [17]. This is possibly because we have not included competition with other T-cell populations, which should be enhanced during infection. Therefore, an important next step would be to include a population of T-cells that reacts to a foreign pathogen, which could respond to immunogenic DC in a deterministic manner.

Table 5.1: Nondimensionalization

ϵ	$\frac{\delta_T}{\delta_D}$	.1
h_1	$\frac{\alpha_T}{\delta_T}$	$<< 1$
h_2	$\frac{\alpha_D}{\delta_D}$	$<< 1$
γ	$\frac{g\alpha_D}{\delta_D\delta_T}$	variable
ω	$\frac{w\alpha_D}{\delta_D\delta_T}$	variable
κ	$\frac{k\delta_T}{\alpha_T}$	$>> 1$
μ	$\frac{m\alpha_T}{\delta_T}$	$<< 1$
c	$\frac{C}{\delta_T}$	$<< 1$

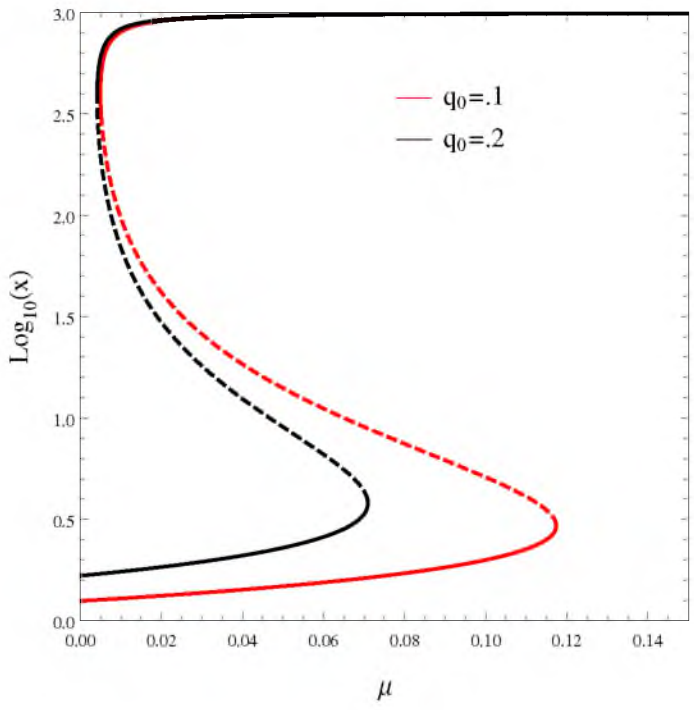

Figure 5.1: Bifurcation diagram of the stable (solid) and unstable (dashed) solutions to (5.4). Parameters: $\epsilon = .1$, $c = \gamma = \omega = 1$,$h_1 = .1$, $h_2 = .01$, $\kappa = 1000$.

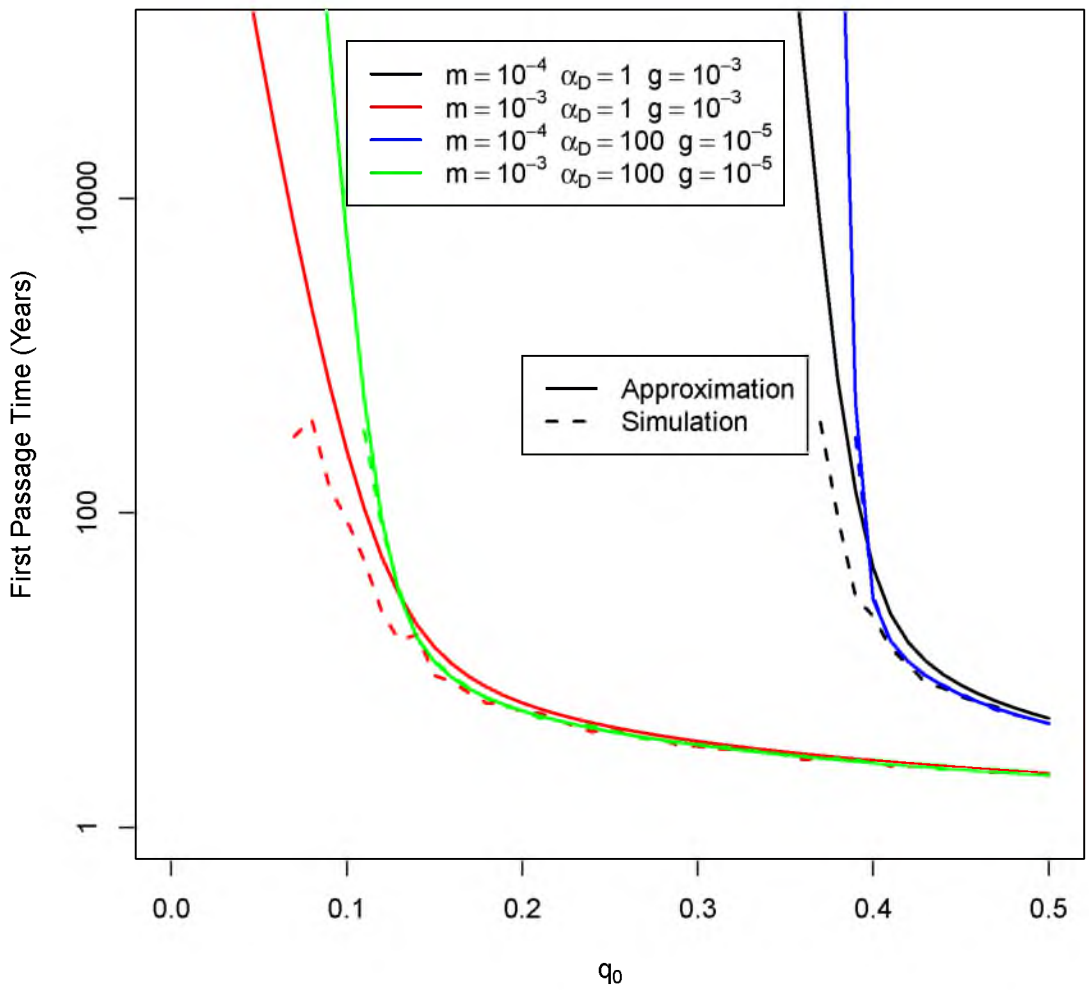

Figure 5.2: Average time to reach the disease state, x_f, as a function of the basal inflammation rate, q_0. Dashed lines: mean of simulations using a gillespie algorithm. Solid lines: derived approximation from (5.18)

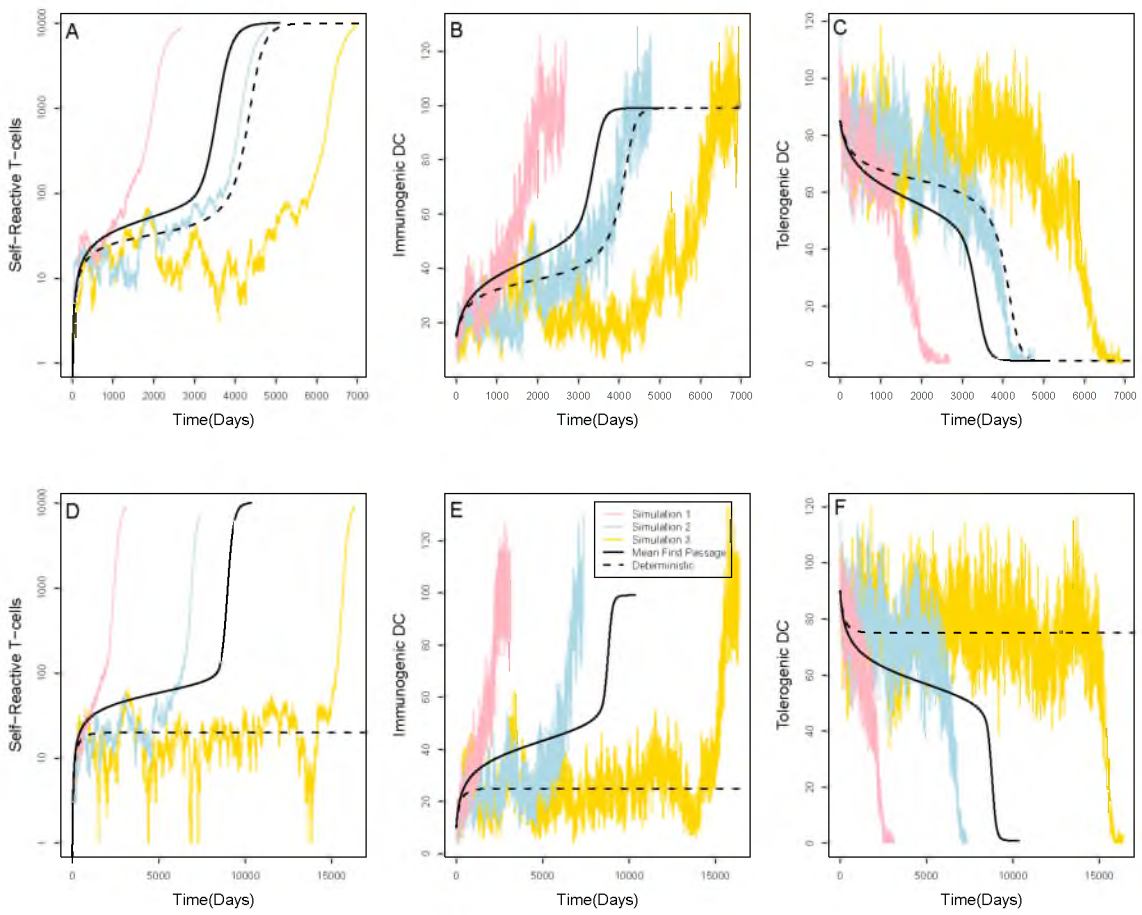

Figure 5.3: Simulation of the stochastic (red, yellow, and blue) and deterministic (black dashed) systems. The mean first passage of the stochastic model is the black dashed lines. A, D: Self T-cell. B, E: Immunogenic DC. C, F: Tolerogenic DC. A-C: $q_0 = .15$. D-F: $q_0 = .1$. All other parameters are common: $m = .01$, $\alpha_T = .1$, $\alpha_D = 10$, $g = w = 10^{-4}$.

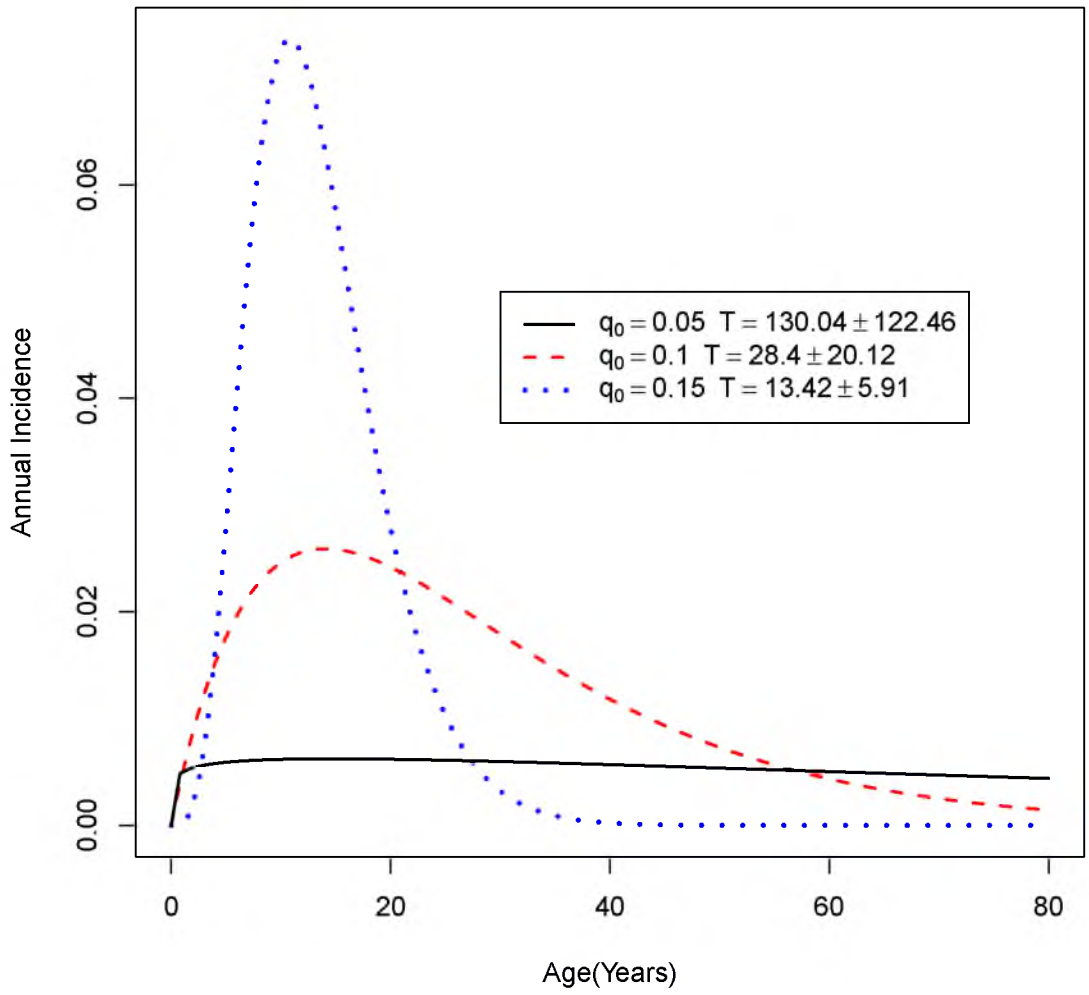

Figure 5.4: Approximate probability density functions of first passage time. We calculate the mean and standard deviation using 5.18, then compute the gamma distribution that shares these statistics.

APPENDIX A

DERIVING PER CAPITA GROWTH RATES

In this appendix, we derive the total proliferation of T-cells due to IL-2 and justify the simplification we use in the model. We consider a population of N DC, each with N_S spots on their surfaces, that binds T-cells according to (2.3). The collection of T-cells bound to a given DC represents a sample from a multivariate hypergeometric distribution [44]. Let B_E and B_R be the total number of bound effectors and Tregs, respectively. The probability that an individual DC binds e effectors and r Tregs is

$$q_{er} = \frac{\binom{B_E}{e}\binom{B_R}{r}\binom{NN_S - B_E - B_R}{N_S - e - r}}{\binom{NN_S}{N_S}}. \tag{A.1}$$

When N is large the hypergeometric distribution approaches a multinomial distribution

$$\lim_{N\to\infty} q_{er} = p_{er} = \binom{N_S}{e}\binom{N_S - e}{r} b_E^e b_R^r (1 - b_E - b_R)^{N_S - e - r} \tag{A.2}$$

where $b_E = B_E/(NN_S)$ and $b_R = B_R/(NN_S)$ are the probabilities that a DC spot binds an effector or Treg, respectively. The per capita growth rate of T-cells bound to such a DC is $\gamma \frac{k_i e}{k_E e + k_R r}$, where $i = E$ or R for effectors and Tregs, respectively. The expected value of the per capita growth rates for effectors and Tregs, respectively, is

$$\hat{\gamma}_E^*(b_e, b_r) = \frac{\sum_{er} \frac{k_E e^2}{k_E e + k_R r} p_{er}}{\sum_{er} e p_{er}} \tag{A.3}$$

$$\hat{\gamma}_R^*(b_e, b_r) = \frac{\sum_{er} \frac{k_R er}{k_E e + k_R r} p_{er}}{\sum_{er} r p_{er}}. \tag{A.4}$$

In this paper, we replace these expressions with a simpler approximation that is far faster to calculate.

$$\hat{\gamma}_E(b_e, b_r) = k_E \frac{1 + b_E(N_S - 1)}{k_E + (k_E b_E + k_R b_R)(N_S - 1)} \tag{A.5}$$

$$\hat{\gamma}_R(b_e, b_r) = k_R \frac{b_E(N_S - 1)}{k_R + (k_E b_E + k_R b_R)(N_S - 1)} \tag{A.6}$$

Figure A.1 shows the relative error of the approximation for $\hat{\gamma}_E$ across the full range of values b_e and b_r. Our approximation has the following qualitative features:

$$\gamma_E(b_E, 0) = \gamma_E^*(b_E, 0) = 1$$
$$\gamma_R(1, 0) = \gamma_E^*(1, 0) = \frac{N_S - 1}{N_S}$$
$$\gamma_E(0, b_r) > 0$$
$$\gamma_R(0, b_r) = \gamma_R^*(0, b_r) = 0$$

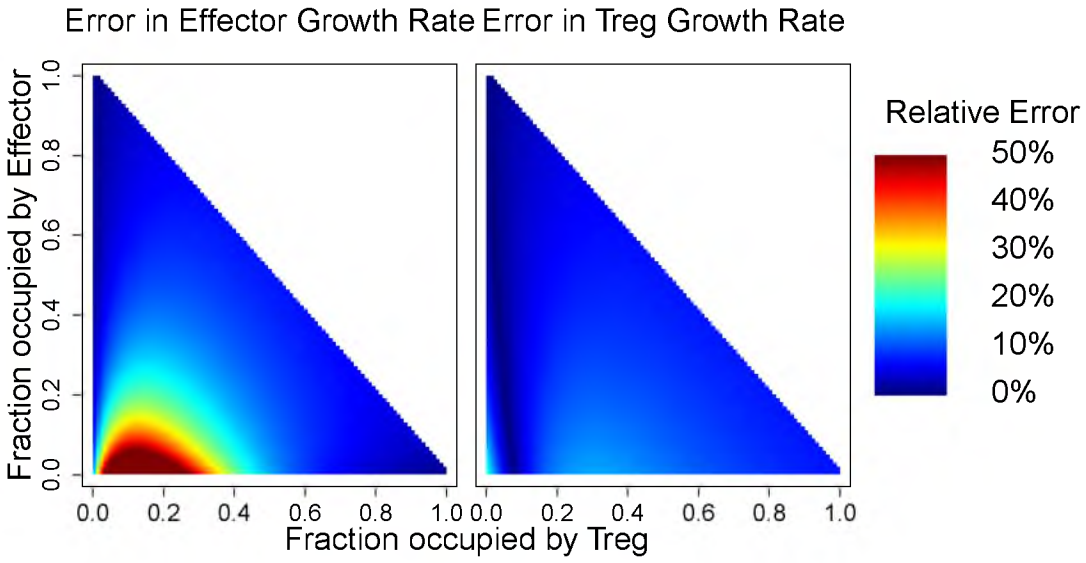

Figure A.1: Relative error of per capita growth rate of effector T-cells used in model ($\hat{\gamma}_E$ and $\hat{\gamma}_R$) compared to the derived values ($\hat{\gamma}_E^*$ and $\hat{\gamma}_R^*$). Parameters: $N_S = 10$, $k_E = 1$, $k_R = 3$.

APPENDIX B

ALL MODELS PERFORM POORLY UNDER EXTREME CONDITIONS

According to Figures 2.7 and B.1, the outcome is poor in all models if ϕ_S and p_I are close to 1. In the absence of Tregs, there is always a sustained self response (Figure B.1 A, D). The foreign response is significant in either case and meets our criteria for 'Immunity'; however, this response is not sustained in the homogenous case (Figure B.1 A). With the addition of killer Tregs (Figure B.1 C, F), the self response is no longer sustained, but the foreign response does not escape suppression by self reactive Tregs. In the heterogenous case (Figure B.1 F), the criteria for immunity or tolerance are met, albeit it narrowly. This represents a tradeoff with the suppressive Treg case (Figure B.1 E), which has a stronger immune response but more self reactive T-cells. Although the self reactive population is not sustained in the lymph node, these cells could potentially trigger immunopathology and eventual autoimmune disease. Killer Tregs bias the system tends toward weaker foreign immune responses rather than autoimmune ones.

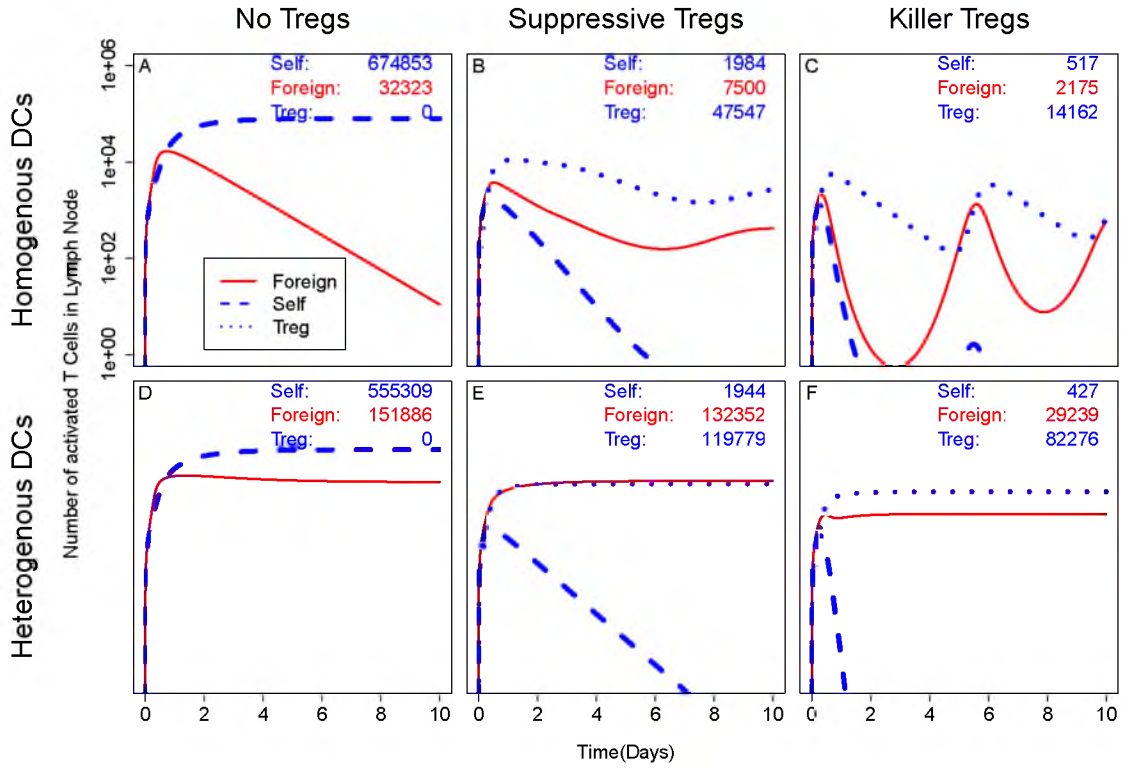

Figure B.1: Activated T-cells versus time (days) for foreign (red), self (blue dashed), and Treg (blue dotted). Each panel represents a different model. The numbers in each plot represent the total number of effector cells of each type that leave the lymph node. Parameters: $\phi_S = 0.8$, $\phi_F = 0.1$, $p_I = 0.9$, $\beta = 1.25$, $k_R = 3$.

REFERENCES

[1] A.K. Abbas, A.H. Lichtman, and S. Pallai, *Cellular and molecular immunology*, sixth ed., 2007.

[2] E.D. Acheson, *Epidemiology of multiple sclerosis*, Br. Med. Bull. **33** (1977), no. 1, 9–14.

[3] E. Akirav, J. A. Kushner, and K. C. Herold, *β-cell mass and type 1 diabetes going, going, gone*, Diabetes **57** (2008), no. 11, 2883–2888.

[4] T. Alanentalo, A. Hörnblad, S. Mayans, A. K. Nilsson, J. Sharpe, Å. Larefalk, U. Ahlgren, and D. Holmberg, *Quantification and three-dimensional imaging of the insulitis-induced destruction of β-cells in murine type 1 diabetes*, Diabetes **59** (2010), no. 7, 1756–1764.

[5] H.K. Alexander and L.M. Wahl, *Self-tolerance and autoimmunity in a regulatory T-cell model*, Bull. Math. Biol. **73** (2011), no. 1, 33–71.

[6] J.F. Allard, O. Dushek, D. Coombs, and P. Anton Van Der Merwe, *Mechanical modulation of receptor-ligand interactions at cell-cell interfaces*, Biophys. J. **102** (2012), no. 6, 1265–1273.

[7] A. Amrani, J. Verdaguer, P. Serra, S. Tafuro, R. Tan, and P. Santamaria, *Progression of autoimmune diabetes driven by avidity maturation of a T-cell population*, Nature **406** (2000), no. 6797, 739–742.

[8] M.S. Anderson and J.A. Bluestone, *The NOD mouse: a model of immune dysregulation*, Annu. Rev. Immunol. **23** (2005), 447–485.

[9] K.C. Atwood and A. Norman, *On the interpretation of multi-hit survival curves*, Proc. Natl. Acad. Sci. **35** (1949), no. 12, 696.

[10] M.E. Bianchi, *Damps, pamps and alarmins: all we need to know about danger*, J. Leukocyte Biol. **81** (2007), no. 1, 1–5.

[11] J.A.M. Borghans, R.J. De Boer, E. Sercarz, and V. Kumar, *T-cell vaccination in experimental autoimmune encephalomyelitis: a mathematical model*, J. Immunol. **161** (1998), no. 3, 1087–1093.

[12] J. Braun and J. Sieper, *Ankylosing spondylitis*, The Lancet **369** (2007), no. 9570, 1379–1390.

[13] N.J. Burroughs, M. Ferreira, B. Oliveira, and A.A. Pinto, *Autoimmunity arising from bystander proliferation of T-cells in an immune response model*, Math. Comput. Model. **53** (2011), no. 7, 1389–1393.

[14] J. Carneiro, K. Leon, Í. Caramalho, C. Van Den Dool, R. Gardner, V. Oliveira, M.L. Bergman, N. Sepúlveda, T. Paixão, J. Faro, et al., *When three is not a crowd: a crossregulation model of the dynamics and repertoire selection of regulatory CD4+ T-cells*, Immunol. Rev. **216** (2007), no. 1, 48–68.

[15] Z. Chen, A.E. Herman, M. Matos, D. Mathis, and C. Benoist, *Where CD4+ CD25+ Treg cells impinge on autoimmune diabetes*, J. Exp. Med. **202** (2005), no. 10, 1387–1397.

[16] K.T. Coppieters, T. Boettler, and M. von Herrath, *Virus infections in type 1 diabetes*, Cold Spring Harb. Perspect. Med. **2** (2012), no. 1.

[17] M.A. D'Angeli, E. Merzon, L.F. Valbuena, D. Tirschwell, C.A. Paris, and B.A. Mueller, *Environmental factors associated with childhood-onset type 1 diabetes mellitus: an exploration of the hygiene and overload hypotheses*, Arch. Pediat. Adol. Med. **164** (2010), no. 8, 732.

[18] B.F. De Blasio, P. Bak, F. Pociot, A.E. Karlsen, and J. Nerup, *Onset of type 1 diabetes: a dynamical instability*, Diabetes **48** (1999), no. 9, 1677–1685.

[19] R.J. De Boer and A.S. Perelson, *Towards a general function describing T-cell proliferation*, J. Theor. Biol. **175** (1995), no. 4, 567–576.

[20] M. Feuerer, Y. Shen, D. R. Littman, C. Benoist, and D. Mathis, *How punctual ablation of regulatory T-cells unleashes an autoimmune lesion within the pancreatic islets*, Immunity **31** (2009), no. 4, 654–664.

[21] B. T. Fife, I. Guleria, M. G. Bupp, T. N. Eagar, Q. Tang, H. Bour-Jordan, H. Yagita, M. Azuma, M. H. Sayegh, and J. A. Bluestone, *Insulin-induced remission in new-onset NOD mice is maintained by the PD-1-PD-L1 pathway*, J. Exp. Med. **203** (2006), no. 12, 2737–2747.

[22] C. Filippi and M. von Herrath, *How viral infections affect the autoimmune process leading to type 1 diabetes*, Cell. Immunol. **233** (2005), no. 2, 125–132.

[23] C.M. Filippi, E.A. Estes, J.E. Oldham, and M.G Von Herrath, *Immunoregulatory mechanisms triggered by viral infections protect from type 1 diabetes in mice*, J. Clin. Invest. **119** (2009), no. 6, 1515.

[24] M.A. Fishman and A.S. Perelson, *Th1/Th2 differentiation and cross-regulation*, Bull. Math. Biol. **61** (1999), no. 3, 403–436.

[25] M. B. French, J. Allison, D. S. Cram, H. E. Thomas, M. Dempsey-Collier, A. Silva, H. M. Georgiou, L. C. Kay, T. W .and Harrison, and A. M. Lew, *Transgenic expression of mouse proinsulin II prevents diabetes in nonobese diabetic mice*, Diabetes **46** (1997), no. 1, 34–39.

[26] W. Fu, G. Wojtkiewicz, R. Weissleder, C. Benoist, and D. Mathis, *Early window of diabetes determinism in NOD mice, dependent on the complement receptor CRIg, identified by noninvasive imaging*, Nat. Immunol. **13** (2012), no. 4, 361–368.

[27] R.S. Fujinami, M.G. Von Herrath, U. Christen, and J.L. Whitton, *Molecular mimicry, bystander activation, or viral persistence: infections and autoimmune disease*, Clin. Microbiol. Rev. **19** (2006), no. 1, 80.

[28] K.M. Gillespie, S.C. Bain, A.H. Barnett, P.J. Bingley, M.R. Christie, G.V. Gill, and E.A.M. Gale, *The rising incidence of childhood type 1 diabetes and reduced contribution of high-risk HLA haplotypes*, The Lancet **364** (2004), no. 9446, 1699–1700.

[29] D. T. Gillispie, *Markov Processes*, Academic Press, San Diego, 1992.

[30] N. N. Gorgani, U. Thathaisong, Violet RS Mukaro, O. Poungpair, A. Tirimacco, C.S.T. Hii, and Antonio Ferrante, *Regulation of CRIg expression and phagocytosis in human macrophages by arachidonate, dexamethasone, and cytokines*, Am. J. Pathol. **179** (2011), no. 3, 1310–1318.

[31] Erica J Graham, *Mathematical models of mechanisms underlying long-term type 2 diabetes progression*, Ph.D. thesis, The University of Utah, 2012.

[32] K.L. Graham, J.A. O'Donnell, Y. Tan, N. Sanders, E.M. Carrington, J. Allison, and B.S. Coulson, *Rotavirus infection of infant and young adult nonobese diabetic mice involves extraintestinal spread and delays diabetes onset*, J. Virol. **81** (2007), no. 12, 6446–6458.

[33] K.L. Graham, N. Sanders, Y. Tan, J. Allison, T.W.H. Kay, and B.S. Coulson, *Rotavirus infection accelerates type 1 diabetes in mice with established insulitis*, J. Virol. **82** (2008), no. 13, 6139–6149.

[34] T.S. Griffith and T.A. Ferguson, *Cell death in the maintenance and abrogation of tolerance: the five ws of dying cells*, Immunity **35** (2011), no. 4, 456–466.

[35] Yenkel Grinberg-Bleyer, Audrey Baeyens, Sylvaine You, Rima Elhage, Gwladys Fourcade, Sylvie Gregoire, Nicolas Cagnard, Wassila Carpentier, Qizhi Tang, Jeffrey Bluestone, et al., *IL-2 reverses established type 1 diabetes in NOD mice by a local effect on pancreatic regulatory T-cells*, J. Exp. Med. **207** (2010), no. 9, 1871–1878.

[36] S.E. Henrickson, T.R. Mempel, I.B. Mazo, B. Liu, M.N. Artyomov, H. Zheng, A. Peixoto, M.P. Flynn, B. Senman, T. Junt, et al., *T-cell sensing of antigen dose governs interactive behavior with dendritic cells and sets a threshold for T-cell activation*, Nat. Immunol. **9** (2008), no. 3, 282–291.

[37] S. Iwami, Y. Takeuchi, Y. Miura, T. Sasaki, and T. Kajiwara, *Dynamical properties of autoimmune disease models: tolerance, flare-up, dormancy*, J. Theor. Biol. **246** (2007), no. 4, 646–659.

[38] A. Jayasimhan, K. P. Mansour, and R. M. Slattery, *Advances in our understanding of the pathophysiology of type 1 diabetes: lessons from the NOD mouse*, Clin. Sci. **126** (2014), no. 1, 1–18.

[39] M. Karvonen, M. Viik-Kajander, E. Moltchanova, I. Libman, R. LaPorte, and J. Tuomilehto, *Incidence of childhood type 1 diabetes worldwide*, Diabetes Care **23** (2000), no. 10, 1516–1526.

[40] A. Khadra, P. Santamaria, and L. Edelstein-Keshet, *The role of low avidity T-cells in the protection against type 1 diabetes: a modeling investigation*, J. Theor. Biol. **256** (2009), no. 1, 126–141.

[41] B. Krishnamurthy, N.L. Dudek, M.D. McKenzie, A.W. Purcell, A.G. Brooks, S. Gellert, P.G. Colman, L.C. Harrison, A.M. Lew, and H.E. Thomas, *Responses against islet*

antigens in NOD mice are prevented by tolerance to proinsulin but not IGRP, J. Clin. Invest. **116** (2006), no. 12, 3258–3265.

[42] J.F. Kurtzke, *Epidemiologic evidence for multiple sclerosis as an infection.*, Clin. Microbiol. Rev. **6** (1993), no. 4, 382.

[43] K. León, A. Lage, and J. Carneiro, *Tolerance and immunity in a mathematical model of T-cell mediated suppression*, J. Theor. Biol. **225** (2003), no. 1, 107–126.

[44] K. Leon, R. Perez, A. Lage, and A. Jorge, *Modelling T-cell-mediated suppression dependent on interactions in multicellular conjugates*, J. Theor. Biol. **207** (2000), no. 2, 231–254.

[45] G. Magombedze, P. Nduru, C.P. Bhunu, and S. Mushayabasa, *Mathematical modelling of immune regulation of type 1 diabetes*, Biosystems **102** (2010), no. 2, 88–98.

[46] J.M. Mahaffy and L. Edelstein-Keshet, *Modeling cyclic waves of circulating T-cells in autoimmune diabetes*, SIAM J. Appl. Math. **67** (2007), no. 4, 915–937.

[47] A.F.M. Marée, R. Kublik, D.T. Finegood, and L. Edelstein-Keshet, *Modelling the onset of type 1 diabetes: can impaired macrophage phagocytosis make the difference between health and disease*, Phil. T. Roy. Soc. A **364** (2006), no. 1842, 1267–1282.

[48] M. Matloubian, C.G. Lo, G. Cinamon, M.J. Lesneski, Y. Xu, V. Brinkmann, M.L. Allende, R.L. Proia, and J.G. Cyster, *Lymphocyte egress from thymus and peripheral lymphoid organs is dependent on S1P receptor 1*, Nature **427** (2004), no. 6972, 355–360.

[49] E.J. McMahon, S.L. Bailey, C.V. Castenada, H. Waldner, and S.D. Miller, *Epitope spreading initiates in the CNS in two mouse models of multiple sclerosis*, Nat. Med. **11** (2005), no. 3, 335–339.

[50] T.R. Mempel, S.E. Henrickson, and U.H. Von Andrian, *T-cell priming by dendritic cells in lymph nodes occurs in three distinct phases*, Nature **427** (2004), no. 6970, 154–159.

[51] J. R Moore, *The benefits of diversity: heterogenous dc populations allow for both immunity and tolerance*, J. Theor. Biol. **357** (2014), 86–102.

[52] K. Murphy, P. Travers, and M. Walport, *Immunobiology*, seventh ed., Garland Science, New York, 2008.

[53] J. Nerup, T. Mandrap-Poulsen, S. Helqvist, H. U. Andersen, F. Pociot, J. I. Reimers, B. G. Cuartero, A. E. Karlsen, U. Bjerre, and T. Lorenzen, *On the pathogenesis of IDDM*, Diabetologia **37** (1994), no. 2, S82–S89.

[54] H.S. Panitch, *Influence of infection on exacerbations of multiple sclerosis*, Annals of Neurology **36** (1994), no. S1, S25–S28.

[55] S. M. Pop, C. P. Wong, D. A. Culton, S. H. Clarke, and R. Tisch, *Single cell analysis shows decreasing FoxP3 and TGFβ1 coexpressing CD4+ CD25+ regulatory T-cells during autoimmune diabetes*, J. Exp. Med. **201** (2005), no. 8, 1333–1346.

[56] M. J. Richer, N. Straka, D. Fang, I. Shanina, and M. S. Horwitz, *Regulatory T-cells protect from type 1 diabetes after induction by coxsackievirus infection in the context of transforming growth factor-β*, Diabetes **57** (2008), no. 5, 1302–1311.

[57] S. Sakaguchi, T. Yamaguchi, T. Nomura, and M. Ono, *Regulatory T-cells and immune tolerance*, Cell **133** (2008), no. 5, 775–787.

[58] M. Samarkos and G. Vaiopoulos, *The role of infections in the pathogenesis of autoimmune diseases*, Curr. Drug Targets **4** (2005), no. 1, 99–103.

[59] B. Schaub, R. Lauener, and E. von Mutius, *The many faces of the hygiene hypothesis*, J. Allergy. Clin. Immun. **117** (2006), no. 5, 969–977.

[60] A. Scheffold, K.M. Murphy, and T. Höfer, *Competition for cytokines: Treg cells take all*, Nat. Immunol. **8** (2007), no. 12, 1285–1287.

[61] D.V. Serreze, E.W. Ottendorfer, T.M. Ellis, C.J. Gauntt, and M.A. Atkinson, *Acceleration of type 1 diabetes by a coxsackievirus infection requires a preexisting critical mass of autoreactive T-cells in pancreatic islets*, Diabetes **49** (2000), no. 5, 708–711.

[62] E. Sgouroudis, A. Albanese, and C. A. Piccirillo, *Impact of protective IL-2 allelic variants on CD4+ Foxp3+ regulatory T-cell function in situ and resistance to autoimmune diabetes in NOD mice*, J. Immunol. **181** (2008), no. 9, 6283–6292.

[63] N. A. Sherry, J. A. Kushner, M. Glandt, T. Kitamura, A. B. Brillantes, and K. C. Herold, *Effects of autoimmunity and immune therapy on β-cell turnover in type 1 diabetes*, Diabetes **55** (2006), no. 12, 3238–3245.

[64] C. M. Smith, M. B. Gill, J. S. May, and P. G. Stevenson, *Murine gammaherpesvirus-68 inhibits antigen presentation by dendritic cells*, PLoS One **2** (2007), no. 10, e1048.

[65] S. Sreenan, A. J. Pick, M. Levisetti, A. C. Baldwin, W. Pugh, and K. S. Polonsky, *Increased beta-cell proliferation and reduced mass before diabetes onset in the nonobese diabetic mouse*, Diabetes **48** (1999), no. 5, 989–996.

[66] R.M. Steinman, D. Hawiger, and M.C. Nussenzweig, *Tolerogenic dendritic cells**, Annu. Rev. Immunol. **21** (2003), no. 1, 685–711.

[67] Q. Tang, J.Y. Adams, C. Penaranda, K. Melli, E. Piaggio, E. Sgouroudis, C.A. Piccirillo, B.L. Salomon, and J.A. Bluestone, *Central role of defective interleukin-2 production in the triggering of islet autoimmune destruction*, Immunity **28** (2008), no. 5, 687–697.

[68] B. Topp, K. Promislow, G. Devries, R. M. Miura, and D. T. Finegood, *A model of β-cell mass, insulin, and glucose kinetics: pathways to diabetes*, J. Theor. Biol. **206** (2000), no. 4, 605–619.

[69] M. Tritt, E. Sgouroudis, E. d'Hennezel, A. Albanese, and C. A. Piccirillo, *Functional waning of naturally occurring CD4+ regulatory T-cells contributes to the onset of autoimmune diabetes*, Diabetes **57** (2008), no. 1, 113–123.

[70] J. D. Trudeau, C. Kelly-Smith, C. B. Verchere, J. F. Elliott, J. P. Dutz, D. T. Finegood, P. Santamaria, and R. Tan, *Prediction of spontaneous autoimmune diabetes in NOD mice by quantification of autoreactive T-cells in peripheral blood*, J. Clin. Invest. **111** (2003), no. 2, 217–223.

[71] J.D. Trudeau, J.P. Dutz, E. Arany, D.J. Hill, W.E. Fieldus, and D.T. Finegood, *Neonatal beta-cell apoptosis: a trigger for autoimmune diabetes*, Diabetes **49** (2000), no. 1, 1–7.

[72] H.J. Van Den Ham and R.J. De Boer, *From the two-dimensional Th1 and Th2 phenotypes to high-dimensional models for gene regulation*, Int. Immunol. **20** (2008), no. 10, 1269.

[73] M. Vellela and H. Qian, *A quasistationary analysis of a stochastic chemical reaction: Keizers paradox*, Bull. Math. Biol. **69** (2007), no. 5, 1727–1746.

[74] J. Verdaguer, D. Schmidt, A. Amrani, B. Anderson, N. Averill, and P. Santamaria, *Spontaneous autoimmune diabetes in monoclonal T-cell nonobese diabetic mice*, J. Exp. Med. **186** (1997), no. 10, 1663–1676.

[75] H Viskari, Johnny Ludvigsson, R Uibo, L Salur, D Marciulionyte, R Hermann, G Soltesz, M Füchtenbusch, A-G Ziegler, A Kondrashova, et al., *Relationship between the incidence of type 1 diabetes and maternal enterovirus antibodies: time trends and geographical variation*, Diabetologia **48** (2005), no. 7, 1280–1287.

[76] H.L. Weiner, A.P. da Cunha, F. Quintana, and H. Wu, *Oral tolerance*, Immunol. Rev. **241** (2011), no. 1, 241–259.

[77] J. D. Wetzel, E. S. Barton, J. D. Chappell, G. S. Baer, M. Mochow-Grundy, S. E. Rodgers, Y. Shyr, A. C. Powers, J. W. Thomas, and T. S. Dermody, *Reovirus delays diabetes onset but does not prevent insulitis in nonobese diabetic mice*, J. Virol. **80** (2006), no. 6, 3078–3082.

[78] K. Wing and S. Sakaguchi, *Regulatory T-cells exert checks and balances on self tolerance and autoimmunity*, Nat. Immunol. **11** (2009), no. 1, 7–13.

[79] A. Yates, R. Callard, and J. Stark, *Combining cytokine signalling with T-bet and GATA-3 regulation in Th1 and Th2 differentiation: a model for cellular decision-making*, J. Theor. Biol. **231** (2004), no. 2, 181–196.

[80] J. Ye, J. R. Ortaldo, K. Conlon, R. Winkler-Pickett, and H. A. Young, *Cellular and molecular mechanisms of IFN-γ production induced by IL-2 and IL-12 in a human NK cell line*, J. Leukocyte Biol. **58** (1995), no. 2, 225–233.

[81] L. Zhang, M. Nakayama, and G. S. Eisenbarth, *Insulin as an autoantigen in NOD/human diabetes*, Curr. Opin. Immunol. **20** (2008), no. 1, 111–118.

[82] Z. J. Zhang, L. Davidson, G. Eisenbarth, and H. L. Weiner, *Suppression of diabetes in nonobese diabetic mice by oral administration of porcine insulin*, Proc. Natl. Acad. Sci. **88** (1991), no. 22, 10252–10256.